

REACTIONS OF  $C_6$  OLEFINS AND m-XYLENE  
OVER ION-EXCHANGED ZEOLITES

BY

BERNARD W. MOLLER, B.Sc.

Thesis submitted for the degree of Doctor of  
Philosophy of the University of Edinburgh  
in the Faculty of Science

December 1974



TO MY WIFE

## Abstract

In this work two test reactions have been utilised to study the nature of zeolite catalysts. Firstly, the isomerisation of 3,3-dimethylbut-1-ene(I), to give 2,3-dimethylbut-1-ene(II) and 2,3-dimethylbut-2-ene(III), was used to study the acidity of a series of copper, zinc and nickel-exchanged zeolites because the reaction is believed to proceed via the formation of carbonium ion intermediates. After a preliminary survey of each series of zeolites a more detailed examination of the isomerisation and exchange reactions of these  $C_6$  olefins over selected catalysts was undertaken. The isomerisation of both I and II was studied and the effect of the presence of  $H_2$  and  $H_2O$  upon such rates examined. The nature of the exchange reactions of the various olefins was investigated using both  $D_2$  and  $D_2O$ .

The results demonstrate that  $CuX$  and  $ZnX$  zeolites display acidic-type behaviour, being much more active than the parent  $NaX$ . Hydrogen was observed to have no effect upon the rate of isomerisation of the olefins over these catalysts but the changes in rate observed when the reactions were carried out in the presence of water could be explained in terms of interaction of water molecules with the transition metal cations. The isomerisation of II was shown to be a more facile process than that of I.

The exchange reactions of I and II with  $D_2$  and  $D_2O$  showed that substantial exchange only took place under conditions where isomerisation occurred. With  $D_2O$  the exchange of I was multiple in character whereas that of II was stepwise. These differences were rationalised in terms of the relative rates of desorption of II and III from the catalyst surface and the rate of formation of a tertiary carbonium ion from the initial olefin. The exchange reactions of the olefins with  $D_2$

all occurred via a stepwise process.

NiX zeolites were observed to display activity of a dual function type. They showed acidic behaviour in being active for the isomerisation of I and the reactions of the olefins with  $H_2O$  or  $D_2O$  could be interpreted as for CuX or ZnX. However, the most striking differences between NiX and CuX or ZnX were observed when reactions of the olefins were studied with  $H_2$  or  $D_2$ . The ability of NiX zeolites to catalyse the hydrogenation of the  $C_6$  olefins and to bring about the low temperature exchange of I with  $D_2$  was well demonstrated. Further detailed study was undertaken with selected CuX and NiX zeolites. The catalysts were subjected to various pretreatments in an attempt to gain more information about the nature of the catalytically active sites.

The second part of the thesis was concerned with studying the exchange reactions of m-xylene over nickel, cobalt and calcium-exchanged zeolites using a temperature-programming technique. The relative reactivities of the different hydrogen atoms in the aromatic molecule is thought to provide information about the operative mechanism. The most important result to emerge was that the nature of the source of labelling isotope ( $D_2$  or  $D_2O$ ) had a profound effect upon the character of the reaction. With  $D_2O$ , ring exchange was found to be faster than side-group exchange over all catalysts, a result indicative of acidic type behaviour. One of the ring hydrogen atoms in m-xylene was observed to react more slowly than the other three and this is believed to be the hydrogen atom ortho to both methyl groups, indicating that steric and not electronic factors are important in the exchange of the ring atoms.

When  $D_2$  was used as the source of deuterium a complete change was observed in the character of the reaction. With NiX side-group exchange was now faster than ring exchange, a result similar to that found over

metals. CoX and CaX were much less active than NiX for exchange with  $D_2$ . Over these two catalysts all of the hydrogen atoms in the molecule were found to be equally reactive and the limiting factor in the exchange appeared to be the ability of the catalysts to activate  $D_2$ .

## CONTENTS

### Part I      General Introduction

#### Chapter 1      Introduction to Adsorption and Catalysis

	<u>Page</u>
1.1      Definition	1
1.2      Mechanism of Heterogeneous Catalysis	2
1.3      Adsorption	3
1.4      Adsorption Isotherms	4
1.5      Techniques in the Study of Adsorption	5
1.6      Kinetics and Mechanism	6
1.7      Catalysts and Catalytic Activity	8
1.8      Classification of Catalysts	9

#### Chapter 2      Molecular Sieve Zeolites

2.1      Introduction	10
2.2      Occurrence/Synthesis	11
2.3      Crystallography	12
2.4      Cation Positions	14
2.5      Ion-Exchange	18
2.6      Adsorption/Dehydration/Stability	20
2.7      Surface Studies	24
2.8      Reactions on Zeolites	26
2.9      Reactivity	30

#### Chapter 3      Exchange Reactions

3.1      Introduction	32
3.2      General Aspects of Exchange Reactions	33
3.2(A)      The Final Equilibrium of Exchange Reactions	33

	<u>Page</u>
3.2(B) The Rate Constants of an Exchange Reaction	34
3.2(C) Kinetics	35
3.2(D) Classification and Mechanism	36
 <u>Chapter 4</u> <u>The Isomerisation of 3,3-Dimethylbut-1-ene</u>	
4.1 Reaction Scheme	40
4.2 Mechanism	40
4.3 Purpose of the Present Work	42
 <u>Part II</u> <u>Experimental and Treatment of Results</u>	
 <u>Chapter 5</u> <u>Experimental</u>	
5.1 Apparatus	43
5.2 The Gas Handling System	43
5.3 Reaction Vessel and Capillary Leak	44
5.4 Volume Calibrations	45
5.5 The MS.10 Mass Spectrometer	46
5.6 Chromatographic Analyses	47
5.7 Materials	48
5.8 Procedure	50
5.9 Other Techniques	51
 <u>Chapter 6</u> <u>Treatment of Results</u>	
6.1 Introduction (Mass Spectrometric Data)	53
6.2 Preliminary Procedure	53
6.3 Background Corrections	54
6.4 Isotope Corrections	54
6.5 Fragmentation Corrections	55
6.6 Arrhenius Plots	57
6.7 H <sub>2</sub> /D <sub>2</sub> Exchange	58
6.8 Treatment of GLC Data	59

Part III      The Reactions of C<sub>6</sub> Olefins over Ion-Exchanged X Type Zeolites

Chapter 7      Results for CuX Zeolites

7.1	Isomerisation of Dimethylbutenes	65
7.2	Exchange Reactions of Dimethylbutenes	67
7.3	The Exchange of I with D <sub>2</sub> O Studied by a Combined GC-MS Technique	70
7.4	Reactions on Treated CuX(10)	71
7.5	Reactions over CuHX Zeolites	73
7.6	Discussion	74

Chapter 8      Results for ZnX Zeolites

8.1	Olefin Isomerisation	95
8.2	Exchange Reactions	95
8.3	Discussion	97

Chapter 9      Results for NiX Zeolites

9.1	Olefin Isomerisation	101
9.2	Reactions over NiX(21)	101
9.3	Reactions over Treated NiX(21)	103
9.4	Reactions over NiX(9)	105
9.5	Discussion	106

Part IV

Chapter 10      The Exchange Reactions of m-Xylene over Ion-Exchanged X Type Zeolites

10.1	Introduction	120
10.2	Object of the Present Study	121
10.3	Experimental	122



	<u>Page</u>
10.4 Treatment of Results	122
10.5 Results for NiX Zeolites	125
10.6 Results for CoX Zeolite	127
10.7 Results for CaX Zeolite	128
10.8 Discussion	128
References	139

## Part I

### General Introduction

## CHAPTER I

### Introduction to Adsorption and Catalysis

#### 1.1 Definition

A catalyst is a substance that isothermally increases the rate at which a chemical reaction reaches equilibrium without itself undergoing overall chemical change. Catalysis is the word used to describe the action of the catalyst.

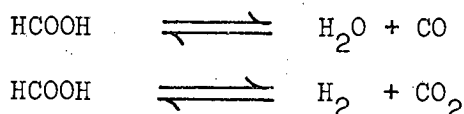
The terms catalyst and catalysis were introduced by Berzelius<sup>1</sup> in 1835, when he reviewed a number of apparently diverse observations having a factor in common; in every case the reaction was influenced by the presence of a substance which remained unchanged. Among the examples quoted were the conversion of starch into sugar by means of acids and the combination of hydrogen and oxygen on spongy platinum.

The first quantitative meaning was given to catalysis by Ostwald<sup>2</sup> who introduced the concept of velocity of change as a measure of catalytic activity.

As a result of the kinetic studies of Bodenstein and Ostwald, and the thermodynamic principles enunciated by Van't Hoff, the following statements must be valid,

- (i) a catalyst can only accelerate a reaction which is already thermodynamically feasible
- (ii) the equilibrium position reached in the presence of a catalyst is the same as that which would ultimately be obtained in its absence
- (iii) a catalyst accelerates equally the rates of the forward and reverse reactions

- (iv) for a given reactant or groups of reactants there may be several reaction paths and by appropriate choice of catalyst one of these paths may be selected. For example, formic acid may be decomposed in two alternative ways,



the first of these changes is catalysed by oxides such as alumina, the second by various metals.

In general, catalysed reactions may be divided into two main classes:

- (a) Homogeneous catalysis in which catalyst and reactants are in the same phase.
- (b) Heterogeneous catalysis which describes the enhancement in rate brought about by the presence of an interface between two phases.

This thesis is concerned only with the latter type of reaction.

## 1.2 Mechanism of Heterogeneous Catalysis

The first attempts to explain the mechanism of heterogeneous catalysis supposed that the molecules of a gas were brought into a chemically active state by mere mechanical impact with the surface of the catalyst, but this theory failed to explain many aspects of catalysis.

Faraday<sup>3</sup> proposed that by virtue of the attraction which the solid exerted on the reacting gases, the latter are concentrated near the surface allowing interaction to occur more readily. In order to explain the specificity of catalytic action Sabatier<sup>4</sup> introduced the concept of unstable surface intermediates. In this

way, a metal such as nickel possessed hydrogenation activity because it could readily form an intermediate hydride, which in turn decomposed to regenerate the free metal.

A much clearer outlook resulted from the work of Langmuir<sup>5</sup>, who suggested that adsorption on a solid surface frequently involved the formation of chemical bonds between the surface and adsorbate and that the amount of gas adsorbed will depend upon the number of sites available for bonding, leading ultimately to the production of a unimolecular layer of adsorbed gas. The formation of surface-adsorbate chemical bonds leads to more favourable reaction pathways as evidenced by the lower activation energies for reactions taking place in the presence of a catalyst.

### 1.3 Adsorption

From the above it follows that in a catalytic reaction at least one of the reactants must become attached in some way, and for a significant period, to the surface of the catalyst. Therefore, in order to appreciate the mechanism of heterogeneous catalysis it is important to understand the characteristics of adsorption. Adsorption may be divided into two main classes: physical adsorption and chemisorption.

#### Physical Adsorption

Physical adsorption<sup>6</sup> is caused by forces of molecular interaction i.e. of the van der Waals type, and is similar in nature and mechanism to the condensation of a vapour on the surface of a liquid. Heats of physical adsorption are generally low and in the neighbourhood of the heat of liquifaction of the adsorbate.

Physical adsorption is important only at temperatures near or below the boiling point of the adsorbate and requires no activation energy, taking place rapidly and reversibly. It is non-specific, occurring on all surfaces under the correct conditions of temperature and pressure and is not restricted to monolayer coverage.

#### Chemisorption

Chemisorption<sup>7</sup> involves the rearrangement of the electrons of the interacting gas and solid with the consequential formation of chemical bonds. Heats of chemisorption may be quite high, being of the order of 40-250 kJ mole<sup>-1</sup>. Chemisorption may take place at temperatures far above the boiling point of the adsorbate and may require an appreciable activation energy. The specificity is great; hydrogen chemisorbs readily on nickel but not on copper. Chemisorption is often irreversible especially at low temperatures and is usually restricted to monolayer coverage of the surface.

The criteria discussed above may be used to distinguish between the two types of adsorption though in some cases the distinction may not be well-defined.

#### 1.4 Adsorption Isotherms

Since physical adsorption is non-specific it can be used to measure the total area of a surface exposed to a gas. This phenomenon is employed in the B.E.T. isotherm<sup>8</sup> (for multi-layer physical adsorption). Physical adsorption also forms the basis of most methods of measuring the porosity of solids<sup>9</sup>.

Due to the large energy changes that it brings about in a molecule, chemisorption of one or more of the reactants is

thought to be a prerequisite of any catalytic reaction.

The relationship between the pressure of a gas and the amount of gas adsorbed on a surface was first treated quantitatively by Langmuir<sup>10</sup> and on the basis of kinetic considerations he derived the Langmuir Isotherm;

$$\theta = \frac{bp}{1+bp}$$

where  $\theta$  is the fraction of the surface covered by adsorbed molecules,  $p$  is the pressure of gas and  $b$  is a constant which contains the heat of adsorption and temperature.

Although it contains a number of weaknesses, principally that it ignores surface heterogeneity which has been taken into account in other isotherms<sup>7</sup>, the Langmuir isotherm has proved to be useful in a number of systems.

#### 1.5 Techniques in the Study of Adsorption

Apart from the utilisation of thermodynamic data, such as heats and entropies of adsorption, it is possible to investigate the intermediates of a catalytic reaction by means of physical techniques. One of the most successful approaches has involved the application of i.r. spectroscopy. The electronic spectra of adsorbed molecules may also be used. Other spectroscopic techniques which have been employed include nmr and epr. Also, techniques which involve following changes in the properties of the catalyst after adsorption have proved useful and these include work function and electrical-resistance measurements. Chemical techniques such as the use of deuterium and other 'tracer' elements have yielded much information concerning the nature and reactivity of surface intermediates. Examples of the use of the

above-mentioned techniques, with reference to zeolite catalysts, will be discussed in later sections.

#### 1.6 Kinetics and Mechanism

The overall rate of a heterogeneously catalysed reaction is likely to be determined by one (or more) of the following consecutive steps ,

- (1) Diffusion of reactant(s) to the surface from the gas phase.
- (2) Chemisorption of one or more reactant species on the surface.
- (3) The surface reaction (adsorbed species reacting among themselves, with physically adsorbed species or with other molecules colliding with the surface).
- (4) Desorption of the products from the surface.
- (5) Diffusion of the products away from the surface.

Steps (1) and (5) would only become important if the reactants were in the liquid phase or if the catalyst were highly porous. They are unlikely to be rate-controlling unless the surface reaction is extremely rapid.

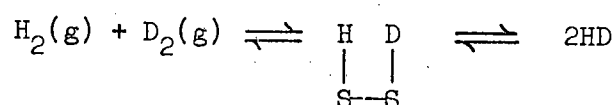
Wheeler<sup>11</sup> has developed methods for determining the effects of diffusion on the overall reaction rate. Diffusion processes are non-activated and do not depend greatly on temperature whereas chemical reactions do, and by studying the reaction at various temperatures, if a linear Arrhenius plot is obtained from widely differing rates then it is unlikely diffusion effects are important.

Steps (2), (3) and (4) are chemical interactions and it is usually found that step (3) is rate-controlling unless the



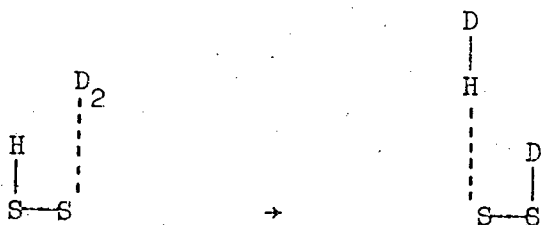
adsorbed species is difficult to form or remove.

Two basic mechanisms have been proposed to explain the combination of reactants at a catalyst surface. The first of these, the Langmuir-Hinshelwood mechanism<sup>12,13</sup>, assumes that the rate of reaction is controlled by reaction of molecules chemically adsorbed on adjacent sites, the adsorption and desorption processes being in equilibrium. According to this scheme, H<sub>2</sub>/D<sub>2</sub> exchange would take place in the following way;



Most of the reactions this mechanism has been applied to occur at high temperatures where rapid adsorption/desorption is to be expected.

The second basic mechanism is known as the Eley-Rideal mechanism<sup>14,15</sup> and is more often applicable at low temperatures. In this case, it is proposed that only one species is chemisorbed and this reacts with a molecule which is either physically adsorbed or in the gas phase and can be represented as follows;



The exact mechanism of the surface reaction is extremely difficult to determine since the nature, properties and concentration of the various chemical species cannot easily be derived from an examination of the kinetics of a catalytic reaction.

## 1.7 Catalysts and Catalytic Activity

### Geometric Factor

Surface geometry and lattice spacing have been shown to play an important role in some heterogeneously catalysed reactions. Beeck<sup>16</sup> found that Ni(110) planes were more active in ethylene hydrogenation than non-orientated films and was able to correlate the activity of a series of metals with their lattice spacing<sup>17</sup>. Balandin's<sup>18</sup> theory on the role of crystal symmetry in which he paid special attention to the benzene  $\rightleftharpoons$  cyclohexane system must also be considered.

However, results from LEED and electron microscopy have led to certain doubts being expressed as to the validity of the geometric factor. It has been shown that the surface atoms of certain films undergo drastic rearrangement after adsorption of gases or during catalysis and may even develop new crystal planes<sup>19</sup>. The actual lattice spacing of surface atoms reactive in catalysis may differ greatly from that in the bulk material.

### Electronic Factor

The basis of the electronic factor has been to relate the collective electronic properties of metals, alloys or semi-conductors to their catalytic activity.

The catalytic activity of a series of transition metals has been related to the percentage d-character of the metals<sup>17,20-22</sup> and for semiconducting oxides the activity has been interpreted either in terms of point defects or the Wolkenstein<sup>23</sup> electronic theory. The view that the activity of transition-metal oxides is determined by the d-electrons<sup>24-26</sup> has been discussed in terms of electron-transfer and augmented by application of crystal field theory<sup>25</sup>.

However, not all of the observed facts of chemisorption can be satisfactorily explained by the electronic theory of solids. The percentage d-character controls the lattice spacing but it does not determine the precise arrangement of the active centres at a given surface and hence concepts such as d-character can only explain the general level of activity of polycrystalline catalysts. It does not explain why faces of the same metal may show greater variations in activity than two metals with significantly different d-character<sup>27</sup>.

A more fruitful approach involves consideration of the properties of individual atoms or complexes at the surface<sup>27-29</sup>. Despite criticism of this approach<sup>30</sup> evidence for the role of factors such as ease of formation and stability of surface intermediates has arisen<sup>31-33</sup> and such considerations may apply to a variety of systems.

### 1.8 Classification of Catalysts

Electrical conductivity has been used to classify heterogeneous catalysts<sup>30</sup> and based upon this scheme the more important reactions catalysed by conductors (metals), semi-conductors (metal oxides and sulphides) and insulators (acids and metal oxides) have been listed. This thesis is concerned with the use of zeolites as catalysts and it has been found that zeolites exhibit electrical conductivity of an ionic type<sup>52</sup>, due to the migration of the cations through the channel structure.

## CHAPTER II

### Molecular Sieve Zeolites

#### 2.1 Introduction

Zeolite minerals were discovered and named by the Swedish minerologist Baron Cronsted in 1756. Some of the important properties shown by zeolites were soon recognized e.g. reversible ion-exchange and dehydration, adsorption of inorganic vapours and the molecular sieving effect. The early literature on zeolites has been summarised by McBain<sup>34</sup> who proposed the term 'molecular sieve'. Smith<sup>35</sup> has defined a zeolite as 'an aluminosilicate with a framework structure enclosing cavities occupied by large ions and water molecules, both of which have considerable freedom of movement, permitting ion-exchange and reversible dehydration', in order to distinguish them from amorphous, gel-type aluminosilicates used for water treatment which are commonly called 'zeolites'.

The early attempts to prepare synthetic forms of zeolite crystals were largely unsuccessful and have been discredited on the basis of improper identification<sup>36,37</sup>. It has only been since the introduction of x-ray diffraction techniques that a more positive identification of complex structures and compositions has been achieved.

Barrer<sup>38</sup> was the first to systematically examine the sorbent properties and the ability to separate mixtures. He reported the synthesis of the zeolite mordenite and several other synthetic varieties<sup>36,37,39</sup>. Union Carbide Corp. attracted

by the potential application of zeolites initiated a programme of research which resulted in the preparation of many synthetic zeolites some of which were not analogs of zeolite minerals found in nature<sup>40,41</sup>. The discovery of synthetic crystalline zeolites has resulted in wide scientific interest and a great variety of applications in industry.

## 2.2 Occurrence/Synthesis

There are over thirty naturally occurring zeolites. They are found in basaltic and diabasic igneous rocks rich in alkalis e.g. in N. Ireland and Iceland<sup>42</sup>, being formed in such media by hydrothermal alteration. They are also found in massive amounts as alteration products in sediments<sup>43</sup>.

The synthesis of zeolites arises from the crystallisation of freshly-prepared, highly reactive aluminosilicate gels at temperatures ranging from 293-423 K at atmospheric or autogeneous pressure<sup>44</sup> (a gel is defined as a hydrous, metal aluminosilicate mixture which is prepared either from aqueous solutions or reactive solid phases). Typical gels are prepared from aqueous solutions of sodium aluminate, sodium silicate and sodium hydroxide. This method is best suited for the alkali metals since they form soluble hydroxides, silicates and aluminates and it is possible to prepare very homogeneous gel mixtures. The gel structure is formed by the polymerisation of the aluminate and silicate ions.

During the crystallisation process, the components of the gel undergo a rearrangement into the ordered crystalline structure, being brought about by a depolymerisation of the gel due to the hydroxyl ions present in the reaction mixture.

Large numbers of crystallite nuclei are formed from the supersaturated gel so that the final product consists of a finely divided white powder of very small crystals, only a few microns in size.

The type of hydrated cation used in the reactant gel is important, sodium containing gels give more open zeolite structures than potassium ones.

By varying parameters such as initial gel composition, crystallisation temperature and type of reactants many zeolite species have been formed in a pure state.

### 2.3 Crystallography

#### Framework Structure

The structures of zeolites consist of a 3-dimensional framework of  $\text{SiO}_4$  and  $\text{AlO}_4$  tetrahedra, with the oxygen atoms at the corners and the T(Si,Al) atoms occupying the centres of the tetrahedra.

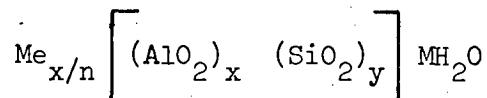
The substitution of  $\text{Al}^{3+}$  for  $\text{Si}^{4+}$  requires the presence of a charge balancing cation to maintain electrical neutrality.

Zeolites have been prepared in which  $\text{Ge}^{4+}$  and  $\text{Ga}^{3+}$  have been substituted for Si and Al respectively<sup>45,46</sup> and more recently phosphorous substitution in the zeolite framework has been reported<sup>47</sup>.

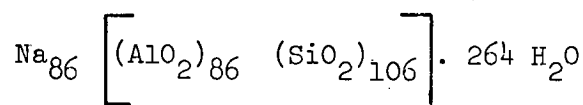
In zeolites the maximum substitution of Al for Si is the ratio of 1:1 and leads to a complete ordering of the Al and Si ions<sup>48</sup>. The minimum ratio is 1:5 in mordenite<sup>49</sup>. Zeolites X and Y are synthetic forms which have the same topology as the mineral faujasite. The Si : Al ratio is 1 to 1.5 for X and

1.5 to 3.0 for Y.

A structural formula of the type



may be used to illustrate the relationship between chemical composition and structure. Me represents the metal cation and x, y and n are integers. For Na 13X zeolite the unit cell composition is



The structures of many zeolites consist of simple arrangements of polyhedra, with each polyhedron being a 3-dimensional array of (Si)AlO<sub>4</sub> tetrahedra in a definite geometric form. The SiO<sub>4</sub> and AlO<sub>4</sub> tetrahedra are the primary building blocks; each corner is shared by two tetrahedra and the linkage of the resulting framework is specified by placing tetrahedral centres at the corners of a truncated octahedron (secondary building block), which in keeping with Euler's theorem contains 8 hexagonal faces, 6 square faces, 24 vertices and 36 edges<sup>50</sup>. The space inside a truncated octahedron is commonly called a sodalite unit or β-cage and has a free diameter of 0.66 nm.

(a) The Sodalite Group

In faujasite and zeolites X and Y the framework consists of a tetrahedral arrangement of truncated octahedra, i.e. the octahedra are linked by hexagonal faces with 6 bridge oxygen ions. This results in a series of wide, nearly spherical cavities (α-cages) 1.2 to 1.3 nm in length, each of which opens by common windows (distorted 12-rings of 0.9 nm diameter) into 4 identical tetrahedrally distributed cavities. Each α-cage is linked to 4

sodalite units through 6-rings and shares 4-rings with 6 other sodalite units. The overall view of the faujasite lattice is that of a tightly packed aggregate of oxygen atoms interlaced with large voids.

In zeolite A<sup>48</sup> each sodalite unit is linked to its neighbour by four bridging oxygen atoms between the square faces.

Although sodalite is not strictly a zeolite, the framework structure is based on similar units. The truncated octahedra share square and hexagonal faces.

(b) Mordenite<sup>49</sup> has only a 2-dimensional tubular pore system. The crystal structure consists of chains of 4- and 5-rings of Si and Al tetrahedra linked laterally so that a system of large, elliptical, parallel channels (0.66 nm diameter) interconnected by smaller cross channels (0.28 nm diameter) is created.

(c) Chabazite Group

Zeolites in this group have frameworks best represented in terms of sheets or layers of linked rings of tetrahedra. The cavities are roughly ellipsoidal linked by distorted 8-rings with dimensions of about 0.44 by 0.31 nm.

2.4 Cation Positions

In order to assess the role played by exchangeable cations in catalysis, it is essential to know what positions the cations may occupy in the zeolite framework and what factors may affect their distributions among the various sites.

Fig. 2.3 shows the cation sites which have been identified and the nomenclature adopted is due to Smith<sup>51</sup>.

Site U is at the centre of the truncated octahedron and lies



at the intersection of 4 axes of inverse 3-fold rotation symmetry; Site I is situated at the centre of the hexagonal prism; I' on a triad axis displaced into the sodalite cage from the hexagonal face shared by the hexagonal prism and sodalite cage; II' on a triad axis but displaced into the sodalite cage from the unshared 6-ring between sodalite cage and supercage; II slightly and II\* considerably displaced into the supercage from the unshared 6-ring; III displaced into the supercage from bridging 4-rings; V displaced slightly from the centre of the 12-ring separating supercages.

The information which is available on cation locations has proved difficult to interpret since several specimens were not fully-exchanged and most dehydrated samples still contain significant amounts of water or other oxygen species. The exchange procedure may lead to the entry of protons instead of the chosen cation and not all single crystals have been completely characterised for cation content.

#### Dehydrated Samples

Calculations of cation distributions are usually based on an electrostatic model although covalent bonding may occur and cations may associate with particular 6-rings containing high amounts of Al. Site I (16 per unit cell) permits a cation to be enclosed by framework oxygens whereas I', II and II' (32 per unit cell) permit only one-sided coordination to oxygens of the adjacent 6-ring. Site I is thus preferred unless electrostatic repulsion or cation-molecule attraction become important.

In zeolite Y the most favoured way electrostatically to distribute 58 monovalent cations would be to place 32 in II, 6 in I and 20 in I' so that no I and I' cations share a 6-ring.

In zeolite X, Breck<sup>52</sup> placed 16 in I, 32 in II and 38 in III but there is no published data on cation positions in monovalent X zeolite.

In zeolite Y, all the divalent cations (29 per unit cell) can be accommodated in I and II. In strongly dehydrated samples site I offers minimum electrostatic energy and is preferred. The occupancy of sites in the sodalite cage (both in strongly and partially dehydrated samples) can be ascribed to cations bonding to residual water molecules<sup>53</sup> or other oxygen species. Dempsey<sup>54</sup> found that for monovalent zeolites calculations of ionic distributions agreed with crystallographic data but that for divalent zeolites divergences could be explained if small amounts of water were retained by the zeolite.

#### Hydrated Samples

The available data for hydrated samples is unsatisfactory since the positions of all the cations and water molecules have not been established. Ion-exchange studies<sup>55,56</sup> are consistent with 16 Na<sup>+</sup> ions in internal sites for NaY and NaX. Multivalent cations present in X and Y zeolites occupy mainly supercage sites where they coordinate to the maximum number of water molecules but with zeolite X, because of the higher cation density, coulombic repulsions will force ions into internal sites. Occupation of site II\* and V is important only in hydrated systems.

Olson<sup>57</sup>, suggested that in hydrated systems cations only occupy site II when there are three Al atoms in the 6-ring to provide a favourable electrostatic environment and hence cations should only occupy site II in zeolite X, in agreement with the experimental evidence.

### Techniques used to Investigate Cation Positions

X-ray diffraction techniques have been most widely used for determining the locations of cations in the zeolite structure. Although the data obtained on atomic positions and occupation frequency appear to be highly precise they are subject to personal interpretation and involve making chemical assumptions<sup>51</sup>. Data from single crystals yield more positive results than from powders but large synthetic crystals have only recently become available.

The infra-red stretching frequency of CO adsorbed on X and Y zeolites has been examined<sup>58,59</sup> and the presence of an absorption band at a frequency higher than that shown by CO in the gas phase was suggested to serve as an indicator of accessible divalent cations in the zeolites. This band was attributed to the electrostatic interaction between the CO molecule and the divalent cation. In this way CoY and NiY, 22 and 20% exchanged respectively, were shown to have cations in surface sites whereas in CaY (35% exchanged) the divalent  $\text{Ca}^{2+}$  ions preferred hidden sites.

Egerton and Stone<sup>64,65</sup> have used the specific adsorption of CO as a means of detecting divalent cations occupying surface sites. In a study of CaY zeolite<sup>64</sup>, from the measured thermodynamic parameters of adsorption, they concluded that only after 55% exchange had taken place were  $\text{Ca}^{2+}$  ions located in surface sites.

Epr studies<sup>59-63</sup> have made useful contributions and have been mainly directed towards zeolites containing  $\text{Cu}^{2+}$  and  $\text{Mn}^{2+}$  ions. Based on their work with  $\text{Mn}^{2+}$  as a probe ion Barry and Lay<sup>61</sup> have given a summary of the factors which are likely to determine cation

location. They concluded that certain transition metals display strong covalent character, preferring sites of specific symmetry rather than sites of higher coordination number, e.g.  $\text{Zn}^{2+}$  prefers tetrahedral coordination in the sodalite unit to the nearly octahedral site I. Cations of higher valency were found to have a tendency to occupy positions in the sodalite unit.

Mikheiken and co-workers<sup>63</sup> utilised epr and optical spectroscopy to study the environment of  $\text{Cu}^{2+}$  ions in CuY zeolite.  $\text{Cu}^{2+}$  ions were found to enter the zeolite in the form of octahedral hexaquo complexes upon ion-exchange. Vacuum thermal treatment (373-673 K) led to the formation of aquo complexes of the  $\text{Cu}^{2+}$  ions with square pyramidal or square planar symmetry and the movement of the cations was hindered. With further increase in temperature the  $\text{Cu}^{2+}$  ions became stabilised in the six-membered windows of the sodalite units of the zeolite.

An example of the use of Mossbauer Spectroscopy would be in the investigation of the local environment of  $\text{Fe}^{2+}$  ions in FeY<sup>66</sup>. It was proposed that while  $\text{Fe}^{2+}$  ions preferentially enter  $\text{S}_\text{I}$ , dehydration leads to  $\text{Fe}^{2+}$  ions in four-fold coordination near the hexagonal windows. The effect of dehydration and the use of adsorbates of varying size and chemical behaviour as an aid in characterising surface sites is discussed.

Information from x-ray and epr studies applicable to the present work will be discussed in later sections.

## 2.5 Ion-Exchange

The ability to undergo reversible cation-exchange is one of the most important properties of zeolites. It provides a means of modifying the electric fields inside zeolite crystals,

which in turn modifies the sorptive and catalytic properties.

The cation-exchange behaviour depends upon the size and charge of the ion or complex ion and the type of zeolite structure.

A suspension of zeolite in water is basic<sup>52</sup> due to a limited amount of hydrolysis of the more loosely bound cations. If the pH of the solution is reduced below a value of about 5 (by addition of an aqueous acid) the aluminium ions are removed from the framework and the structure is destroyed. However, a hydrogen form can be prepared by first exchanging the alkali metal cations with ammonium ions and subsequently heating at 673 K to decompose the ammonium cation<sup>67</sup>. With zeolite X, up to about 50% exchange can be tolerated whereas with zeolite Y and mordenite greater exchange is possible.

Theoretical cation exchange capacities for the synthetic zeolites are quite high<sup>52</sup>, e.g. 4.7 milliequivalents/g hydrated zeolite X, although the extent of exchange tends to decrease with increasing Debye-Hückel parameter ( $a$ ) of the ions.

The presence of two independent 3-dimensional networks of cavities with cations located in both networks causes double sieving effects. One network is dense and contains little water (sodalite cages and hexagonal prisms) and the other network is open and highly hydrated. These two networks exhibit differing thermodynamic ion-exchange properties<sup>68,69</sup>. The sites in the supercage show a thermodynamic preference for higher charged ions over lower charged ones, and among univalent cations the preference depends upon the aluminium content or framework charge. In the small cages of X and Y, there is a preference

for ions with the smallest ionic radius and lowest charge, this effect being more marked with zeolite Y.

There are two steps in the exchange of polyvalent ions for  $\text{Na}^+$  ions, the slow step involving the exchange of  $\text{Na}^+$  in internal or hidden sites. The exchanging cations may not occupy the same sites or have the same distribution of sites as did the leaving ion.

Barrer<sup>70,71</sup> has shown that in faujasite the lattice constant changes from 2.49 nm to 2.56 nm upon introducing divalent nickel or cobalt ions into the zeolite.

## 2.6 Adsorption/Dehydration/Stability

### Adsorption

The crystalline solid remaining after dehydration is a highly selective adsorbent for gases and vapours. Molecular size voids permeate the crystal, forming the internal surface area or adsorption space. The entry of adsorbates into the channel systems of the zeolite is controlled by the free dimensions of the windows giving access into the cavities and not by the free dimensions of the cavities themselves.

From adsorption isotherms for various adsorbates at their saturation pressures, the limiting adsorption capacity has been determined and some typical results are shown in Table 2.1 for zeolite X. The adsorption of tertiary amines has been used to estimate the size of the channels<sup>72</sup>; the effective pore diameter of NaX was 0.9 to 1.0 nm whereas calcium or barium exchange reduced this to 0.8 to 0.9 nm.

It is possible to form zeolite encapsulates by forcing

TABLE 2.1 LIMITING ADSORPTION CAPACITIES FOR X TYPE ZEOLITES

adsorbate	kinetic diameter/nm	temp./K	pressure/k Nm <sup>-2</sup>	no. adsorbed mol/ cavity for NaX
H <sub>2</sub> O	0.265	298	3.3	33
Ar	0.340	90	101.3	17.6
O <sub>2</sub>	0.346	90	101.3	18.6
Kr	0.360	90	2.3	14.5
N <sub>2</sub>	0.364	77	93.3	16.6
Xe	0.396	195	93.3	9.3
n-pentane	0.430	298	27.3	4.3
cyclohexane	0.600	298	6.0	3.9
benzene	0.600	298	10.1	5.6
neopentane	0.620	298	93.3	3.6
(C <sub>4</sub> H <sub>9</sub> ) <sub>3</sub> N	0.810	298	0.1	2.1
(C <sub>4</sub> F <sub>9</sub> ) <sub>3</sub> N	1.020	323	0.1	0.1

otherwise non-adsorbed molecules into the zeolite cavities at elevated temperatures and pressures. When cooled, the gases remain trapped in the cavities. Encapsulates have been formed with zeolite A and  $\text{CH}_4$ , Ar and Kr<sup>52</sup>.

The molecular sieve properties of zeolites can be used in hydrocarbon separations. There are several factors which govern the molecular sieve behaviour. Small molecules cannot diffuse through 4- or 5-rings and  $\text{NH}_3$  and  $\text{H}_2\text{O}$  require an activation energy for passage through the 6-ring of sodalite<sup>73</sup>. The ease of penetration increases with ring size and diffusion is more rapid through the larger rings of faujasite. Due to puckering and non-planarity not all rings containing the same number of atoms are equivalent in size. Ring distortion affects the free diameter of the orifices<sup>74</sup>.

The number, size, valency and location of cations affect the size and shape of the entry pores and tend to partially obstruct intracrystalline channels<sup>75</sup>. NaA does not adsorb n-butane but many straight-chain hydrocarbons are readily adsorbed when about one-third of the sodium ions are replaced by calcium ions<sup>52</sup>.

The Si to Al ratio will affect the ring size because Si-O bonds are shorter than Al-O bonds<sup>76</sup>. Decreasing the Si to Al ratio will result in an increased charge density, decreasing the diffusion of polar molecules.

The molecular dimensions and polarity of the adsorbate must obviously be important.

The framework of zeolites has a lack of rigidity and hence dehydration will cause lattice distortions and changes in



cation occupation<sup>77</sup>.

Variations in temperature cause changes in pore size and the sensitivity is increased by lowering the temperature<sup>74</sup>, e.g. at 77 K oxygen is freely adsorbed on NaA whereas nitrogen is excluded although it is only 0.02 nm larger<sup>78</sup>.

The rates of diffusion and sorption in zeolites may be important in catalysis and the factors which govern them have been reviewed in detail<sup>79</sup>.

### Dehydration

The presence of water molecules is known to affect the distribution of exchangeable cations in zeolites but they do not appear to have any primary structural function and can be removed reversibly without disrupting the framework structure. Water molecules form hydration complexes with the cations and interact electrostatically with the framework oxygens. The hydration complexes of monovalent cations are weakly bonded and dehydration is achieved fairly readily whereas with multivalent cations the hydration complexes are more strongly held and the cation may polarise the water molecules causing them to split into a hydroxyl group (which bonds to the cation) and a proton which becomes attached to a framework oxygen<sup>80</sup>.

### Stability

The thermal stability depends upon the Si/Al ratio. Zeolite X is stable up to 973 K, zeolite Y up to 1023 K before structural collapse occurs.

When the zeolites are subjected to water vapour at elevated temperatures the stability of X and Y are found to differ

appreciably, X being less stable than Y<sup>35</sup>.

The thermal stability of the zeolite also depends upon the cations present. Barrer and Bratt<sup>81</sup> found that SrX and CoX were less stable than other monovalent and divalent forms. CeX and LaX were observed to show greater thermal and hydrolytic stability<sup>72</sup>.

Under certain conditions, oxygen and aluminium may be removed from the zeolite framework. Controlled dehydration and deamination of  $\text{NH}_4\text{Y}$  yields HY; containing one proton for every  $\text{Na}^+$ -free  $\text{AlO}_2$  unit. At higher temperatures, above 723 K at  $10^{-4}$   $\text{Nm}^{-2}$  or 873 K at  $8 \times 10^4$   $\text{Nm}^{-2}$  dehydroxylation occurs, the protons from HY are lost through the elimination of one mole of water per pair of  $\text{Na}^+$ -free  $\text{AlO}_2$  units<sup>82,83</sup>.

Kerr<sup>83</sup> found that heating HY in a dry atmosphere led to a material with a low thermal stability due possibly to crystalline defects. Heating to 973-1073 K in an inert static atmosphere with water remaining near the zeolite produced a substance of high thermal stability, the 'ultrastable' zeolite of McDaniel and Maher<sup>84</sup>, in which about 25% of the aluminium is present as exchangeable cations, suggesting that 12 aluminiums per unit cell had left the framework.

## 2.7 Surface Studies

Infra-red spectroscopy is one of the most powerful techniques for investigating the surface properties of zeolites. A number of studies have been reported on the nature of the structural hydroxyl groups on zeolites and they have been reviewed by Ward<sup>85</sup>. In general, alkali cation forms, when non-cation deficient, contain no detectable structural hydroxyl groups. Hydroxyl groups on Group IA zeolites probably arise from cation deficiencies caused by partial hydrolysis

and small amounts of siliceous impurities. Only hydroxyl groups terminating the giant lattice are expected. The alkaline earth, transition-metal and rare-earth forms possess several different kinds of hydroxyl groups which are probably similar to those in HY although they appear to be less reactive. One is attributed to silica-type hydroxyl groups present either as impurity or terminating the crystal lattice. A further two are attributed to structural silanol groups, one residing in the supercages, the other in the hexagonal prisms. Additional bands whose frequencies depend upon the cation have been observed and are attributed to  $\text{MOH}^+$  groups formed by dissociation of bound water.

Infra-red spectroscopy has been used to study the surface acidity of zeolites using basic molecules such as ammonia, pyridine and piperidine as probes. The interactions of these basic molecules with Bronsted acid sites, Lewis acid sites and cations, and their hydrogen-bonding interactions can be detected by ir spectroscopy. From these studies it has been found that Group IA zeolites are in general non-acidic whereas other zeolites (Group IIA, TM and RE) show Bronsted and/or Lewis acidity depending on the calcination temperature. The Bronsted acid sites on cation and hydrogen zeolites are the same and are believed to be two hydroxyl groups which have different acid strengths<sup>85</sup>. The Lewis acid sites are thought to be tricoordinated aluminium atoms. Hydroxyl groups, cations and aluminium atoms can function as adsorption sites. The interaction of zeolites with organic and inorganic molecules has been discussed<sup>85</sup>.

The oxidising properties of zeolites have been reported<sup>62,82</sup> and the conditions that produce maximum concentrations of radicals

from molecules of low ionisation potential studied in some detail<sup>86</sup>. Flockhart et al.<sup>87</sup>, have studied the reducing activity of HY for TCNE as a function of activation temperature and attempted to elucidate the nature of the sites at which electron transfer occurs.

Other techniques which may be used include the use of indicators which form stable carbonium ions<sup>88</sup>. Calorimetric studies, both heats of adsorption<sup>89</sup> and immersion<sup>90</sup> have been used to measure the acidity of sites in zeolite X and to suggest that the electrostatic field is the source of activity. Bolton<sup>91</sup> has combined it with thermogravimetric analysis to show that one water molecule is associated with each rare-earth cation. Tung<sup>92</sup>, from measurements of dielectric response to temperature and electrical frequency changes found considerable ionic movement over the zeolite surface and proposed the concept of dynamic Bronsted acidity.

The mobility of cations has been studied by radiochemical techniques<sup>93</sup>, X-ray diffraction<sup>94</sup> and epr<sup>95</sup>. UV spectroscopy gives information about the nature of adsorbed species and cation environments<sup>96</sup>, and nmr<sup>97</sup> can be used to give precise information about the location of protons in the zeolite structure.

## 2.8 Reactions on Zeolites

### Olefin Transformations

These include the fundamental carbonium ion type reactions of olefins including double-bond and carbon skeleton isomerisation, polymerisation, isotopic exchange and hydrogen transfer. The most important and recurring factor is the transfer and redistribution of hydrogen.

Hex-1-ene<sup>98</sup> undergoes isomerisation and polymerisation over REX with the formation of occluded intracrystalline polyolefins as

large as  $C_{30}H_{60}$  but no aromatics are formed. Over  $HY^{99}$  hex-1-ene undergoes complex changes with increase of temperature; a polyene is formed at 423 K and aromatic ring formation takes place at 533 K.  $C_2$  to  $C_5$  olefins follow similar patterns. Habgood et al.<sup>100</sup> found that the isomerisation of cyclopropane over deuterated NaY was promoted by small amounts of water and a mechanism proceeding via the formation of a non-classical carbonium ion was proposed. But-1-ene isomerisation has been used<sup>101-103</sup> to indicate the nature of the reaction occurring over a series of X-type zeolites.

#### Electrophilic Aromatic Substitution and Related Reactions

The process involves the attack of a positive species (electrophile) on an aromatic ring with the formation of a new bond and elimination of a proton. There are many ways of generating electrophiles, e.g. from an olefin by protonation, from a saturated hydrocarbon by hydride abstraction or a proton itself may behave as an electrophile.

Alkylations catalysed by zeolites generally proceed via carbonium ion mechanisms showing great similarity to the corresponding reactions carried out in the presence of strong protonic acids. The nature of the reaction may be deduced from analysis of the structures of the products, patterns of substrate reactivity and side reaction pathways. In general, ortho-para orientation is observed and in competitive studies selectivity for attack on the more nucleophilic aromatic nucleus is shown. A Rideal type mechanism is thought to be operative<sup>98</sup>, which requires rapid, reversible and non-competitive adsorption of the olefin on the catalyst acid sites.

Mays and Pickert<sup>104</sup> reported that multivalent cation-exchanged and decationated Y zeolites were excellent catalysts for

alkylation of aromatic molecules with  $C_2$  to  $C_{12}$  olefins or alkyl halides. An extensive amount of work has been done in the area of alkylaromatic isomerisation-transalkylation, dealkylation and related areas<sup>79</sup>. Ward<sup>105-108</sup> has conducted a series of investigations into the relationship between catalytic activity in reactions such as cumene dealkylation and o-xylene isomerisation, and the structural properties of the zeolites utilising techniques such as infrared spectroscopy. In many of these reactions catalytic activity was related to Bronsted acidity. Bolton et al.<sup>109</sup> proposed that isomerisation of diethylbenzenes over modified Y zeolites occurs via a transalkylation mechanism involving diphenylethane type intermediates. A similar mechanism has been proposed for xylene isomerisation<sup>110</sup> and this can only occur however if  $\alpha$ -hydrogens are available. Csicsery and Hickson<sup>111</sup> found that two independent reactions were occurring with 2-methyl-1-ethylbenzene over a series of Y zeolites. Isomerisation to 3-ethyl-1-methylbenzene and 4-ethyl-1-methylbenzene and transethylation to toluene and diethylmethylbenzenes took place. They explained the results by proposing that isomerisation took place on Bronsted acid sites whereas the transethylation was primarily a Lewis acid catalysed reaction.

#### Oxidation, Dehydrogenation and Related Reactions

Most crystalline aluminosilicates appear to have little intrinsic catalytic activity for hydrogenation-dehydrogenation type reactions excluding hydrogen transfer reactions<sup>112,113</sup>. When metallic or chalcogen functions are introduced into zeolites the situation changes but it is not clear whether the influence of the

zeolite structure is important or whether it functions only as a support.

X and A type zeolites containing Ni, Co, Fe or Cr have shown moderate paraffin dehydrogenation activity<sup>112,113</sup>. Among other reports there is dehydrogenation of cyclohexane over NiX<sup>114</sup> and of simple alcohols to ketones or aldehydes over CrX and CrA zeolites.

Oxidation reactions over zeolites have been reported mainly by transition metal zeolites. Examples are, the oxidative dehydrogenation of ethylbenzene to styrene and the selective oxidation of benzyl alcohol to benzaldehyde over MnY<sup>98</sup>. Propylene has been oxidised to formaldehyde, CO<sub>2</sub> and minor quantities of acrolein and acetaldehyde over CuY<sup>115</sup>.

#### Catalytic Cracking

Catalytic cracking has been one of the major applications of zeolite catalysts. The first publication showed that NaX was more active than conventional silica alumina catalysts for the cracking of large n-paraffins and that the activity was enhanced by replacing Na<sup>+</sup> by Ca<sup>++</sup> ions<sup>116</sup>. With NaX there were no branched chain products (indicative of a radical type mechanism) whereas CaX gave branched products indicating carboniogenic activity. In general, this type of reaction is of a carbonium ion nature over zeolites, and an extensive review has been given by Rabo and Poutsma<sup>117</sup>.

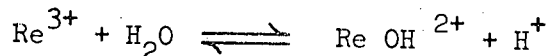
The most successful cracking catalysts have been those employing rare-earth faujasites because they possess high thermal and hydrothermal stability, are not subject to poisoning by metal impurities and display great selectivity. One of the standard test reactions for the characterisation of cracking catalysts is the

cracking of cumene. It is of the Friedel-Crafts type and is rationalised in terms of proton attack at an aromatic carbon atom with displacement of the side-chain as a carbonium ion.

A great deal of work is still being done on cracking catalysts and there is a growing interest in the use of mordenite and erionite zeolites.

## 2.9 Reactivity

The activity of zeolites was initially attributed to the strong electrostatic fields near polyvalent surface cations which polarised the reactant molecules to form carbonium ion type intermediates<sup>118</sup>. However, there were many points which could not be satisfactorily explained by this theory. It was proposed<sup>88,123</sup> therefore that hydroxyl protons were the locus of activity, being introduced through hydrolysis of the cation<sup>88</sup>,



and that the cation influences the geometry and acidity of the protonic sites<sup>123</sup>. The presence of Bronsted acid sites was reported based on acid indicator tests<sup>119</sup> and spectroscopic studies have shown that active catalysts possess acidic hydroxyl groups<sup>85</sup> and that bases poison the catalysts<sup>120</sup>. It is also known that cation zeolites are not Lewis acids and that the activity is enhanced by proton donors<sup>121,122</sup>. For cation zeolites several reactions correlate with Bronsted acidity concentrations<sup>62,79,80,106,108,124</sup> but there are a number of exceptions to this simple picture particularly with transition metal zeolites.

For many reactions of HY it has been shown that Lewis acidity



is not the primary active site<sup>79</sup>, activity being found to decrease as the calcination temperature was increased. The maximum activity of HY does not occur at the maximum Bronsted acid concentration or hydroxyl group content but after some dehydroxylation has taken place<sup>80,125,126</sup>. It is possible that only certain acid site strengths are important and that these are influenced by the cations or Lewis acid sites<sup>62,88,108,124,126</sup> or a dual site mechanism may be involved utilising both Bronsted and Lewis acid sites<sup>124,127</sup>. In general, it appears that in most carbonium ion type catalysis the primary role of zeolite cations is in the generation of hydroxyl groups through hydrolysis and they may further enhance the activity by a cooperative effect, intervening through the lattice or reactant.

In non-carbonium ion type catalysis e.g. radical cracking, hydrogenation and oxidation, the role of the cations appears to be direct, through interaction between reactant and surface cations. The need for this direct contact is illustrated both in the dehydrogenation of cumene<sup>128</sup> and in the trimerisation of acetylene<sup>117</sup>.

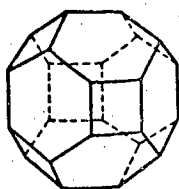


Fig.2.1(a). Truncated octahedron or sodalite unit: vertices represent Si or Al atoms; lines represent oxygens.

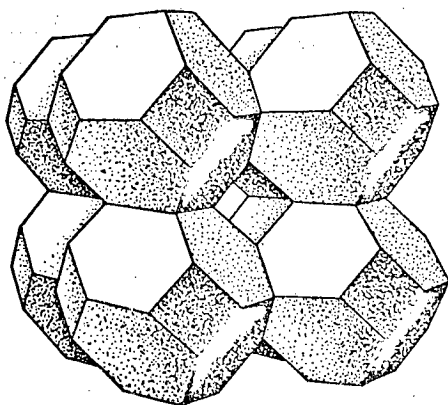


Fig.2.1(b). Line drawing of sodalite structure.

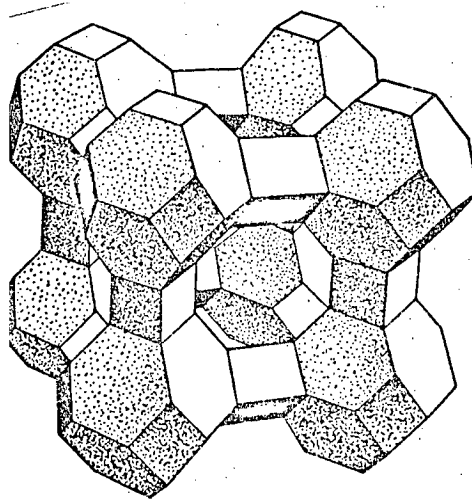
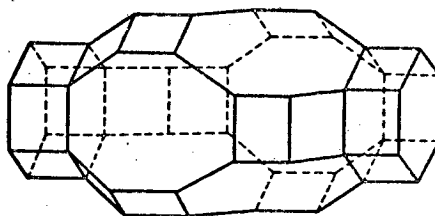


Fig.2.1(c). Line drawing of zeolite type A structure.

(i)



(ii)

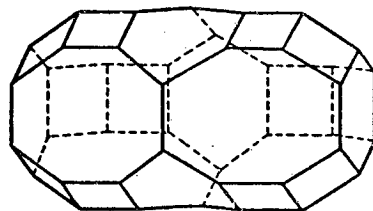


Fig.2.1(d). Line drawings of (i) chabazite and (ii) erionite structures.

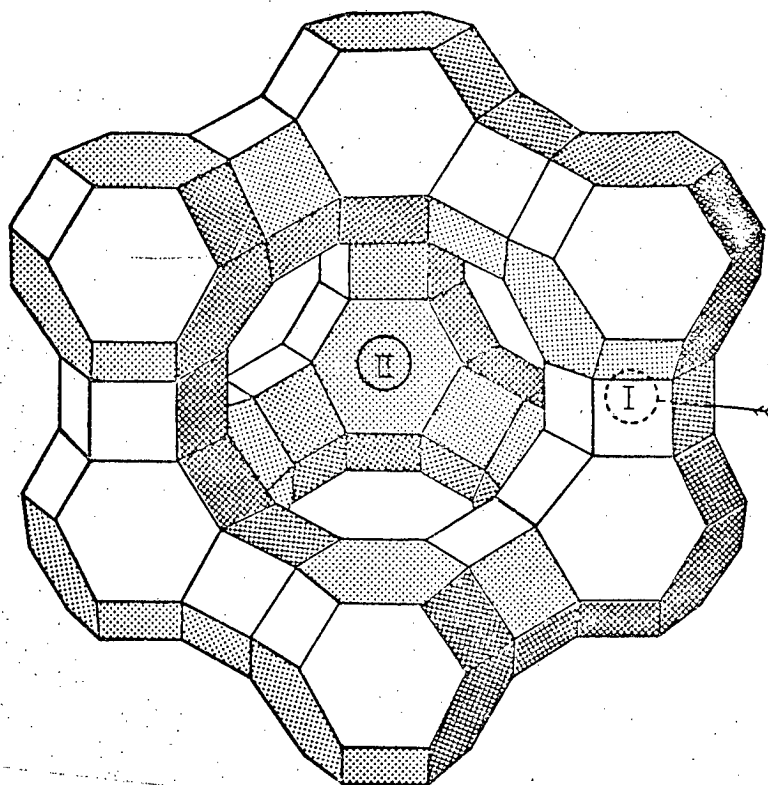


Fig.2.2(a). Line drawing of the faujasite structure  
Type I and II sites are indicated.

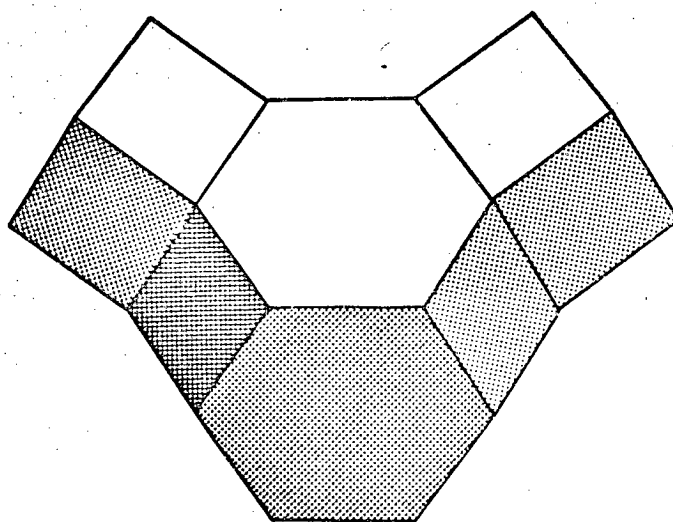


Fig.2.2(b). A perspective view of a sodalite unit  
and two hexagonal prisms.

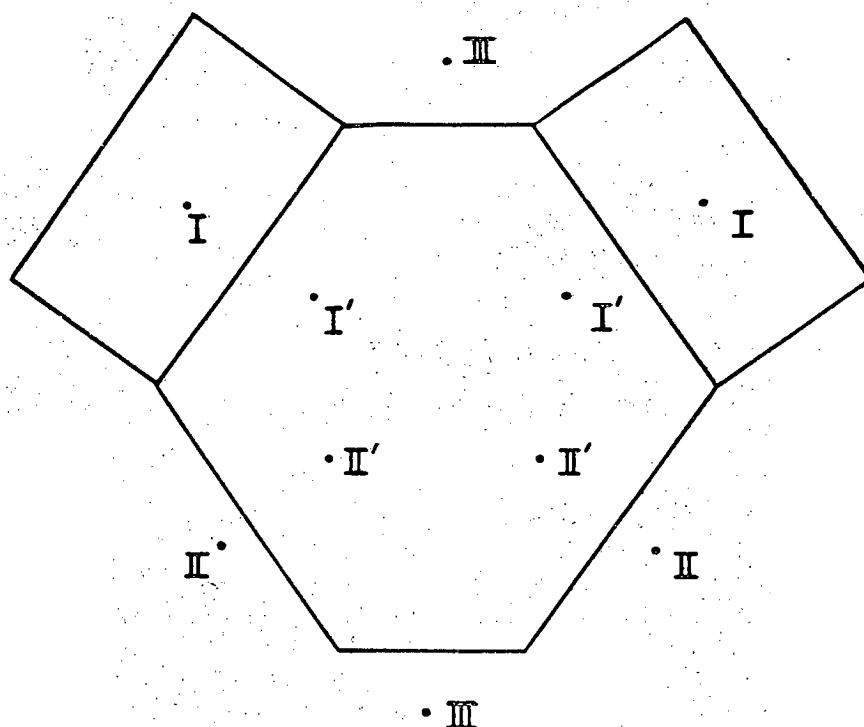


Fig.2.3. A sodalite unit and two hexagonal prisms. The I' sites face the I sites across the six-membered rings joining the hexagonal prisms to the sodalite units. II' sites lie inside the sodalite units close to the six-membered windows to the large supercages.

Site	No. per unit cell	Nature of site
I	16	In hexagonal prisms, co-ordination to six oxygen atoms in approximate octahedron. Not accessible to water.
II	32	In large supercages with one-sided, three-fold co-ordination.
III	48	No structural evidence but see reference (59)
I'	32	In sodalite cages close to type I sites, one-sided, three-fold co-ordination.
II'	32	In sodalite cages close to type II sites, one-sided, three-fold co-ordination.

## CHAPTER III

### Exchange Reactions

#### 3.1 Introduction

The study of exchange reactions provides a means of assessing the activity of catalysts for the making and breaking of chemical bonds, and provides much information about the adsorbed intermediates and the types of reaction which they can undergo.

The exchange between saturated hydrocarbons and  $D_2$  (or the exchange between different isotopic species of saturated hydrocarbon in the absence of added  $D_2$ ) is a pure exchange and results in no overall change in the chemical composition of the reactant gases, except for cracking which may occur at higher temperatures. However, in the exchange of unsaturated hydrocarbons with  $D_2$ , deuteration may also occur and the possibility of isomerisation processes may exist<sup>129</sup>.

The earlier work on exchange reactions employed techniques such as thermal conductivity to measure the dilution of the deuterium by hydrogen, examination of the hydrocarbons by ir spectroscopy and determination of the total deuterium in the hydrocarbon by combustion. However, the deuterium content so measured is only a mean value and it was only after the introduction of the mass-spectrometric technique of following exchange reactions that it was possible to discover what happens to a molecule during one sojourn at the catalyst surface.

The earlier investigations established several important points, namely that (1) the exchange of hydrocarbons with  $D_2$  occurs much more readily than the cracking of hydrocarbons despite the fact that C-H bonds are much stronger than C-C bonds, (2) a dissociative mechanism

is involved and (3) the ease of exchange depends upon the hydrocarbon.

### 3.2 General Aspects of Exchange Reactions

There are a number of features common to all exchange reactions and the methods which are used to interpret experimental data and to classify exchange reactions will be described below.

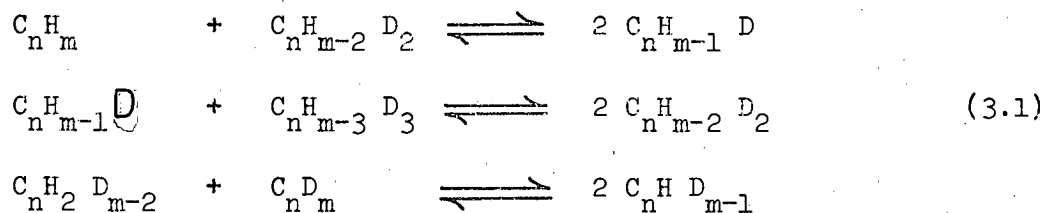
#### A. The Final Equilibrium of an Exchange Reaction

The exchange reaction between a hydrocarbon  $C_n H_m$  and  $D_2$  will result in two kinds of equilibria being established.

(1) There will be an equilibrium distribution between the total amount of deuterium in the hydrocarbon and the total amount of deuterium in the hydrogen.

(2) The relative amounts of the different isotopic species of hydrocarbon will be in equilibrium, as will be the case for the different isotopic species of hydrogen.

The interconversion equilibria for the hydrocarbon may be represented as follows,



The equilibrium constants in equation (3.1) are given by the general expression

$$K_i = \frac{\binom{i}{m}}{\binom{i-1}{m} \binom{i+1}{m}} \quad (3.2)$$

where the symbol  $\binom{i}{m}$  represents the number of ways of selecting  $i$  objects from a group of  $m$  identical objects. The equilibrium constants calculated using equation (3.2) have been found to be in good agreement

with experimental values<sup>130-132</sup>. It is found that the ratio of D/H in the hydrocarbon is greater than that expected from a random distribution of deuterium between the hydrocarbon and hydrogen<sup>133</sup>.

#### B. The Rate Constants of an Exchange Reaction

The rate of an exchange reaction may be determined from the parameter  $\phi$ , defined by

$$\phi = \sum_{i=1}^m i d_i \quad (3.3)$$

where  $d_i$  represents the percentage of the isotopic species containing  $i$  deuterium atoms. If all the hydrogen atoms in the molecule are equally susceptible to exchange and the influence of isotopic composition on the reaction rate is ignored, the course of an exchange reaction will be given by the first-order equation

$$\frac{d\phi}{dt} = k_{\phi} (1 - \phi/\phi_{\infty}) \quad (3.4)$$

where  $k_{\phi}$  is a rate constant equivalent to the number of deuterium atoms entering 100 molecules of the hydrocarbon in unit time at the start of the reaction and  $\phi_{\infty}$  is the equilibrium value of  $\phi$ .

Integration of equation (3.4) gives

$$-\log_{10} (\phi_{\infty} - \phi) = \frac{k_{\phi} t}{2.303 \phi_{\infty}} - \log_{10} (\phi_{\infty} - \phi_0) \quad (3.5)$$

where  $\phi_0$  is the initial value of  $\phi$ .

Failure to obey equation (3.5) may be due to the presence of groups of hydrogen atoms of differing reactivity but may also be caused by poisoning of the catalyst.

A second rate constant  $k_o$  may be determined from the empirical first-order equation

$$-\log_{10} (x_o - x_\infty) = \frac{k_o t}{2.303 (100 - x_\infty)} - \log_{10} (100 - x_\infty) \quad (3.6)$$

where  $k_o$  represents the initial rate of disappearance of the light hydrocarbon  $C_n H_m$  in percentage per unit time,  $x_o$  is the percentage of  $C_n H_m$  present at time  $t$ , and 100 and  $x_\infty$  are the initial and final percentages of this species.

The parameter  $M$ , defined by

$$M = \frac{k_\phi}{k_o} \quad (3.7)$$

represents the mean number of hydrogen atoms replaced in each molecule of the hydrocarbon undergoing exchange in the initial stages of the reaction.

### C. Kinetics

The true kinetics of an exchange reaction can be determined only by means of a series of experiments with different mixtures of the reactants. The course of a reaction with a single mixture follows the apparent first-order equation (3.5).

When a reaction mixture is admitted to a catalyst two things will occur.

- (1) The surface concentrations of the species involved will build up, reach their equilibrium values and then remain constant.
- (2) The exchange reaction will commence and lead to isotopic equilibrium between all species in the system including molecules in the gas phase as well as adsorbed species.

Process (1) will be complete after only a very small fraction



of the molecules present have been adsorbed and desorbed but process (2) cannot be completed until all of the gas phase has been adsorbed and desorbed. Therefore there will be equilibrium concentrations of adsorbed species on the surface for practically the whole of the time required for the exchange reaction. The only factor which reduces the rate of exchange from the initial value is the approach of the isotopic content of the 'hydrogen' and the hydrocarbon to their equilibrium values and this factor leads to the apparent first-order behaviour.

#### D. Classification and Mechanism

Stepwise Exchange Reactions in which only one hydrogen atom of the hydrocarbon is exchanged at each residence of the molecule at the surface. Isotopic species containing two or more deuterium atoms are only formed by successive interactions at the surface. For this class of reaction the following criteria will be obeyed.

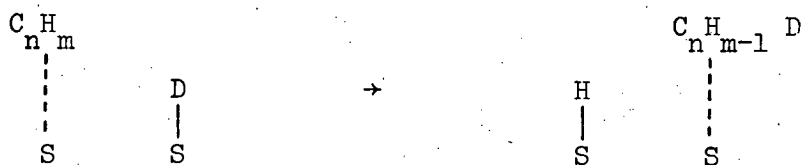
- (1) The value of  $M$  defined by equation (3.7) will be unity.
- (2) The only initial product will be the monodeutero species  $C_n H_{n-m-1} D$ .
- (3) The distribution of the various isotopic hydrocarbons at any time calculated on the basis that equilibrium is established between them will be found to be in agreement with the observed distribution if all the hydrogen atoms in the molecule are equivalent.

The first two criteria are obvious, the third may be proved quite readily<sup>134,135</sup>.

The following possible mechanisms may be considered.

- (a) The hydrocarbon molecule is not chemisorbed except during

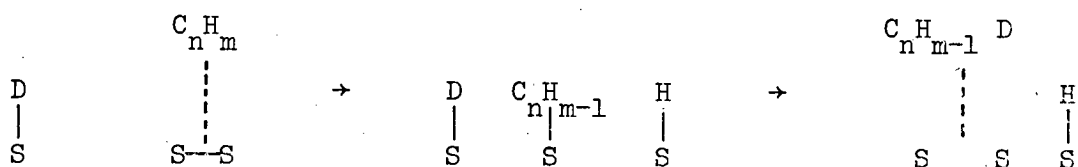
the actual exchange, which takes place with a chemisorbed atom or ion.



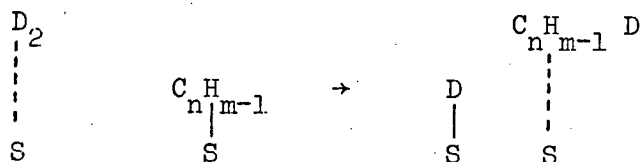
(b) The mechanism may be dissociative and involve adsorbed radicals or ions  $\text{C}_n\text{H}_{m-1}^\cdot$ .

(c) The mechanism may be associative and involve adsorbed species of the type  $\text{C}_n\text{H}_{m+1}$  (ions or radicals).

Mechanism (b) must be followed by saturated hydrocarbons if they exchange and unsaturated molecules will show mechanism (c) but could go either by (b) or (c). However, (b) and (c) may be visualised as proceeding through either a Langmuir-Hinshelwood<sup>12,13</sup> or an Eley-Rideal mechanism<sup>14,15</sup>.



or



In a stepwise exchange process the adsorbed intermediate must be a fairly stable species and have little tendency to undergo further reaction otherwise this would lead to the formation of initial

products containing more than one deuterium atom per molecule.

Multiple Exchange Reactions in which more than one hydrogen atom is exchanged on each interaction of the molecule with the catalyst surface. The following characteristics are shown.

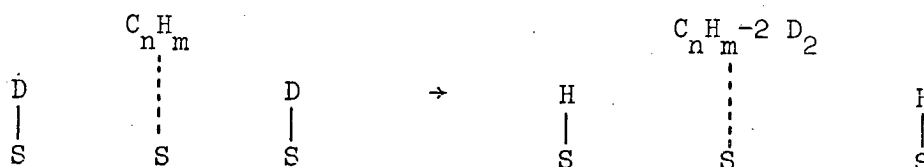
- (1) The value of M is greater than unity and will give the average number of deuterium atoms introduced to each molecule at the beginning of the reaction.
- (2) The initial products will contain species having more than one deuterium atom and the initial product distribution may indicate the type of process occurring.
- (3) The observed distribution will be richer in the more highly deuterated species than one based on a binomial distribution.

Multiple and stepwise exchange processes must lead to the same equilibrium distribution of isotopic species.

In the study of multiple exchange reactions it is desirable to employ a high ratio of  $D_2$  to hydrocarbon in order to minimise the effect of isotopic dilution of the deuterium on the rate of production of the more highly deuterated species during the early stages of reaction. The reaction should be studied at low conversions to exclude the possibility of molecules having had more than one residence at the surface.

Four possible mechanisms may be considered.

- (a) No chemisorption of the hydrocarbon except during the actual exchange



- (b) The formation of a single type of dissociated species involving the loss of at least two hydrogen atoms from the original molecule.
- (c) The formation of a single type of associated species having at least two hydrogen atoms more than the original molecule.
- (d) The existence of two or more types of adsorbed species of different states of hydrogenation with multiple exchange resulting from the interconversion of these species on the surface of the catalyst.

Mechanism (d) is the most probable.

On metals, radical intermediates are known to be involved<sup>133,136,137</sup> but on oxides and other non-metallic catalysts ionic species or at least polarised intermediates are important for exchange and other reactions<sup>138-140</sup>.

## CHAPTER IV

### The Isomerisation of 3,3-Dimethylbut-1-ene

The isomerisation of 3,3-dimethylbut-1-ene (I) is a useful test reaction for investigating the acidic properties of catalyst surfaces. While double-bond migration in olefins may arise from base<sup>141</sup> as well as acid catalysis<sup>142</sup>, the skeletal isomerisation of I depends upon the ability of a catalyst surface to form carbonium ions from the olefin.

#### 4.1 Reaction Scheme

The experimental evidence for the reaction scheme was obtained by Haag and Pines<sup>143</sup> from a kinetic analysis of the isomerisation of I over alumina. A complex mixture of olefins containing up to eleven hexene isomers was obtained<sup>144</sup>. In the isomerisation of I, a series of consecutive reactions involving 1,2 methyl shifts is taking place. 2,3-Dimethylbut-2-enes (II) and 2-methylpentenes (III) are the first and second intermediates respectively, with II being the only primary product of isomerisation. 2-Methylpentenes (III) and 3-methylpentenes (IV) are not formed in parallel reactions but at low conversion II is exclusively converted to III. n-Hexenes (IV) are believed to be formed from III on mechanistic grounds.

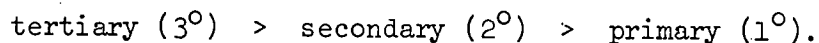
Fig. 4.1 shows the reaction scheme in which, for simplicity, only one of the possible isomers is shown for each skeletal structure, while double-bond isomers are formed in their relative equilibrium concentrations.

#### 4.2 Mechanism

The proposed mechanism is shown in fig. 4.2. The relative

ease of skeletal rearrangement of olefins depends not only on the rates of interconversion of isomeric carbonium ions but also on the rates of formation of the carbonium ions and to some extent on the stabilities of the corresponding olefins.

Although the magnitude of the energy barriers involved in the interconversion of isomeric carbonium ions are not known but depend strongly on the nature of anions present, the relative rates of carbonium ion rearrangements can be estimated from the relative stabilities of the carbonium ions involved, which is



Hence, in the proposed mechanism, step IIb (which involves conversion of a 3° ion to a 1° ion) should proceed more slowly than step IIa (involving conversion of a 2° to a 3° ion). In a similar manner, the conversion of 2-methyl-pentene to n-hexenes should also proceed slowly.

Haag and Pines<sup>143</sup> put forward several points which support the idea that a carbonium ion mechanism is involved. The 2-methyl-pentenes were nearly equilibrated before any noticeable amounts of 3-methylpentene were formed in agreement with the view that hydrogen migration (to produce double bond isomers) is faster than migration of alkyl groups in reactions involving carbonium ion species. Small amounts of 2-methylbut-2-ene, isobutane and isobutene were formed which is indicative of an acid catalysed dimerisation of the hexenes and similar olefins followed by cracking<sup>145-147</sup>. Compound II was formed faster than III as would be expected from such a mechanism.

The isomerisation of I will therefore give information about the acidity of the surface but the depth of isomerisation should

reflect the strength of the acid sites. Rearrangements proceeding formally through  $1^\circ$  ions should require relatively strong acid sites (or high temperatures) whereas those involving  $2^\circ$  or  $3^\circ$  ions should take place on both strong and weak acid sites.

#### 4.3 Purpose of the Present Work

Kemball, Leach, Skundric and Taylor<sup>148</sup> examined the exchange of I with  $D_2$  and  $D_2O$  on a number of oxide catalysts and they also followed the isomerisation of the molecule to form 2,3-dimethylbut-1-ene (II) and 2,3-dimethylbut-2-ene (III) under equivalent conditions to those used for the exchange experiments. Very extensive incorporation of deuterium into the  $C_6$  olefins formed by the isomerisation of I was observed on catalysts capable of forming carbonium ions from the olefin when  $D_2O$  was used as the source of labelling isotope. In contrast, on catalysts which were not active for isomerisation of the olefin by a carbonium ion mechanism, only three hydrogen atoms could be readily replaced, in a stepwise manner, in I. Stepwise exchange was also observed when  $D_2$  gas was employed as the source of labelling isotope.

The present study is concerned with a more detailed examination of the exchange and isomerisation reactions of these  $C_6$  olefins over a series of copper, nickel and zinc-exchanged 13X type zeolites. Kinetic measurements of the isomerisation of both I and II were made, and the effect of the presence of hydrogen or water upon such rates examined. The nature of the exchange reactions of the various olefins was investigated using both  $D_2$  and  $D_2O$ . Hence by studying the reactions of the dimethylbutenes it was hoped to obtain more information about the nature of the active sites on these zeolite catalysts.

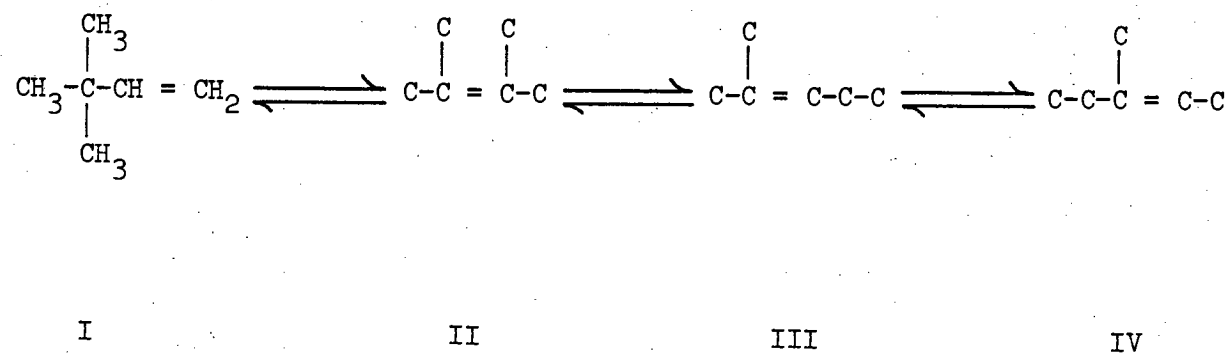


Figure 4.1 - Consecutive Reaction Scheme for Isomerisation of I.



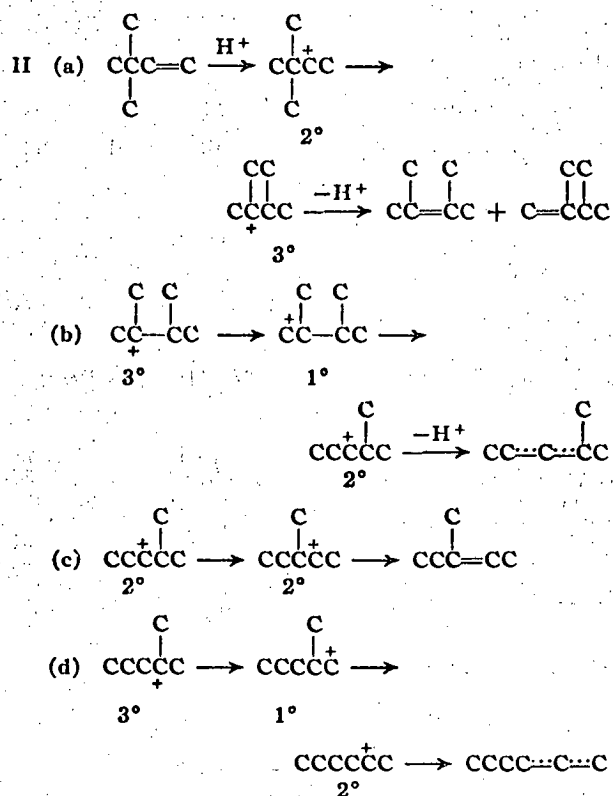


Fig.4.2- Mechanism for Isomerisation of Dimethylbutenes.

## Part II

### Experimental and Treatment of Results

## CHAPTER V

### Experimental

#### 5.1 Apparatus

The work was carried out on two gas-handling systems which will be designated Gas Line A and B. Gas Line A was used for mass spectrometric studies and will be described in detail whereas B, which was of similar design, was employed in GLC studies and therefore only the important features will be discussed. Gas Line A consisted of essentially three parts;

- (1) a high vacuum gas-handling system which enabled mixtures of pure gases and liquid vapours of definite composition to be prepared
- (2) a reaction vessel coupled to a fine capillary leak and
- (3) a mass spectrometer which enabled the composition of the gas mixture in the reaction vessel to be analysed continuously.

#### 5.2 The Gas-Handling System

The design of the gas-handling system together with reaction vessel is shown diagrammatically in fig. 5.1. The apparatus was constructed throughout of 'Pyrex' glass and all ground glass taps and joints were lubricated with 'Apiezon L' vacuum grease. There were two pumping systems each consisting of a mercury diffusion pump (Admiralty type) and cold trap ( $T_2$ ) backed by a two stage 'Speedivac' rotary pump enabling a vacuum of  $133 \mu \text{Nm}^{-2}$  to be obtained. The vacuum was checked using a McLeod gauge (N) of volume  $2.85 \times 10^{-4} \text{ m}^3$ . One pumping system was used exclusively

for evacuating the reaction vessel and the other for pumping the remainder of the apparatus.

Gases could be stored in the gas bulbs (G) and liquids or condensable vapours in sample tubes attached at 'S'.

Two diaphragm vacuum gauges were used for measuring pressures in the coarse vacuum range, with the scale calibrated in Torr ( $\equiv 133 \text{ Nm}^{-2}$ ), one connected between taps 6 and 10 and the second to the mixing volume 'M'.

Two palladium thimbles ( $P_1$  and  $P_2$ ) were used for purifying  $\text{H}_2$  and  $\text{D}_2$ .

### 5.3 Reaction Vessel and Capillary Leak

Cylindrical reaction vessels, 35 mm in diameter and 130 mm in length, and constructed from 'Pyrex' glass were connected to the apparatus by a B24 ground glass joint which fitted into a water cooled socket. The reaction vessel was heated by a close fitting furnace, the temperature of which was kept constant using a Eurotherm temperature controller which was accurate to  $\pm 0.5 \text{ K}$ . The actual temperature was measured by a chromel ( $T_1$ ) - alumel ( $T_2$ ) thermocouple, using ice/water for the cold junction, and the thermocouple voltages were measured by an EXEL digital voltmeter (type XL1000).

The leakage of the reaction mixture into the mass spectrometer was controlled by a fine capillary 0.12 m in length, which gave a leak rate of about  $2.67 \text{ kNm}^{-2}$  of air into a volume of  $2 \times 10^{-5} \text{ m}^3$  in 20 minutes with a pressure differential of one atmosphere. The capillary, similar to that used by Nier<sup>149</sup>, allowed about 3% of the gas in the reaction vessel to flow into the mass spectrometer per hour, giving ample gas for

analysis without affecting appreciably the amount of gas in the reaction vessel.

The properties of capillary leaks and the importance of leak design have been discussed by various authors<sup>130,150,151</sup>.

Gas flow through a capillary leak can occur by either of two processes;

- (a) viscous flow
- (b) molecular flow.

If viscous flow predominates the gas leaking into the mass spectrometer will have the same composition as that in the reaction vessel whereas if molecular flow is occurring there will be discrimination against the higher mass elements in the gas mixture. The long capillary tubing prevents back diffusion and hence fractionation of the mixture.

In exchange reactions of hydrocarbons the relative difference in mass among the various isotopic species is so small that molecular flow can be ignored. In  $H_2/D_2$  exchange reactions however, the relative mass difference is large and any molecular flow into the mass spectrometer will make the mixture richer in  $H_2$  and this must be taken into account when analysing the results.

#### 5.4 Volume Calibrations

Calibration of the volumes of the various sections of the apparatus was performed by expanding hydrogen from a measured standard bulb, and the following values were obtained ( $\times 10^{-6} m^3$ )

Dosing volume	121
Mixing volume	627
Ice trap	83
Reaction Vessel	185

## 5.5 The MS.10 Mass Spectrometer

An A.E.I. MS.10 mass spectrometer was used in the present study. It was a general purpose,  $180^\circ$  sector instrument and is shown schematically in fig. 5.2.

### Principle

The gas is introduced to the analyser tube where the constituent molecules are ionised within the 'ion source cage' C by subjecting them to bombardment by a controlled beam of electrons originating from a hot-wire rhenium filament F. The ions are then accelerated by the 'accelerating voltage' applied to the cage and describe circular orbits due to the influence of the variable magnetic field. The radius  $R$  of the orbit varies for each particular type of ion and is determined by the mass  $m$ , charge  $e$ , accelerating voltage  $V$  and the applied magnetic field  $H$ . The total ion beam is thus separated by the action of the magnetic field into individual beams containing ions corresponding to one particular mass. From equation 5.1 it follows that individual ion beams can be brought in turn to focus on the collector 'I', where the ions give up their charge, by passing through the slits  $S_1$ ,  $S_2$  and  $S_3$  which are called the resolving, defining and collector slits respectively.

$$m/e = R^2 H^2 / 2V \quad 5.1$$

The ion current was preamplified using an electrometer head type ME 1403 with an input resistance of  $10^{11}$  ohm and a time constant of 1s. Spectra were displayed on a Honeywell potentiometric recorder (no. 5401) using a 10 mV range plug.

The resolution and sensitivity of the instrument were governed primarily by the size of the slits  $S_1$  and  $S_3$ , and by choosing appropriate values (1.02, 3.56 and 0.013 mm for  $S_1$ ,  $S_2$  and  $S_3$  respectively) the resolution approached 300.

An electromagnet whose field strength could be varied up to 9 kG was employed, enabling a mass range of up to 400 to be covered. In the present work an accelerating voltage of 500 V was used which enabled a mass range of 0-200 to be scanned. For  $H_2/D_2$  exchange reactions a permanent magnet (1830 gauss) was used and the accelerating voltage was varied.

#### Apparatus

The pumping system in the MS.10 consisted of a cold trap (filled with liquid nitrogen) which separated the tube unit from the diffusion and backing pumps. The diffusion pump was a 'Metrovac' type 0330 operated with Apiezon B.W. oil and backed by a 'Metrovac' type GDR1 two stage rotary pump equipped with a  $P_2O_5$  trap and discharge tube.

The pressure inside the ionisation chamber was measured by an insertion ionisation gauge at 'A', type Metrovac VC3A. Various protection circuits were employed against vacuum failure.

#### 5.6 Chromatographic Analyses

Chromatographic analyses were carried out on Gas Line B, which was of similar design to Gas Line A, and has been described in detail by Brookes<sup>152</sup>. A linear scale McLeod gauge was incorporated for use in poisoning studies, allowing small doses of material to be measured accurately.

A Perkin-Elmer F.11 gas chromatograph was employed for the analyses. The reaction vessel could be connected through a 3-way

tap to a Perkin-Elmer F.11 sampling valve and the sampling volume was such that 2-3% of the gas phase reaction mixture was removed each time a sample was taken. Samples were introduced in this way to the chromatographic column with nitrogen as the carrier gas. The resolved components were eluted to a hydrogen/air flame ionisation detector and the resulting signals were displayed on a Servoscribe potentiometric recorder (Smith's Industries Ltd.), parallel signals were fed to a Kent 'Chromalog 3' Digital Integrator allowing integrated peak areas to be assigned to the components of the mixture as recorded.

Two chromatographic columns were employed,

(a) 1.5 m column of propylene carbonate (35% w.w.) on Chromosorb P operated at 293 K with inlet pressures for air, hydrogen and nitrogen of 172, 138 and 83 kNm<sup>-2</sup> respectively.

(b) 4 m column of hexan-2,5-dione (25% w.w.) on Chromosorb P operated at 273 K with a carrier gas pressure of 83 kNm<sup>-2</sup>.

Column (b) was used only to separate 3,3-dimethylbut-1-ene and 2,2-dimethylbutane and for all other work column (a) was utilised.

A typical analysis, showing the resolution achieved for the dimethylbutenes is given in fig. 5.3. The relative sensitivity of the chromatographic arrangement for the various hydrocarbons was determined by preparing and analysing mixtures of known composition.

## 5.7 Materials

### A. Catalysts

#### Preparation of Ion-Exchanged Zeolites

The starting material in all cases was Linde Na 13X Molecular Sieve obtained from B.D.H. Ltd., in powder form, free of



clay binder. The bulk sample had a silicon to aluminium ratio of  $1.27 \pm 0.02$ <sup>153</sup>.

Zeolites containing (a) cobalt and calcium were prepared by McCosh<sup>153</sup>, (b) zinc and nickel prepared by Cross<sup>154</sup> and (c) copper and nickel prepared by Coutts<sup>155</sup> by a process of single exchange whereby the sodium zeolite was contacted with the desired salt solution overnight. Details of the preparation and analyses of the zeolites have been described<sup>153-155</sup>.

A series of CuX zeolites were prepared by a method developed by Rudham and Sanders<sup>156</sup> in which the pH of the slurry of molecular sieve in water was reduced to about 6 by the addition of aliquots (0.5 ml) of 1 M HCl before adding the desired amount of  $\text{CuSO}_4 \cdot 5\text{H}_2\text{O}$  dissolved in 250 ml of deionised water. The mixture was stirred for 16 h at room temperature, filtered, washed with deionised water, oven dried at 393 K and finally stored over saturated calcium nitrate solution in a desiccator.

#### Analysis

The percentage exchange was obtained from measurements of (a) the sodium content of the ion-exchanged forms using flame photometric methods<sup>157</sup> and (b) the copper content using atomic absorption spectroscopy. In the subsequent text, the samples will be referred to as CuX(n) where n represents the percentage of the original  $\text{Na}^+$  replaced by  $\text{Cu}^{2+}$ .

#### Chemicals

Deuterium (99.5%) was obtained from the Matheson Co. and was purified by diffusion through a palladium thimble followed by two liquid nitrogen traps in series.

Hydrogen was obtained from the British Oxygen Co. and was purified

as for deuterium.

Carbon Monoxide (Matheson Co.) was passed through liquid nitrogen traps before use.

Oxygen and Nitrogen (B.O.C.) were passed through liquid nitrogen traps before use. For surface area determinations, nitrogen was dried by passage through  $P_2O_5$  and dehydrated molecular sieve (5A) prior to storage.

For GLC use hydrogen, nitrogen and air were used without further treatment.

m-xylene (99.9%) was obtained from the Chemical Standards Division of the N.P.L. and was used without further purification.

Mesitylene (SLR) was obtained from Fisons.

Dimethylbutenes were obtained from Fluka Ltd., and Dimethylbutanes from Koch Light Lab. Ltd., and were all degassed by repeated cycles of freeze-pump-thaw.

Deuterium Oxide (99.7%) was obtained in 25 g containers from I.C.I. Ltd. and degassed before use.

#### 5.8 Procedure

Fresh 0.1 g samples of hydrated catalyst were used for each experiment and the standard activation treatment involved outgassing at 673 K for 12 h at a pressure of  $2 \times 10^{-4}$  Nm<sup>-2</sup>, the temperature being raised to this value over the first 2 h period. The reaction vessel was then isolated from the pumps and cooled under vacuum. A charge of between 3 and  $9 \times 10^{19}$  molecules of olefin, equivalent to 1.0 to 3.0 molecules per supercage, was used for experiments at or above 403 K. For work at lower temperatures more reactant was needed to give a sufficient pressure in the gas

phase for analysis; at 273 K a pressure of olefin equivalent to 5.0 molecules per supercage was used. Deuterium and deuterium oxide when used, were in six-fold excess relative to the olefin. For hydrogen-deuterium exchange reactions, equal pressures of  $H_2$  and  $D_2$  were used and the total charge was  $3 \times 10^{20}$  molecules.

The reactions were followed by either (a) sampling the gas phase and analysing by GLC or (b) scanning the mass spectrum at regular intervals.

### 5.9 Other Techniques

X-Ray Diffraction traces were measured on a Philips instrument utilising  $CuK\alpha$  radiation.

Surface Area measurements were performed on an adsorption balance<sup>154</sup> using nitrogen as the adsorbate.

Epr spectra were recorded using a Decca X-1 spectrometer operating at 9270 MHz with a field modulation of 100 kHz.

A combined gas chromatograph-mass spectrometer technique in which the olefins were directly analysed by a fast-scanning mass spectrometer after gas chromatographic separation<sup>158</sup>. Separation of the olefins was provided by a Perkin-Elmer F.11 gas chromatograph fitted with a 1.5 m column of propylene carbonate (35%) on 60/80 mesh Chromosorb P operated at 289 K with a helium carrier gas inlet pressure of  $83 \text{ kNm}^{-2}$ . The effluent from the column was fed into an AEI MS.20 "Rapid" mass spectrometer, a single-focusing  $\pi$ -radian deflexion instrument used with magnetic scanning. An acceleration potential of 250 V and ionising electrons at 20 eV were employed. During the experiment the mass spectrometer scanning rate was 1s per decade of mass. As the spectrometer scanned from preset mass limits of 100 to 10, the



signals generated by the spectrometer were fed to an analogue-to-digital convertor (ADC) of an 'on-line' computer (PDP 11 Digital Equipment Corp., Maynard, Massachusetts, U.S.A.). Subsequent processing<sup>159</sup> of the data enabled isotopic product distributions to be obtained for each reactant olefin.

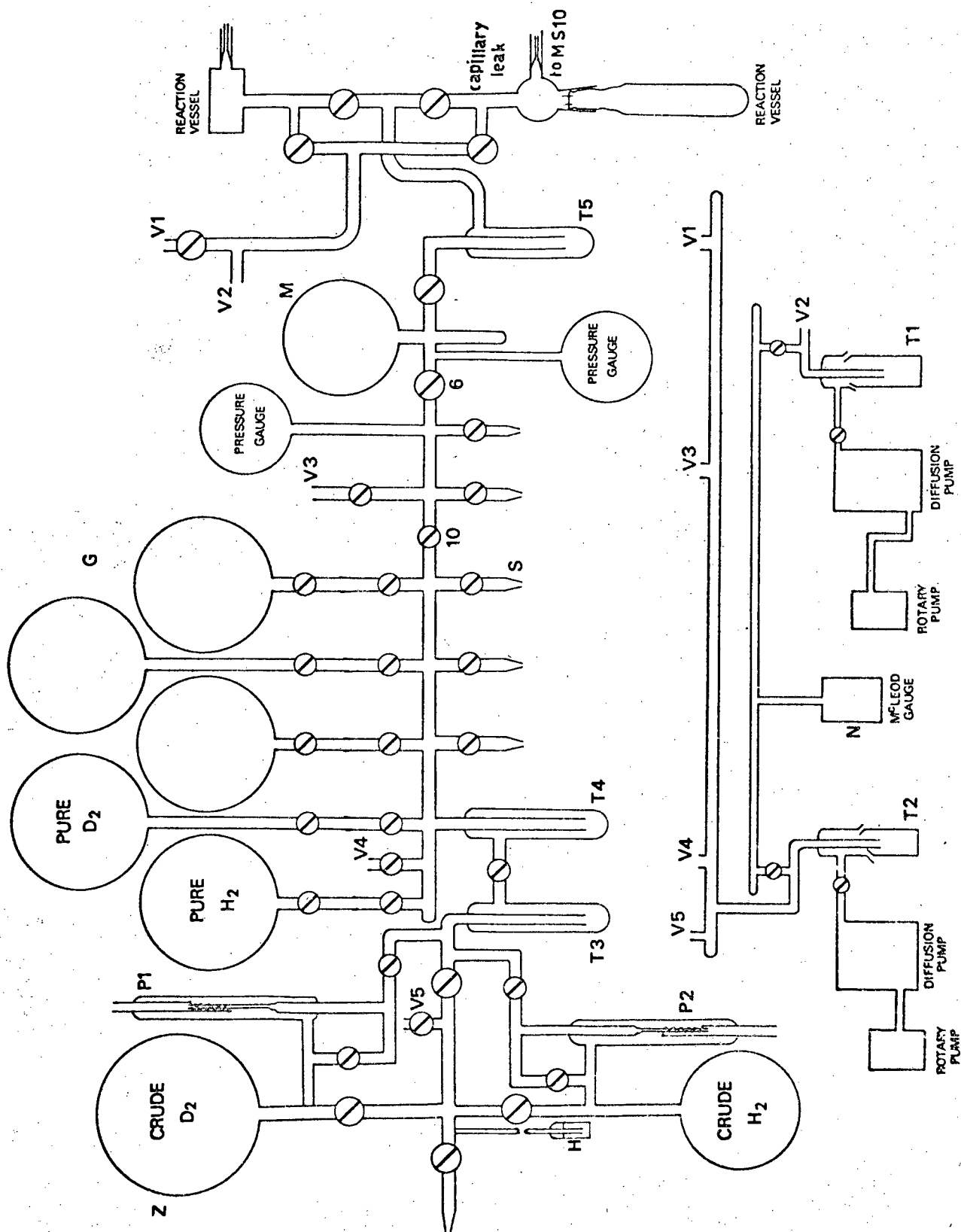


Fig.5.1 APPARATUS.

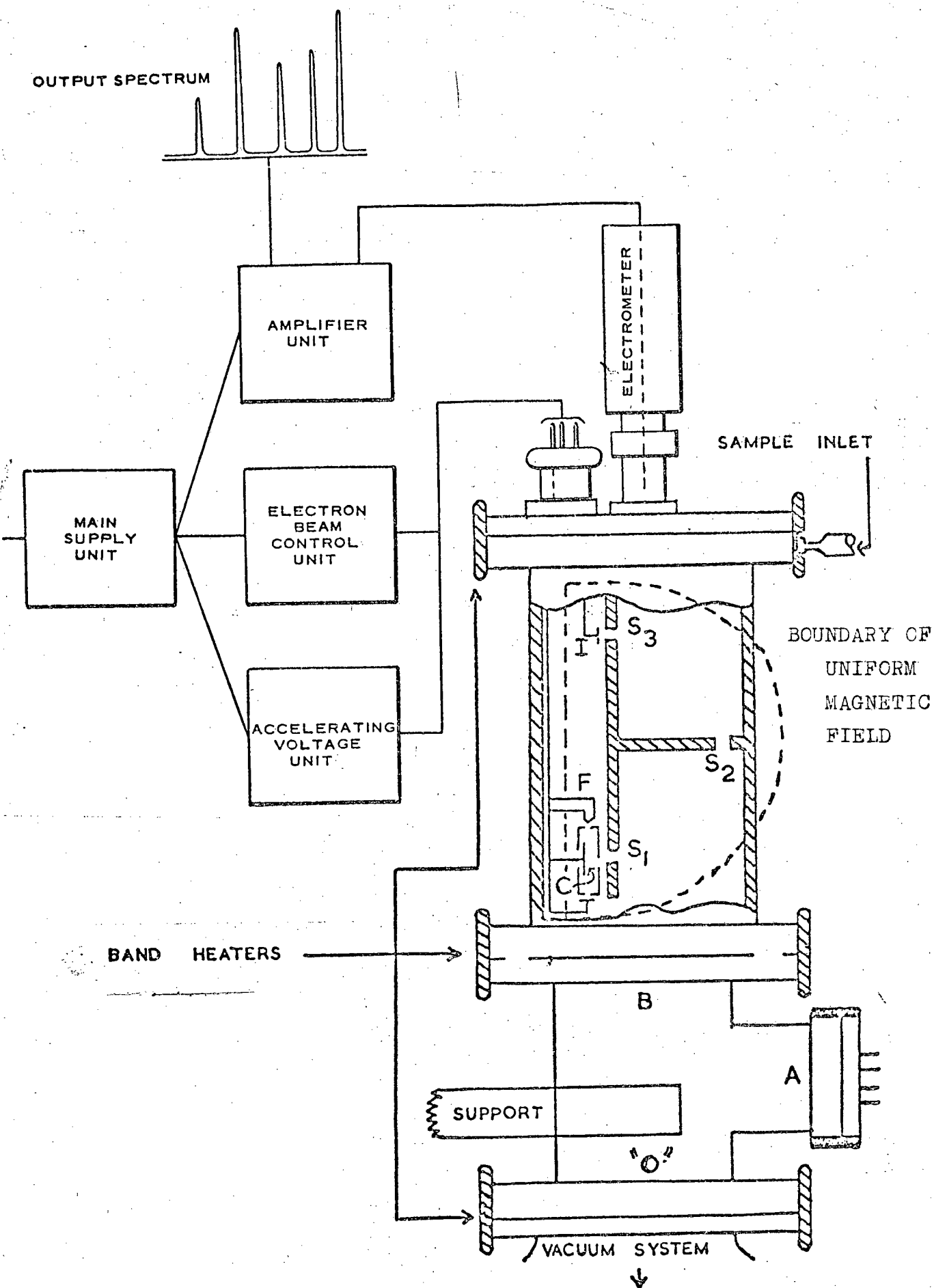


Fig.5.2 SCHEMATIC ARRANGEMENT OF MS10 MASS SPECTROMETER.

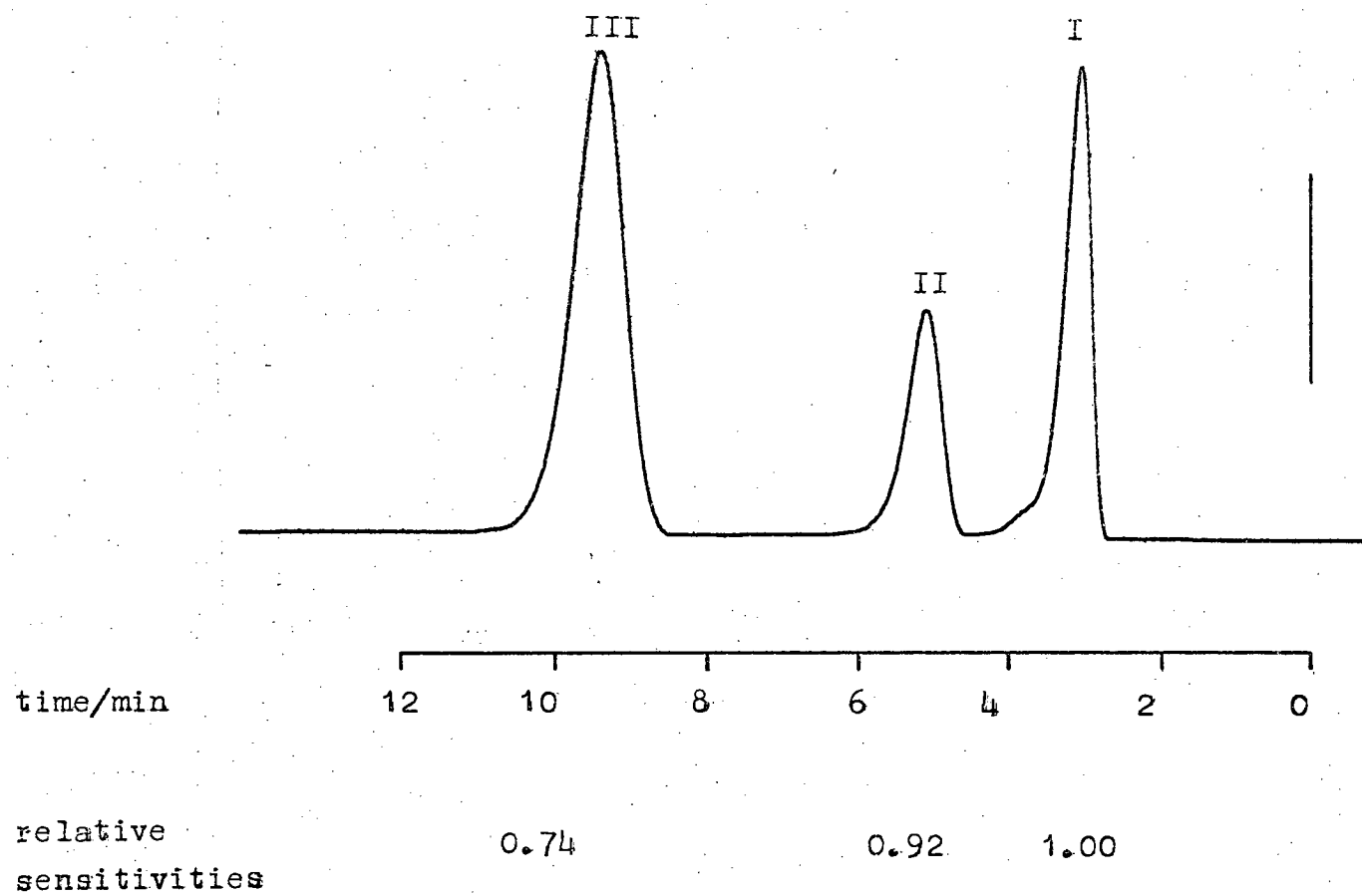


Fig. 5.3- Chromatographic analysis of dimethylbutenes  
using a 1.5m column of 35% w/w propylene  
carbonate on Chromosorb P.

## CHAPTER VI

### Treatment of Results

#### Mass Spectrometric Data

##### 6.1 Introduction

Certain conditions must be satisfied for the accurate quantitative analysis of components in a mixture<sup>160</sup>;

- (1) the mass spectrum of any component must be unaffected by the presence of another component and that when spectral peaks superimpose at any mass number the intensities due to the various components must be linearly additive
- (2) the cracking patterns and sensitivities of the various components must not change with time
- (3) the ion beam intensity for any component must be proportional to the partial pressure of that component in the reaction vessel.

##### 6.2 Preliminary Procedure

Reactions were studied by following the changes in the relative peak height of the parent molecule and those at higher masses.

The first process carried out when analysing mass spectrometric results was to plot the peak heights of the various isotopic species against time so that by drawing smooth curves through these points an accurate assessment of how the peak heights were changing could be obtained. Since in any scan of the mass spectrum each peak was recorded at a slightly different time, then graphs like those above had to be used in order to obtain a measure of the relative amounts of each particular mass at any one particular time; this became



more important as the rate of reaction increased. A number of points at suitable time intervals were then selected and subjected to further treatment as described below.

### 6.3 Background Corrections

Two sources were responsible for background in the mass spectrometer;

- (a) background spectra produced by ionisation of air, water and carbon monoxide which are always present in the ion chamber and
- (b) from hydrocarbon species left over from previous experiments which had adsorbed on the walls of the mass spectrometer and inlet tube. As leakage into the mass spectrometer took place, some of the molecules from the reaction mixture could displace those adsorbed previously. If background spectra were too large the mass spectrometer was baked before use. In the present work, due to the mass ranges examined, background corrections were found to be negligible.

### 6.4 Isotope Corrections

Many of the elements as they occur in nature contain small amounts of heavy isotopes. Carbon and hydrogen are found in two main isotopic forms  $^{12}\text{C}$  and  $^{13}\text{C}$ , and  $^1\text{H}$  and  $^2\text{H}(\text{D})$  respectively. In the mass spectrum of a hydrocarbon there will be peaks at mass numbers higher than that of the parent molecule due to the presence of heavy isotopes and this must be taken into account when calculating how much exchange has taken place.

The ratios  $100 \frac{^{13}\text{C}}{^{12}\text{C}}$  and  $100 \text{ D/H}$  are found to be constant throughout the range of naturally occurring hydrocarbons with values of 1.108 and 0.016 respectively (i.e. for a molecule with one carbon atom, the probability of it being  $^{13}\text{C}$  is 0.01108 or  $^{12}\text{C}$  is 0.98892).

For a hydrocarbon  $C_nH_m$  of mass  $M$ , the peak heights at masses  $M+1$ ,  $M+2$  etc., can be calculated relative to the peak  $P_M$  at mass  $M$  from statistical considerations, and the following relationships are found,

$$100 \frac{P_{M+1}}{P_M} = n(1.108) + m(0.016)$$

and

$$100 \frac{P_{M+2}}{P_M} = \frac{n(n-1)}{2!} (1.108)^2 + \frac{m(m-1)}{2!} (0.016)^2$$

The isotopic contribution due to  $^{13}C$  is not affected by the exchange process but replacing H by D will diminish the contribution due to naturally occurring D. So for any isotopic species  $C_nH_{m-x}D_x$  the above values of  $P_{M+1}/P_M$  and  $P_{M+2}/P_M$  are found by substituting  $(m-x)$  for  $m$  in these equations.

Isotope corrections were carried out in a systematic manner working from low to high mass. The isotopic contributions from the peak at the lowest mass in the spectrum were subtracted from the peaks at one and two mass units higher and the corrected peak heights at every mass were used to calculate the contribution to higher masses. Corrections to peaks more than two mass units higher were usually very small and could be neglected.

## 6.5 Fragmentation Corrections

When a hydrocarbon molecule is bombarded by the ionising electrons it may lose an electron to form the molecular or parent ion, lose one or more hydrogen atoms so that the mass spectrum of a hydrocarbon of mass  $M$  will show peaks at  $M-1$ ,  $M-2$  etc. due to these fragmentation processes or form other fragments through the dissociation of C-C bonds. It is therefore necessary when determining

the isotopic content of partially exchanged hydrocarbon molecules to take into account the contribution of one isotope to those at lower mass numbers caused by the fragmentation process.

The choice of electron energy is important because it is desirable to have the parent peak as large as possible with respect to the fragment ions. However, because ionisation efficiency (sensitivity) decreases with the electron voltage a compromise has to be reached between sensitivity and fragmentation and so electron energies of between 10 and 20 eV were employed to make the corrections as small as possible.

Only fragment ions formed by the loss of hydrogen will be considered here. Fragmentation factors  $f_i$  (the chance of losing  $i$  hydrogen atoms) were determined from the amount and pattern of fragmentation of the light hydrocarbon and were measured before each experiment.  $f_i$  is defined by

$$f_i = \frac{C_n H_{m-i}}{C_n H_m}$$

where  $C_n H_m$  and  $C_n H_{m-1}$  represent the heights of the parent and fragment peak respectively after correction for naturally occurring isotopes.

There are three methods which may be used to calculate fragmentation patterns for the deuterio-isomers.

(a) The fragmentation patterns are calculated on a statistical basis assuming that H and D are lost equally readily. This method is illustrated in Tables 6.1 and 6.2 for dimethylbutenes and *m*-xylene.

(b) For many hydrocarbons it is found that H is lost more readily than D, and this method involves determination of a fragmentation

factor  $f_i'$  (for loss of  $i$  deuterium atoms) for the perdeutero compound if possible. The two sets of factors  $f_i$  and  $f_i'$  can then be used in a statistical scheme such as that devised by Gault and Kemball<sup>161</sup>.

(c) A further improvement can be achieved by allowing for the dependence of fragmentation of a C-H or C-D bond on the nature of the other bonds in the molecule<sup>162-165</sup>. An empirical method of calculating fragmentation factors has been devised which incorporates statistical factors, the preferential rupture of C-H compared with C-D bonds and the influence of other bonds<sup>166</sup>.

Allowing for the loss of different kinds of hydrogen in a molecule is difficult and is usually ignored. In the present work fragmentation patterns were calculated according to method (a) and proved to be satisfactory. Fragmentation corrections were carried out in a similar way to isotope corrections only this time working from high to low mass. The contribution of the heavier compound to the lighter one being the product of the fragmentation factor and the peak height.

## 6.6 Arrhenius Plots

After the above corrections had been made the resultant peak heights were used to calculate the isotopic distributions of the hydrocarbon. Isotopic distributions were calculated at a number of reaction times at a given temperature and then plots of  $\log(\phi_\infty - \phi)$  and  $\log(d_0 - d_\infty)$  versus time were drawn according to equations 3.5 and 3.6, from which  $k_\phi$ ,  $k_O$  and  $M$  were obtained.

From the Arrhenius equation,

$$k = Ae^{-E/RT}$$

$$\log k = \log A - E/2.303 RT \text{ where}$$

$k$  = rate constant / molecule  $s^{-1} \text{ dg}^{-1}$

$A$  = frequency factor / molecule  $s^{-1} \text{ dg}^{-1}$

$E$  = apparent activation energy /  $\text{kJ mole}^{-1}$

$R$  = gas constant /  $\text{joule mole}^{-1} \text{ K}^{-1}$

$T$  = absolute temperature / K

Values of  $E$  and  $\log A$  were obtained from a plot of  $\log k$  against  $K/T$ .

### 6.7 $\text{H}_2/\text{D}_2$ Exchange

In these studies an ionising beam of 25 eV was employed since this gave good sensitivity without the complication of fragmentation. The absence of fragmentation was seen from the mass spectrum of pure deuterium which only gave a peak at mass 3 corresponding to about 5% HD impurity. The purity of the reactants was checked regularly for impurities such as  $\text{N}_2$ , CO and  $\text{O}_2$ .

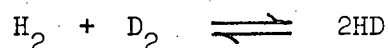
The mass spectrometer had different sensitivities towards  $\text{H}_2$ , HD and  $\text{D}_2$  and although the absolute values changed from time to time the relative sensitivities remained essentially constant. Calibration curves of the type shown in fig. 6.1(b) were obtained after each run, allowing the experimental peak heights to be converted into pressures. It can be seen that  $\text{D}_2$  is more sensitive than  $\text{H}_2$  at all pressures. The pressure of HD was found by assuming the sensitivity to be intermediate between those of  $\text{H}_2$  and  $\text{D}_2$ . It could also be found from the relationship

$$K = \frac{(hxb)^2}{P_{\text{D}_2} \cdot P_{\text{H}_2}}$$

where  $K$  is the theoretical equilibrium constant of Urey and Rittenberg<sup>167</sup>,  $h$  is the peak height of mass 3,  $b$  is the unknown

calibration factor and P indicates the equilibrium pressure. In the present work the former method was adopted and found to give satisfactory results.

The exchange reaction



was followed by monitoring the peaks at masses 2, 3 and 4, and the rate of the reaction was calculated using the first order equation (6.1)

$$\log_{10} (\text{HD}_{\infty} - \text{HD}_t) = \frac{-kt}{2.303} + \log_{10} \text{HD}_{\infty} \quad (6.1)$$

where k is the rate constant for exchange,  $\text{HD}_{\infty}$  and  $\text{HD}_t$  are the percentages of HD present at equilibrium and at time t respectively. The equilibrium constant K in equation (6.2) varies with temperature as shown in fig. 6.1(a) and from this graph the appropriate value was selected for use in equation (6.2) allowing  $\text{HD}_{\infty}$  to be calculated for a particular temperature

$$K = \frac{P_{\text{HD}}^2}{P_{\text{H}_2} \cdot P_{\text{D}_2}} \quad (6.2)$$

#### 6.8 Treatment of GLC Data

The results were analysed by initially plotting the percentage composition against time to give a general picture of the course of the reaction including initial product ratio.

The rate of disappearance of reactant (dimethylbutene) was found from the first order reversible equation (6.3)

$$\log_{10} (X - X_e) = \frac{-kt}{2.303 (100 - X_e)} + \log_{10} (100 - X_e) \quad (6.3)$$

where X is the percentage olefin at time t, 100 and  $X_e$  are the initial and equilibrium percentages of olefin respectively and k is the first

order rate constant of the forward reaction.

The equilibrium data for C<sub>6</sub> olefins has been calculated by Kilpatrick et al.<sup>168</sup> and because the value of X<sub>e</sub> for 3,3-dimethyl-but-1-ene was very small compared to X, it was found that it could be neglected without affecting the accuracy of the results and equation (6.3) reduced to

$$\log_{10} (X) = \frac{-kt}{2.303} + 2 \quad (6.4)$$

By studying the reaction at a series of temperatures Arrhenius parameters could be obtained.

TABLE 6.1 STATISTICAL WEIGHTING FACTORS FOR FRAGMENTATION CORRECTIONS  
FOR DIMETHYLBUTENES

Compound	Mol. wt.	Reduction in mass			
		-1	-2	-3	-4
$C_6D_{12}$	96	-	$f_1$	-	$f_2$
$C_6^{HD}_{11}$	95	$\frac{1}{12} f_1$	$\frac{11}{12} f_1$	$\frac{22}{132} f_2$	$\frac{110}{132} f_2$
$C_6H_2D_{10}$	94	$\frac{2}{12} f_1$	$\frac{10}{12} f_1 + \frac{2}{132} f_2$	$\frac{40}{132} f_2$	$\frac{90}{132} f_2 + \frac{60}{1320} f_3$
$C_6H_3D_9$	93	$\frac{3}{12} f_1$	$\frac{9}{12} f_1 + \frac{6}{132} f_2$	$\frac{54}{132} f_2 + \frac{6}{1320} f_3$	$\frac{72}{132} f_2 + \frac{162}{1320} f_3$
$C_6H_4D_8$	92	$\frac{4}{12} f_1$	$\frac{3}{12} f_1 + \frac{12}{132} f_2$	$\frac{64}{132} f_2 + \frac{24}{1320} f_3$	$\frac{56}{132} f_2 + \frac{288}{1320} f_3$
$C_6H_5D_7$	91	$\frac{5}{12} f_1$	$\frac{7}{12} f_1 + \frac{20}{132} f_2$	$\frac{70}{132} f_2 + \frac{60}{1320} f_3$	$\frac{42}{132} f_2 + \frac{420}{1320} f_3$
$C_6H_6D_6$	90	$\frac{6}{12} f_1$	$\frac{6}{12} f_1 + \frac{30}{132} f_2$	$\frac{72}{132} f_2 + \frac{120}{1320} f_3$	$\frac{30}{132} f_2 + \frac{540}{1320} f_3$
$C_6H_7D_5$	89	$\frac{7}{12} f_1$	$\frac{5}{12} f_1 + \frac{42}{132} f_2$	$\frac{70}{132} f_2 + \frac{210}{1320} f_3$	$\frac{20}{132} f_2 + \frac{630}{1320} f_3$



$C_6H_8D_4$	88	$\frac{8}{12} f_1$	$\frac{4}{12} f_1 + \frac{56}{132} f_2$	$\frac{64}{132} f_2 + \frac{336}{1320} f_3$	$\frac{12}{132} f_2 + \frac{672}{1320} f_3$
$C_6H_9D_3$	87	$\frac{9}{12} f_1$	$\frac{3}{12} f_1 + \frac{72}{132} f_2$	$\frac{54}{132} f_2 + \frac{504}{1320} f_3$	$\frac{6}{132} f_2 + \frac{648}{1320} f_3$
$C_6H_{10}D_2$	86	$\frac{10}{12} f_1$	$\frac{2}{12} f_1 + \frac{90}{132} f_2$	$\frac{40}{132} f_2 + \frac{720}{1320} f_3$	$\frac{2}{132} f_2 + \frac{540}{1320} f_3$
$C_6H_{11}D$	85	$\frac{11}{12} f_1$	$\frac{1}{12} f_1 + \frac{110}{132} f_2$	$\frac{22}{132} f_2 + \frac{990}{1320} f_3$	$\frac{330}{1320} f_3$
$C_6H_{12}$	84	$f_1$	$f_2$	$f_3$	-

TABLE 6.2 STATISTICAL WEIGHTING FACTORS FOR FRAGMENTATION CORRECTIONS  
FOR m-XYLENE

Compound	Mol. wt.	Reduction in mass			
		-1	-2	-3	-4
$C_8D_{10}$	116	-	$f_1$	-	$f_2$
$C_8H^D_9$	115	$\frac{1}{10} f_1$	$\frac{9}{10} f_1$	$\frac{18}{90} f_2$	$\frac{72}{90} f_2$
$C_8H^D_2D_8$	114	$\frac{2}{10} f_1$	$\frac{8}{10} f_1 + \frac{2}{90} f_2$	$\frac{32}{90} f_2$	$\frac{36}{90} f_2 + \frac{48}{720} f_3$
$C_8H^D_3D_7$	113	$\frac{3}{10} f_1$	$\frac{7}{10} f_1 + \frac{6}{90} f_2$	$\frac{42}{90} f_2 + \frac{6}{720} f_3$	$\frac{42}{90} f_2 + \frac{126}{720} f_3$
$C_8H^D_4D_6$	112	$\frac{4}{10} f_1$	$\frac{6}{10} f_1 + \frac{12}{90} f_2$	$\frac{48}{90} f_2 + \frac{24}{720} f_3$	$\frac{30}{90} f_2 + \frac{216}{720} f_3$
$C_8H^D_5D_5$	111	$\frac{5}{10} f_1$	$\frac{5}{10} f_1 + \frac{20}{90} f_2$	$\frac{50}{90} f_2 + \frac{60}{720} f_3$	$\frac{20}{90} f_2 + \frac{300}{720} f_3$
$C_8H^D_6D_4$	110	$\frac{6}{10} f_1$	$\frac{4}{10} f_1 + \frac{30}{90} f_2$	$\frac{48}{90} f_2 + \frac{120}{720} f_3$	$\frac{12}{90} f_2 + \frac{360}{720} f_3$

$C_8H_7D_3$	109	$\frac{7}{10} f_1$	$\frac{3}{10} f_1 + \frac{42}{90} f_2$	$\frac{42}{90} f_2 + \frac{210}{720} f_3$	$\frac{6}{90} f_2 + \frac{378}{720} f_3$
$C_8H_8D_2$	108	$\frac{8}{10} f_1$	$\frac{8}{10} f_1 + \frac{56}{90} f_2$	$\frac{32}{90} f_2 + \frac{336}{720} f_3$	$\frac{2}{90} f_2 + \frac{336}{720} f_3$
$C_8H_9D$	107	$\frac{9}{10} f_1$	$\frac{1}{10} f_1 + \frac{72}{90} f_2$	$\frac{18}{90} f_2 + \frac{504}{720} f_3$	$\frac{216}{720} f_3$
$C_8H_{10}$	106	$f_1$	$f_2$	$f_3$	-

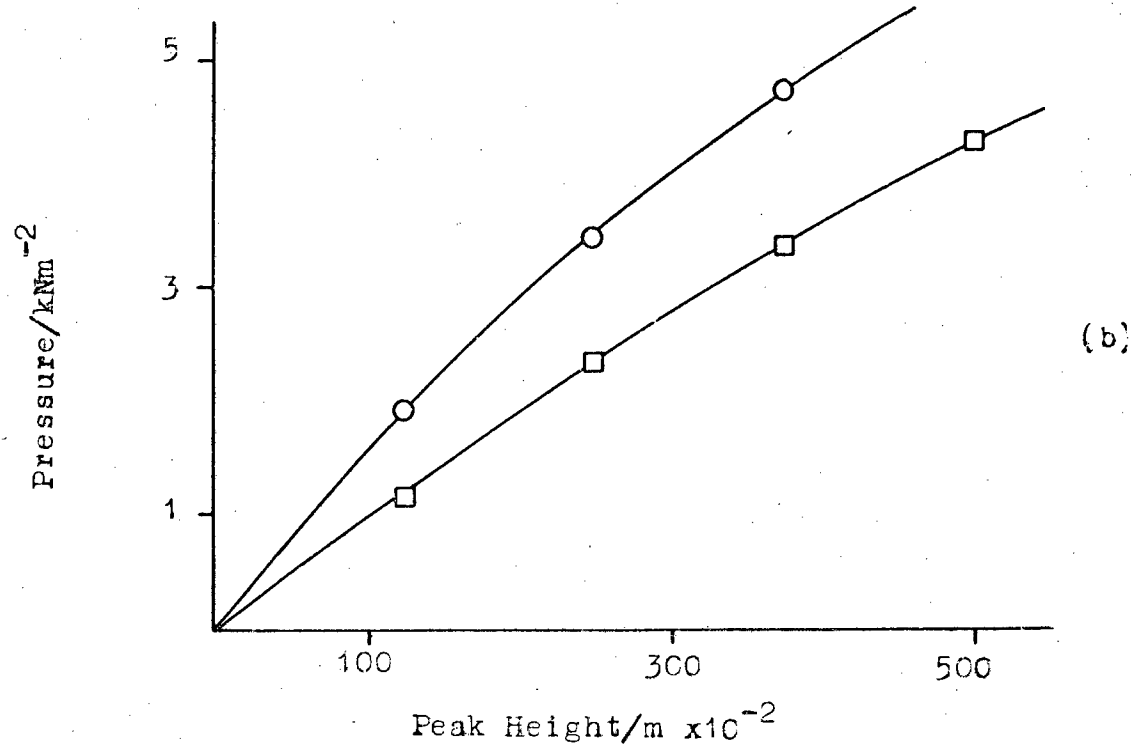
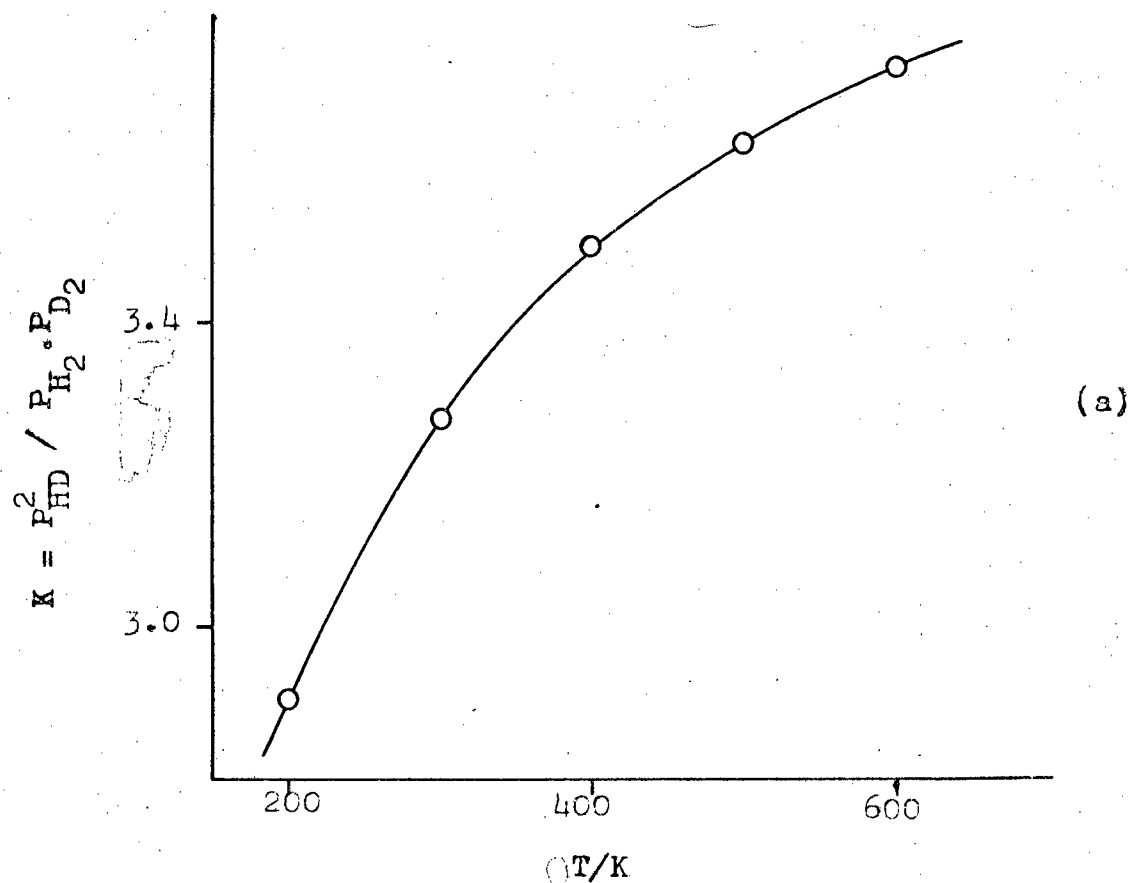


Fig.6.1- (a) Variation of equilibrium constant  $K$ , for the  $H_2/D_2$  exchange reaction, with temperature.  
 (b) Calibration of the MS 10 mass spectrometer for hydrogen ( O ) and deuterium ( □ ).

### Part III

#### The Reactions of C<sub>6</sub> Olefins over Ion-Exchanged X Type Zeolites

## Chapter VII

### Results for CuX Zeolites

#### 7.1 Isomerisation of Dimethylbutenes

The isomerisation reactions were followed by gas chromatographic techniques as discussed in Chapter V. The isomerisation of I to give 2,3-dimethylbut-1-ene (II) and 2,3-dimethylbut-2-ene (III) was studied over four CuX catalysts exchanged to differing extents and over the parent NaX for reference purposes. A typical reaction plot is shown in fig. 7.1 (a) and this illustrates not only the preferential formation of III but also that the product ratio ( III / II ) remained effectively constant during the course of the reaction. The product ratio did not change appreciably from the initial value (which was determined from the initial slopes) at zero conversion. The rate of disappearance of I was found to obey first order kinetics (equation 6.4) in all experiments and this is demonstrated in fig. 7.1 (b).

The results for the isomerisation of I over the various CuX catalysts are presented as Arrhenius plots in fig. 7.2 and the derived parameters are summarised in Table 7.1. Temperatures of above 523 K were required to obtain measurable reaction rates over NaX but the isomerisation process occurred readily over the CuX zeolites at appreciably lower temperatures - the higher the copper content of the zeolite the lower the reaction temperature. The results in fig. 7.2 emphasise the effect of varying the degree of cation exchange upon the catalytic activity.

Experiments were carried out in which the catalyst was evacuated at 673 K for 1 h after a normal isomerisation run, a fresh dose of I admitted and the reaction followed again. For CuX(10) it was found that the first order rate of disappearance of I was virtually unaffected by repeated use whereas the activity of the more highly exchanged CuX catalysts decreased significantly on second and subsequent runs.

The effect of hydrogen and water on the isomerisation rate of I was examined over CuX(10) at 448 K and these data are incorporated into fig. 7.2. The presence of hydrogen produced no change in the observed rate but there was a significant decrease in rate (by a factor of approximately 7) in the presence of water. Similar observations were obtained with CuX(65) at 358 K; hydrogen produced no change in rate whereas water completely inhibited the reaction.

The isomerisation of II to III was examined over NaX and CuX(10). The reaction was more facile than that of I and the temperature range of observation was appreciably lower, as indicated in Table 7.1 where the data are listed. The corresponding Arrhenius plots are shown in fig. 7.3. The major feature of the reaction was the conversion of II to III, with very little formation of I at the relatively low temperatures. The treatment of the kinetic data was as for I, with the rate of disappearance of II obeying first order kinetics (equation 6.4). Once again the effect of replacing  $\text{Na}^+$  by  $\text{Cu}^{2+}$  was very pronounced, e.g. the extrapolated rate of isomerisation of II over CuX(10) at 333 K being some 110 times greater than the rate observed over NaX. In a blank experiment, adopting the standard experimental procedure but without any

zeolite catalyst, a temperature of 573 K was required before significant isomerisation of II occurred ( $k = 8.3 \times 10^{15}$  molecule  $s^{-1}$  dg $^{-1}$ ).

As in the reactions of I, hydrogen had no effect upon the isomerisation rate of II over CuX(10) but the poisoning effect of water was even more marked in this instance. In the presence of water it was necessary to raise the temperature to 393 K in order to obtain a rate ( $6.7 \times 10^{15}$  molecule  $s^{-1}$  dg $^{-1}$ ) similar to that observed at 273 K in the absence of water. Extrapolation of the data to 393 K indicated a decrease in rate by a factor of approximately 145.

## 7.2 Exchange Reactions of Dimethylbutenes

The exchange reactions of I and II with deuterium and deuterium oxide were examined in detail over CuX(10), and the exchange of I with deuterium oxide was studied over NaX for reference purposes. The results were plotted according to the first order reversible equations 3.5 and 3.6 from which the parameters  $k_o$ ,  $k_\phi$  and M were obtained. Under the experimental conditions used, the mass spectrometric data refers to the isotopic content of the combined C<sub>6</sub> olefins and not to the individual olefins.

### Exchange with D<sub>2</sub>O

The exchange of I with D<sub>2</sub>O was studied over both NaX and CuX(10) and the results for  $k_o$  (in absolute units of molecule  $s^{-1}$  dg $^{-1}$ ) presented as Arrhenius plots in figs. 7.3 and 7.4. The enhancement of activity on exchanging Cu<sup>2+</sup> into the zeolite matrix is again well demonstrated. The derived parameters are summarised in Table 7.2. A feature of the reactions of I with D<sub>2</sub>O over both



NaX and CuX(10) was the multiple exchange character, i.e. the initial exchanged products contained an average of 8-10 deuterium atoms per molecule but the important point was that all twelve hydrogen atoms in the molecule could be exchanged. A typical reaction plot is shown in fig. 7.5 and illustrates how the isotopic composition of the olefins changes with time. The initial product distribution for the reaction of I with D<sub>2</sub>O over CuX(10) at 448 K is shown in Table 7.3, it was determined from plots of the amounts of the various isotopic olefins against time. Also included is a calculated binomial distribution for the same average deuterium content (on the basis that all twelve hydrogen atoms in the C<sub>6</sub> olefin are equally susceptible to exchange) and comparison of the two distributions shows that they are similar but not in perfect agreement. A similar comparison of the experimental and binomial distributions after an extended period of time gave excellent agreement (Table 7.4).

Fig. 7.4 shows the Arrhenius plot for the exchange of I with D<sub>2</sub>O over CuX(10) and the isomerisation of I (dotted line) for comparison, and it is apparent that the rate of isomerisation of I in the presence of water agrees very well with the rate of disappearance of the light hydrocarbon indicating that isomerisation and exchange must be occurring simultaneously. For NaX (fig. 7.3) the temperature range necessary to examine the exchange of I with D<sub>2</sub>O was similar to that required for the isomerisation process.

The exchange of II with D<sub>2</sub>O was observed to take place over CuX(10) at a measurable rate at 393 K. The rate of

disappearance of the  $d_0$  species ( $1.31 \times 10^{16}$  molecule  $s^{-1} dg^{-1}$ ) correlates closely with the rate of isomerisation of II in the presence of water i.e. the simultaneous occurrence of isomerisation and exchange was once again indicated. The reaction took place in a stepwise manner and good agreement was obtained at all stages of the reaction between the experimental product distribution and a binomial distribution calculated on the assumption that all the hydrogen atoms in the molecule are equally reactive.

#### Exchange with Deuterium

The reaction of I with  $D_2$  was studied over  $CuX(10)$ , the results are given in Table 7.2 and the corresponding Arrhenius plot in fig. 7.4. The reactions were stepwise in nature, with an M value close to unity, and good agreement was exhibited at all stages of the reaction between the experimental isotopic product distribution and the corresponding binomial distribution as illustrated in Table 7.5. The data of Table 7.5 are calculated on the assumption that the various isomeric forms of the deuterated olefins have similar fragmentation patterns. The agreement exhibited can be taken as an indication that any divergences from such an assumption have no serious effects. Fig. 7.6 is a typical plot showing the change in the distribution of isotopic species with time and this should be contrasted with the multiple exchange character observed with  $D_2O$ .

A temperature of 473 K was necessary in order to obtain a significant rate of exchange of II with deuterium over  $CuX(10)$ , this process also being stepwise in nature. The temperatures required for the exchange of I and II with deuterium were appreciably higher than those required for isomerisation of

is a comparison between experimental product distributions calculated using, (a) a statistical approach assuming random loss of H or D, and (b) the method of Dowie et al. (section 6.5) which takes into account the preferential rupture of C-H compared with C-D bonds and the influence of other bonds. The two sets of distributions agree very closely showing that a purely statistical approach is sufficient for the  $C_6$  olefin system. In the initial stages of reaction virtually all of the deuterium is incorporated into the products of isomerisation II and III, and only a trace is found in I (and there is no significant increase in this amount with time). II and III are highly deuterated and all twelve hydrogen atoms in the molecules can be exchanged. The value of  $M_D$  increases initially and then drops as the reaction proceeds, as expected for an equilibrium  $M_D$  value of 7. As can be seen from Table 7.6, II and III are richer in the more highly deuterated species in the early stages of reaction than expected from the binomial distribution with the same  $M_D$  value (this effect is more pronounced for III) but at later stages of the reaction there is excellent agreement between the two distributions. In the final stages of reaction there appears some deuterium incorporation into I (traces of the  $d_5$  to  $d_{12}$  compounds) which must result from the back reaction of II and III isomerising to I.

#### 7.4 Reactions on Treated CuX(10)

A. The isomerisation of I was examined over CuX(10) catalysts which had been subjected to different pretreatments in order to gain more information about the nature of the active sites and the interactions which take place. The results are shown as additional points on fig. 7.2.

### Hydrogen Pretreatment

The catalyst was heated in hydrogen ( $2 \text{ kN m}^{-2}$ ) at 623 K for 1 h and then evacuated at 293 K for 15 minutes. This increased the rate of isomerisation of I at 413 K by a factor of 5.

When the catalyst was treated with hydrogen ( $4 \text{ kN m}^{-2}$ ) at 673 K for 1 h and then evacuated at this temperature for 15 minutes, the rate of isomerisation of I was too fast to follow at 448 K.

### Carbon Monoxide Pretreatment

The catalyst was heated in CO ( $2 \text{ kN m}^{-2}$ ) at 623 K for 6 h and then evacuated at 473 K for 30 minutes. This reduced the rate of isomerisation of I at 433 K by a factor of 3.

### B. Hydrogen-Deuterium Exchange

In this series of experiments hydrogen-deuterium exchange was used as a test reaction for detecting changes in the nature of CuX(10) catalysts after various pretreatments. All of the reactions (listed below) were carried out at 398 K and the results are summarised in Table 7.7.

- (1) Reaction on a normally outgassed catalyst.
- (2) Reaction carried out in the presence of I. A charge of I equivalent to 1.5 molecules per supercage was preadsorbed on to the catalyst.
- (3) Reaction on an oxygen pretreated catalyst. The catalyst was pretreated with oxygen ( $3 \text{ kN m}^{-2}$ ) at 673 K for 1 h followed by evacuation at this temperature for 15 minutes.
- (4) Reaction on a hydrogen pretreated catalyst. The catalyst was pretreated with hydrogen ( $4 \text{ kN m}^{-2}$ ) at 673 K for 1 h followed by evacuation at this temperature for 15 minutes.

- (5) Reaction carried out in the presence of carbon monoxide, a charge equivalent to 1.5 molecules per supercage.

#### 7.5 Reactions over CuHX Zeolites

A series of CuX zeolites were prepared by the method developed by Rudham and Sanders<sup>156</sup>, this method being employed to prevent the formation of a catalyst with a supported oxide component. Analysis of the samples showed that extensive loss of sodium from the zeolite had occurred in addition to that replaced by copper and that the samples had suffered an appreciable loss of surface area.

The catalysts have been designated CuHX(n), where n represents the percentage of the original  $\text{Na}^+$  replaced by  $\text{Cu}^{2+}$ . The NaHX catalyst was subjected to the same treatment as the CuHX catalysts except that no exchange with the transition metal salt took place. The results for the isomerisation of I are presented in Table 7.8 and it can be seen that all four catalysts show comparable activity and that there is no correlation between catalytic activity and copper content. The activity of the copper is masked by the activity of hydrogen ions which have presumably replaced  $\text{Na}^+$  ions and the behaviour appears to be more typical of a series of HX zeolites and hence the nomenclature adopted for this series of catalysts.

The reactions of CuHX(2) will be described since the behaviour shown by this catalyst is typical of the series. The catalyst had a surface area of  $600 \text{ m}^2 \text{ g}^{-1}$  and 26% of the sodium ions were lost from the zeolite in addition to those replaced by copper ions. Hydrogen was found to have no effect upon the rate of isomerisation of I at 458 K but the

presence of water caused an enhancement in rate by a factor of 3. The results are shown on the Arrhenius plot in fig. 7.7, together with those for NaX and CuX(10) for comparison. The reaction of I with D<sub>2</sub>O resulted in multiple exchange with initial products containing an average of 9-10 deuterium atoms per molecule. The reaction was studied in the temperature range 423-448 K and the results are shown in fig. 7.7 and summarised in Table 7.8. It can be seen that there is good correlation between the rate of isomerisation of I in the presence of water and the rate of disappearance of the light hydrocarbon.

For all the catalysts of this series, evacuating at 673 K for 1 h after reaction followed by admission of a fresh dose of reactant gave a well-behaved reaction i.e. the first order rate of disappearance of I was virtually unaffected by carrying out successive runs on the same sample of catalyst.

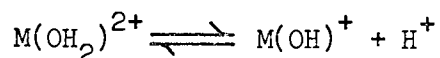
## 7.6 Discussion

### Isomerisation Reactions

The isomerisation of I has been used as a test reaction for investigating the acidity of zeolite catalysts because the reaction is believed to proceed via carbonium ion intermediates. As discussed earlier, evidence for such a reaction scheme was obtained by Haag and Pines<sup>143</sup> and further support for such a scheme arose from the work of Kemball, Leach, Skundric and Taylor<sup>148</sup> who found that the isomerisation of I occurred readily over silica-alumina and X-type zeolites containing Ce, Ca and Ni whereas over MgO the process was much more difficult. It is worthwhile emphasising the important features of the proposed reaction scheme which is shown in fig. 7.8. The initial formation

of a  $2^\circ$  ion is followed by rearrangement to the more stable  $3^\circ$  ion and the subsequent loss of  $H^+$  from this species results in the formation of II and III. The detailed kinetic data presented in this work for the isomerisation of I clearly demonstrates the ability of copper-exchanged zeolites to display acidic-type catalytic activity. The parent NaX is normally regarded as having very little such activity and indeed it is noted here that isomerisation of I only occurred over NaX at elevated temperatures ( $>523$  K).

Infra-red investigations by Ward<sup>105,108,169</sup> and by Nacacche and Ben Taarit<sup>170,171</sup> have provided evidence that copper-exchanged Y zeolites possess acidic properties. Two types of acidic structural hydroxyl group were identified; one located in the hexagonal prisms of the zeolite structure, the other in the zeolite supercage. The CuY zeolites exhibited Bronsted acidity but not Lewis acidity at low activation temperatures. It has been postulated<sup>79,172</sup> that such acidic hydroxyl groups arise from the fission of adsorbed water molecules according to the following scheme,



with the released proton attaching itself to a lattice oxygen to form an acidic hydroxyl group. Ward<sup>108</sup> did not find any evidence of Bronsted acidity in an infra-red examination of a CuX zeolite but substantial structural collapse of his sample had occurred. On the other hand infra-red studies have shown that pure NaX zeolite possesses no acidic properties<sup>85</sup> and Lambardo et al.<sup>173</sup> have proposed that the activity of NaY zeolite is associated

with Bronsted acid sites formed by interaction of water with divalent cations e.g.  $\text{Ca}^{2+}$  present as impurities or by decationation through hydrolysis.

The pronounced enhancement in catalytic activity upon incorporation of copper cations into the zeolite lattice emphasises the important role that this cation must play in the mechanism. Fig. 7.9 gives a striking illustration of the variation in catalytic activity (expressed in terms of the first order rate constant) as a function of the extent of cation exchange. The data were obtained from the results in fig. 7.2, extrapolated to a common temperature of 453 K. However, the positions occupied by the cations in the zeolite framework must also have an important bearing upon the catalytic activity. With the lowest exchanged sample CuX(10), it is possible for all the  $\text{Cu}^{2+}$  ions (4.3 per unit cell) to be accommodated in the relatively inaccessible SI sites (16 per unit cell) within the hexagonal prisms of the lattice where they would have little catalytic effect. If the  $\text{Cu}^{2+}$  ions preferentially enter SI sites a marked change in activity would be expected when the zeolite contains 16  $\text{Cu}^{2+}$  ions per unit cell, i.e. when 32 of the 86  $\text{Na}^+$  ions (37%) have been exchanged, for once all the SI positions are occupied at least some of the  $\text{Cu}^{2+}$  ions can be expected to enter surface sites. If on the other hand  $\text{Cu}^{2+}$  ions preferentially enter SI' positions (32 per unit cell) then only after 74% exchange had taken place would  $\text{Cu}^{2+}$  ions occupy accessible sites although a more limited occupation of SI' would be anticipated due to cation-cation interactions. However, this is clearly not the situation as fig. 7.9 indicates, CuX(10) is very much more active (by a factor of approximately



1000) than the parent NaX. Therefore even at low levels of exchange some of the  $\text{Cu}^{2+}$  ions are accessible to reactant molecules.

An esr investigation<sup>174</sup> of this CuX(10) sample also suggested that the copper cations were present in at least two different environments, with the cations in one such environment being preferentially reactive towards a variety of simple reactant molecules. In a more recent and detailed esr study<sup>175</sup> the more reactive copper cations were postulated to occupy site II' in the sodalite unit whereas the less reactive cations were placed in SI' positions. The spectra of the  $\text{Cu}^{2+}$  species were shown to be affected by the adsorption of I, but only at temperatures which closely parallel those at which the zeolite is active for isomerisation. Such data provide clear evidence of the importance of interaction between the olefin and the copper cation. It has been postulated that reversible reduction of  $\text{Cu}^{2+}$  to  $\text{Cu}^+$  occurs with the formation of a  $\text{Cu}^+$ -hydrocarbon complex. The esr data also revealed that under reaction conditions migration of copper cations to more accessible positions in the zeolite lattice takes place.

Gallezot et al.<sup>176</sup> in an X-ray diffraction study of a copper-exchanged Y zeolite showed that the cupric ions have a great affinity for SI' and less for SI in the dehydrated zeolite, and that adsorption of ammonia (which can penetrate the sodalite cage) does not produce important displacements of cations when introduced in small amounts, whereas for larger adsorbates such as pyridine and naphthalene chemisorption results in a marked migration of cupric ions towards the supercage. Further evidence for the mobility of cupric ions under the influence

of reagent molecules has been obtained by several other workers<sup>177-179</sup>.

The inhibiting effect of water upon the isomerisation of I can be readily explained in terms of complex formation. Preferential adsorption of water to give a copper aquo complex would prevent the formation of the postulated copper-hydrocarbon species; consequently higher temperatures would be necessary to promote the isomerisation. No such complex is likely to be formed with hydrogen, hence the fact that hydrogen does not affect the isomerisation rate. However, Ward<sup>169</sup> observed that water was simply physically adsorbed on CuY zeolite and desorbed without interacting chemically with the zeolite framework whereas for the other transition metal cations studied dissociation of the water occurred and structural hydroxyl groups were formed. This effect was unexpected since if copper ions were present in the divalent form the polarising power of the cupric ion would be greater than the other cations studied, and it was proposed that since the first ionisation state is readily available copper ions may be present in the monovalent state with a subsequent low polarising power.

Haag and Pines<sup>143</sup> observed the formation of methylpentenes and hexenes in their studies on alumina catalysts but a temperature of 623 K was employed. In the present study the isomerisation of I over the CuX zeolites was limited to the products II and III. Further rearrangement of the olefin structure presumably occurs on more strongly acid sites or at higher temperatures. This latter point is illustrated in fig. 7.10(a) which shows that a complicated mixture containing at least eight compounds was obtained when the isomerisation reaction was left for an extended period of time at 473 K, and strongly suggests that further isomerisation

of the dimethylbutenes has occurred.

A feature of the isomerisation studies of I was the manner in which the product ratio ( III / II ) remained effectively constant during the course of the reaction-varying very little from the initial product ratios quoted in Table 7.1 (and these values were in good agreement with those obtained from reactions left for an extended period of time). When the experimental product ratios are compared with those extrapolated from the data of Kilpatrick et al.<sup>168</sup> (fig. 7.10(b)) it can be seen that both sets of data are in very close agreement, and it is possible to calculate the heat of interconversion from them for the reaction  $II \rightleftharpoons III$ ; values of  $-7.2 \pm 0.5$  and  $-6.8 \pm 0.6$  kJ mole<sup>-1</sup> were obtained from the experimental and theoretical points respectively. The evidence strongly indicates that the isomers II and III are formed in equilibrium proportions during the isomerisation of I.

The ease of isomerisation of II, relative to that of I, is shown over both NaX and CuX zeolites. Such enhanced reactivity is compatible with the scheme of fig. 7.8 for acidic catalysts as a 3° ion can be formed directly from either II or III. However it should be remembered that the  $II \rightleftharpoons III$  interconversion does not necessarily involve intermediates of this type. The efficiency of MgO<sup>148</sup> as a catalyst for this reaction was explained in terms of carbanion intermediates. Loss of an H<sup>+</sup> from II or III would produce an allylic carbanion which would be capable of forming copper complexes of the type previously discussed. Such an allylic species cannot of course be formed directly from I, only after isomerisation to II and/or III. The effect of hydrogen and water on the isomerisation can be explained as for I, but the more severe poisoning effect of water

may be attributed to the greater adsorption of water at the lower temperatures employed.

### Exchange Reactions

The temperature ranges necessary in order to observe the exchange reactions with deuterium oxide of both I and II over NaX and CuX(10) were similar to those required for isomerisation. This is particularly demonstrated for the CuX(10) data where the correlation between rates of exchange and of isomerisation in the presence of water is striking. It is consequently apparent that significant exchange with deuterium oxide only occurs under conditions where substantial isomerisation also takes place. The exchange of II with deuterium oxide over CuX(10) was seen at significantly lower temperatures than the exchange of I, which is to be expected in terms of fig. 7.8. It is envisaged that heterolytic splitting of deuterium oxide over the zeolite catalysts provides a ready source of  $D^+$  species, and consequently the exchange of II (or of III) will take place via the reversible formation of a  $3^{\circ}$  ion. In such an exchange mechanism interconversion of II and III must also be occurring.

A feature of the exchange reactions of I with deuterium oxide over CuX(10) was the multiple exchange character exhibited, similar to that previously reported<sup>148</sup> over silica-alumina and other cation exchanged X-type zeolites. This behaviour together with that exhibited by the II plus deuterium oxide reaction system can be rationalised in terms of the scheme shown in fig. 7.8. At the relatively low reaction temperatures at which II exchanged, desorption of III (or II) is faster than the surface interconversion processes and consequently stepwise exchange is observed. This

stepwise character incidentally precludes any explanation of the multiple character of the exchange of I in terms of diffusion control. At the somewhat higher temperatures required to form the  $2^{\circ}$  ion from I, then interconversion on the surface is apparently faster than desorption of II or III. Consequently, it is feasible to envisage several interconversions taking place between II and III under such conditions (with loss of  $H^{+}$  and gain of  $D^{+}$  possible at each stage) before the olefinic species returns to the gas phase where it is observed as a multiply exchanged product.

The experimentally observed equilibrated product ratio of III/II is consistent with such a picture of the multiple exchange process. It is also pertinent to point out that an initial M value of 10 implies that each reacting  $C_6$  olefin has equilibrated with approximately thirty deuterium oxide molecules. Such a value is an indication of the ease of mobility of water molecules within the zeolite lattice under reaction conditions.

When the MS10 mass spectrometer was employed to follow the exchange of I with  $D_2O$  only the isotopic content of the combined  $C_6$  olefins could be determined, but despite this limitation further support for the proposed reaction scheme comes from the distribution of isotopic species produced during the reaction. A molecule such as I possesses at least two groups of non-equivalent hydrogen atoms, those in the methyl groups and those in the vinyl positions and if no isomerisation of I was occurring during exchange one would not expect all the hydrogen atoms to be equally reactive, e.g. in the exchange of I with  $D_2$  over  $MgO^{148}$  three hydrogen atoms were observed to exchange faster than the remaining nine. However, in the present case it was observed that all twelve hydrogen atoms in the molecule exchanged at the same rate and this is evidence for the  $3^{\circ}$  ion intermediate, in which all hydrogen atoms are equivalent, being involved.

The results from the combined GC-MS study of the reaction of I with  $D_2O$  demonstrate quite convincingly that I must isomerise if exchange is to occur but further detailed information is obtained about the proposed reaction scheme (fig. 7.8). In the initial stages of reaction virtually all of the deuterium is incorporated into the products II and III, and therefore  $k_3 \gg k_{-2}$ . The  $2^\circ$  ion which is formed from I is converted to the  $3^\circ$  ion and does not revert back to I, because if this did occur one would expect to form exchanged I containing the  $d_1$  and possibly  $d_2$  compounds during the reaction. In the proposed reaction scheme the rate controlling step is the formation of the  $2^\circ$  ion from I. In the initial stages, II and III are richer in the more highly deuterated compounds than expected from the corresponding binomial distribution. This may be due to a kinetic isotope effect arising in the following way; the first molecules to exchange do so with a large surface pool of deuterium ( $D^+$ ) and the interconversion between II and III via the  $3^\circ$  ion intermediate may take place many times involving preferential loss of  $H^+$  and gain of  $D^+$  at each stage with the loss of  $H^+$  being greater relative to that predicted on a purely statistical basis and as the molecule becomes richer in deuterium  $H^+$  will be lost less readily overall but more readily than expected from statistical considerations. In this way all twelve hydrogen atoms in the molecule may be exchanged during one sojourn at the surface. As the reaction proceeds dilution of the deuterium pool results in a lowering of the  $M_D$  value. In the later stages of the reaction there is evidence of some back isomerisation of II and III to I.

It has been shown that hydrogen does not affect the rate of isomerisation of the olefins. It is therefore clear that at the temperatures necessary for the exchange reactions with deuterium one is concerned with exchange of an equilibrated mixture of the  $C_6$  olefins

rather than with the individual hydrocarbons. The close correspondence of the data for the I plus deuterium and II plus deuterium systems (fig. 7.4) provides further evidence of this point. The limiting factor in the exchange reactions of the  $C_6$  olefins with deuterium would appear to be the activation of the deuterium.

Hydrogen-deuterium exchange has been noted over CuX(10) in the temperature range 353-393 K<sup>180</sup> and at 398 K in the present study, and the higher temperatures required for exchange might reflect a change in the character of the reaction. Although the hydrogen-deuterium reaction is envisaged as proceeding via homolytic fission it might well be necessary in the present study to supply deuterium in the form of  $D^+$  (a less facile process). It has been shown that pretreatment of the CuX(10) catalyst with I had a significant poisoning effect upon the subsequent activity for hydrogen-deuterium exchange. Thus an alternative explanation for the different temperature ranges of the exchange processes is preferential adsorption of the olefin, with the consequent blocking of the sites active for the hydrogen-deuterium exchange reaction. However, it may well be that both factors are important. The stepwise nature of the exchange reactions with deuterium could reflect the fact that deuterium is less efficient (relative to deuterium oxide) in providing a sufficient supply of  $D^+$  species to sustain the multiple character of the reaction.

#### Treated CuX(10)

The CuX(10) sample was subjected to various pretreatments with hydrogen and carbon monoxide in an attempt to gain a better understanding of the factors responsible for the catalytic activity. Induction periods have been observed for butene<sup>101</sup> and methylcyclopropane<sup>155</sup> isomerisation over CuX zeolites and it was postulated<sup>101</sup> that the induction periods were associated with a reduction process,  $Cu^{2+} \rightarrow Cu^+$ . Leith and Leach<sup>175</sup> have shown that adsorption of I, or but-1-ene, produces changes in the

esr spectrum of  $\text{Cu}^{2+}$  at temperatures which closely parallel those at which isomerisation of the olefin occurs, with the reversible reduction of  $\text{Cu}^{2+}$  to  $\text{Cu}^+$  and the formation of a copper-hydrocarbon complex. Leith<sup>181</sup> in a more detailed examination of n-butene isomerisation over the CuX(10) sample used in the present work, observed induction periods after oxygen pretreatment of the catalyst (to ensure that no reduced copper species were present) and, at a given temperature, was able to correlate the length of the induction period for the isomerisation reaction with the time required for the olefin to cause reduction of  $\text{Cu}^{2+}$  to  $\text{Cu}^+$  as evidenced by esr spectroscopy.

In the present study induction periods were not observed for the isomerisation of I, but I is known to be a more efficient reducing agent than but-1-ene, reduction of  $\text{Cu}^{2+}$  occurring readily at 423 K<sup>175</sup>. It is therefore clear that interaction between the olefin and cupric ions plays an important role in determining the catalytic activity. The consequence of complex formation could be that since complexed copper ions are no longer available to balance the net negative charge on the lattice, the double bond  $\pi$ -electrons of the olefin provide electron transfer to the copper d-orbitals and the interaction between cupric ions and the olefin releases protons from the olefin which react with the framework oxygens to form new hydroxyl groups. In support of this, it is known that CuY zeolites possess oxidising properties<sup>170,182</sup> and that electron transfer occurs at the cupric ion. Therefore, the rate of but-1-ene isomerisation would be proportional to the concentration of  $\text{H}^+$  brought about by this reduction process and the induction period may be attributed to the reaction accelerating until a constant  $\text{Cu}^+$  concentration is attained. However, hydroxyl groups which are known to be present in dehydrated transition-metal zeolites could also function as Bronsted acid sites, so that the protons released by the copper-olefin interaction may not be essential for activity.

The observed enhancement in the rate of isomerisation of I



following hydrogen pretreatment of the catalyst suggests the participation of protonic sites produced during this pretreatment. Pretreatment of CuX zeolites with hydrogen is known to reversibly reduce  $\text{Cu}^{2+}$  to  $\text{Cu}^{+}$  <sup>175,183</sup> but under more severe conditions the formation of  $\text{Cu}^0$  or metal clusters may result <sup>170</sup>. Nacacche <sup>170</sup> proposed the reaction scheme shown in fig. 7.11 to account for the kinetics of hydrogen reduction observed in his work, and such a scheme provides a satisfactory explanation for the results observed in this work. Pretreatment at 623 K may lead to partial reduction of  $\text{Cu}^{2+}$  to  $\text{Cu}^{+}$  whereas pretreatment at 673 K may result in virtually complete reduction of the  $\text{Cu}^{2+}$  ions to  $\text{Cu}^0$  with the consequent greater production of  $\text{H}^{+}$  and thus enhanced activity. On the other hand pretreatment with carbon monoxide resulted in a decrease in the rate of isomerisation of I. This result supports the conclusion that protonic sites are necessary, since it is known <sup>170,175</sup> that such a pretreatment leads to the formation of  $\text{Cu}^{+}$  but without the production of protonic sites. The proposed reduction scheme is shown in fig. 7.12. Therefore, in summary, although the hydroxyl groups present initially in the dehydrated catalyst contribute to the isomerisation activity, the interaction of the olefin with cupric ions results in the reduction of the latter to cuprous ions with the formation of additional catalytically active Bronsted ( $\text{H}^{+}$ ) acid sites.

#### $\text{H}_2/\text{D}_2$ Exchange

The results show that  $\text{H}_2/\text{D}_2$  exchange is not a sensitive test reaction for detecting changes in the properties of CuX(10) after various pretreatments. The observed changes in activity were so small that no definite conclusions can be drawn regarding the nature of the active sites for this reaction. The most striking effect was shown by preadsorbing I, which led to complete inhibition

of the reaction at 398 K but I is not a specific 'poison' for a particular site within the zeolite framework.

#### CuHX Catalysts

The results clearly demonstrate that the CuHX zeolites showed behaviour typical of acidic catalysts, and in the main the results can be interpreted as for the CuX zeolites. The most striking difference shown by the CuHX catalysts was the enhancement in the rate of isomerisation of I caused by the presence of water. For these catalysts an appreciable number of sodium ions are thought to have been replaced by hydrogen ions so that dehydration of the samples may lead to the formation of Lewis acid sites. The addition of water would convert the Lewis acid sites into Bronsted acid sites.

TABLE 7.1    ARRHENIUS   PARAMETERS   FOR   THE   ISOMERISATION   OF   DIMETHYLBUTENES

catalyst	reactant	temp. range/K	activation energy/kJ mole <sup>-1</sup>	log <sub>10</sub> (A/ molecule s <sup>-1</sup> dg <sup>-1</sup> )	initial product ratio*
NaX	I	523-598	118	26.3	2.2
CuX(10)	I	433-463	85	26.1	3.5
CuX(25)	I	398-428	99	28.7	4.2
CuX(43)	I	363-393	83	26.5	5.1
CuX(65)	I	343-373	77	27.7	6.1
NaX	II	333-383	33	20.4	
CuX(10)	II	250-303	31	21.9	

\* values for the initial product ratio, III/II, were determined at the lowest temperature quoted for each catalyst.

TABLE 7.2      ARRHENIUS PARAMETERS FOR THE EXCHANGE REACTIONS OF  
3,3-DIMETHYLBUT-1-ENE

catalyst	reactants	temp. range/K	E/kJ mole <sup>-1</sup>	log <sub>10</sub> (A/molecule s <sup>-1</sup> dg <sup>-1</sup> )	M
NaX	I+D <sub>2</sub> O	523-598	62	20.8	8
CuX(10)	I+D <sub>2</sub> O	448-483	143	32.1	10
CuX(10)	I+D <sub>2</sub>	463-503	123	29.3	1

TABLE 7.3 INITIAL PRODUCT DISTRIBUTION FROM EXCHANGE OF I WITH  
D<sub>2</sub>O ON CuX(10) AT 448 K

	d <sub>5</sub>	d <sub>6</sub>	d <sub>7</sub>	d <sub>8</sub>	d <sub>9</sub>	d <sub>10</sub>	d <sub>11</sub>	d <sub>12</sub>	M <sub>D</sub> <sup>a</sup>
expt.	4.2	6.2	9.4	18.9	19.8	20.6	15.7	5.2	9.0
binomial <sup>b</sup>	1.2	4.0	10.4	19.4	25.8	23.3	12.7	3.2	9.0

<sup>a</sup> M<sub>D</sub> gives the average number of deuterium atoms in the product. For initial products M<sub>D</sub> should be equivalent to the value of M determined from the ratio  $k_{\phi}/k_o$ .

<sup>b</sup> Binomial distribution calculated on the basis that all twelve hydrogen atoms in the olefins are exchangeable, and that the average composition is nine deuterium atoms and three hydrogen atoms.

TABLE 7.4      FINAL DISTRIBUTION OF PRODUCTS FROM THE EXCHANGE OF I WITH  
D<sub>2</sub>O ON CuX(10) AT 448 K

	d <sub>0</sub>	d <sub>1</sub>	d <sub>2</sub>	d <sub>3</sub>	d <sub>4</sub>	d <sub>5</sub>	d <sub>6</sub>	d <sub>7</sub>	d <sub>8</sub>	d <sub>9</sub>	d <sub>10</sub>	d <sub>11</sub>	d <sub>12</sub>	M <sub>D</sub>
expt.	0.8	2.8	8.0	16.2	21.5	21.3	15.9	8.6	3.5	0.9	0.2	0.1	0.1	4.56
binomial	0.3	2.4	8.0	16.3	22.5	22.1	15.8	8.3	3.2	0.9	0.2	0.0	0.0	4.56

TABLE 7.5 PRODUCT DISTRIBUTION DURING EXCHANGE OF I WITH D<sub>2</sub> ON CuX(10) AT 483 K

	d <sub>0</sub>	d <sub>1</sub>	d <sub>2</sub>	d <sub>3</sub>	d <sub>4</sub>	d <sub>5</sub>	d <sub>6</sub>	d <sub>7</sub>	d <sub>8</sub>	M <sub>D</sub>
expt.	21.0	35.2	26.0	12.4	4.1	1.0	0.2	0.1	-	1.47
binomial <sup>a</sup>	20.7	34.9	26.9	12.5	4.0	0.9	0.1	-	-	1.47

<sup>a</sup> Binomial distribution calculated assuming all twelve hydrogen atoms in the olefin molecule are exchangeable.

TABLE 7.6 PRODUCT DISTRIBUTION DURING EXCHANGE OF I WITH D<sub>2</sub>O ON CuX(10)

% I isomerised	olefin		d <sub>0</sub>	d <sub>1</sub>	d <sub>2</sub>	d <sub>3</sub>	d <sub>4</sub>	d <sub>5</sub>	d <sub>6</sub>	d <sub>7</sub>	d <sub>8</sub>	d <sub>9</sub>	d <sub>10</sub>	d <sub>11</sub>	d <sub>12</sub>	M <sub>D</sub>
24.5	I	expt.	99.06	0.93												0.01
		binomial	99.0	1.0												0.01
24.5	II	expt.	0.0	0.1	0.1	0.1	0.1	0.5	0.9	1.5	8.5	21.5	32.8	25.4	8.6	9.91
		binomial	0.0	0.0	0.0	0.0	0.0	0.1	0.8	3.3	9.9	20.8	29.5	25.5	10.1	9.91
24.5	III	expt.	0.1	0.8	0.3	0.9	0.4	0.8	1.4	3.9	9.0	19.5	28.9	24.8	9.2	9.65
		binomial	0.0	0.0	0.0	0.0	0.0	0.3	1.4	4.9	12.7	23.2	28.7	21.4	7.4	9.65
60.0	I	expt.	97.62	2.31												0.03
		binomial	97.1	2.9												0.03
60.0	II	expt.	0.0	0.0	0.0	0.5	0.2	0.8	2.1	7.1	16.9	25.8	26.0	16.3	4.4	9.27
		binomial	0.0	0.0	0.0	0.0	0.1	0.7	2.7	7.9	16.8	25.4	25.9	16.0	4.5	9.27
60.0	III	expt.	0.1	0.1	0.1	0.5	0.4	0.8	2.6	7.3	16.1	25.2	26.1	16.3	4.5	9.24
		binomial	0.0	0.0	0.0	0.0	0.1	0.7	2.9	8.2	17.2	25.5	25.5	15.5	4.3	9.24
		expt. <sup>a</sup>	0.1	0.1	0.1	0.5	0.4	0.8	2.7	7.5	16.1	25.1	26.0	16.2	4.5	9.22
77.5	I	expt.	97.35	1.76	0.41					0.03	0.12	0.19	0.09	0.03	0.02	0.07
		binomial	92.9	6.8	0.3											0.07
77.5	II	expt.	0.0	0.0	0.0	0.7	0.1	0.9	4.8	11.6	20.8	26.1	22.2	10.6	2.1	8.83
		binomial	0.0	0.0	0.0	0.1	0.3	1.5	5.0	11.9	20.7	25.6	21.4	10.9	2.5	8.83
77.5	III	expt.	0.0	0.0	0.0	0.4	0.3	1.4	4.6	11.6	20.7	26.1	21.5	11.1	2.2	8.82
		binomial	0.0	0.0	0.0	0.1	0.3	1.5	5.0	12.0	20.8	25.6	21.4	10.8	2.5	8.82

<sup>a</sup> calculated using the fragmentation scheme of Dowie, Whan and Kemball<sup>158</sup>.



TABLE 7.7     HYDROGEN-DEUTERIUM EXCHANGE ON  
CuX(10) AT 398 K

reaction	$(r/\text{atom s}^{-1} \text{ dg}^{-1}) \times 10^{16}$
1	10.4
2	no reaction
3	13.0
4	6.2
5	4.0

TABLE 7.8    ARRHENIUS PARAMETERS FOR THE ISOMERISATION OF I ON CuHX ZEOLITES

catalyst	temp. range/K	E/kJ mole <sup>-1</sup>	log <sub>10</sub> (A/molecule s <sup>-1</sup> dg <sup>-1</sup> )
NaHX	463-503	97	26.8
CuHX(2)	453-493	78	24.6
CuHX(5)	483-523	85	25.0
CuHX(10)	448-503	70	23.3
CuHX(2) <sup>†</sup>	423-448	110	28.8

<sup>†</sup> Arrhenius parameters for exchange of I with D<sub>2</sub>O.

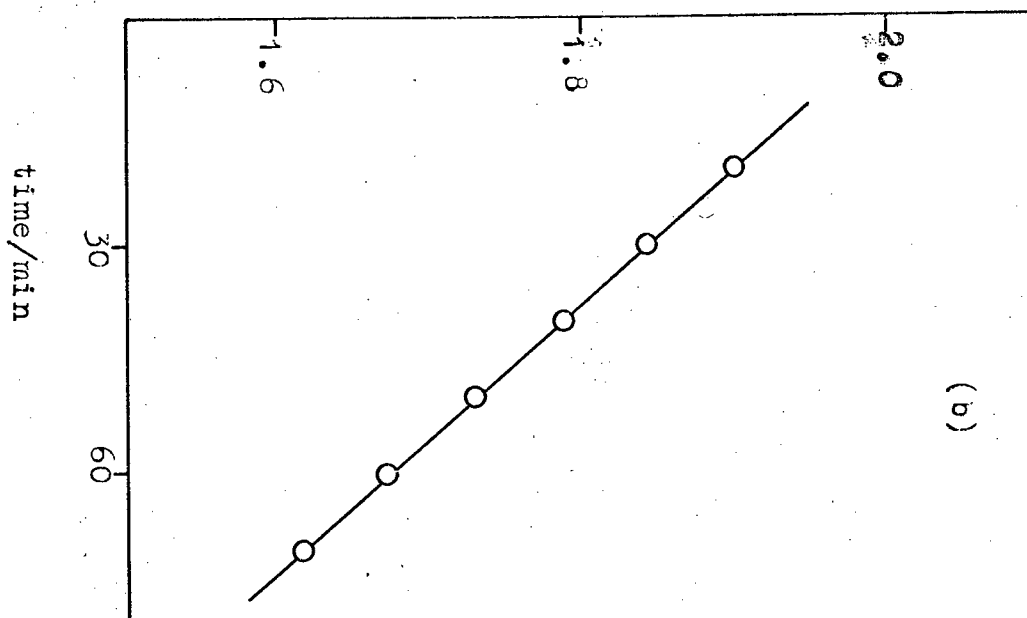
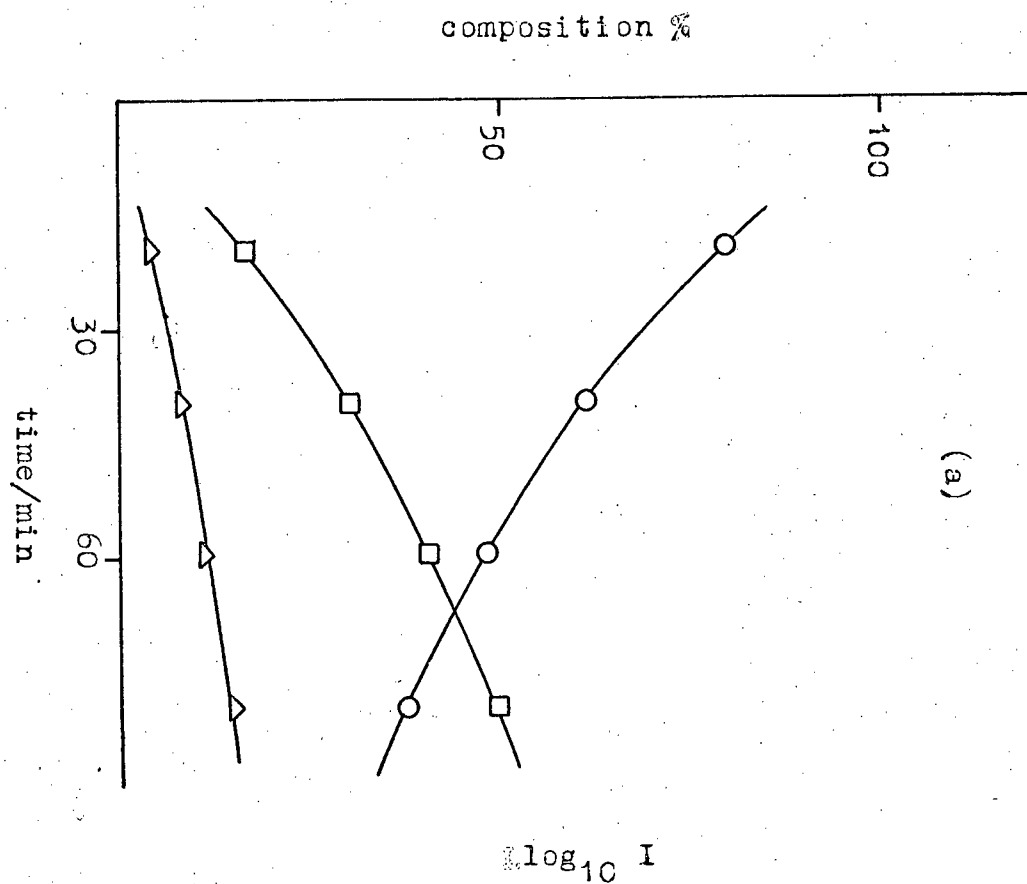


Fig.7.1- (a) Isomerisation of 3,3-dimethylbut-1-ene over CuX(10) at 448K. O = I,  $\Delta$  = II, and  $\square$  = III.

(b) First order plot of disappearance of I from data in fig.7.1(a).

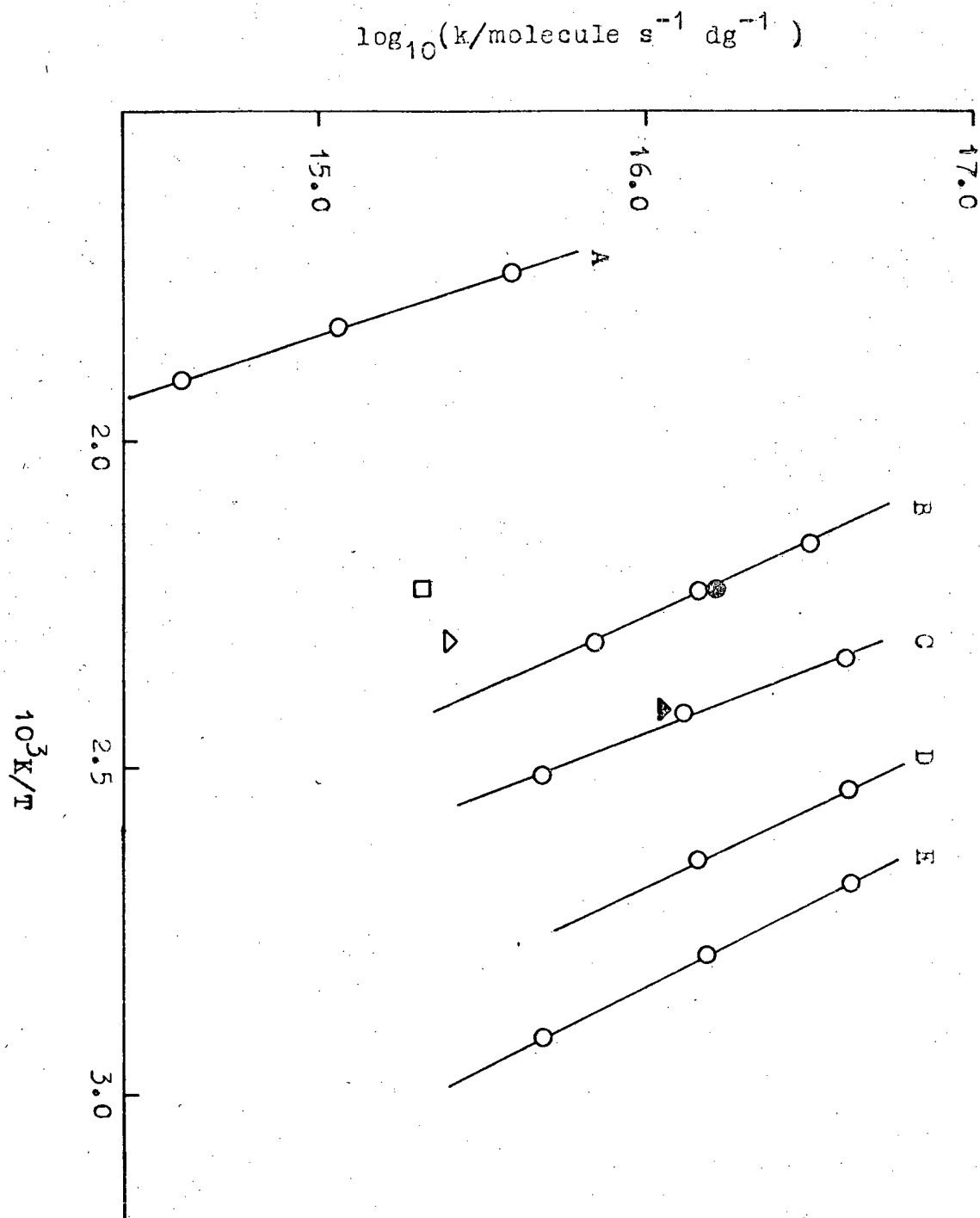


Fig.7.2- Isomerisation of I over NaX and CuX.

A = I over NaX, B = I over CuX(10),  
 C = I over CuX(25), D = I over CuX(43),  
 E = I over CuX(65),  $\square$  = I+H<sub>2</sub>O over CuX(10),  
 $\bullet$  = I+H<sub>2</sub> over CuX(10),  $\Delta$  = I over CuX(10)  
 after CO pretreatment, and  $\blacktriangle$  = I over  
 CuX(10) after hydrogen pretreatment.

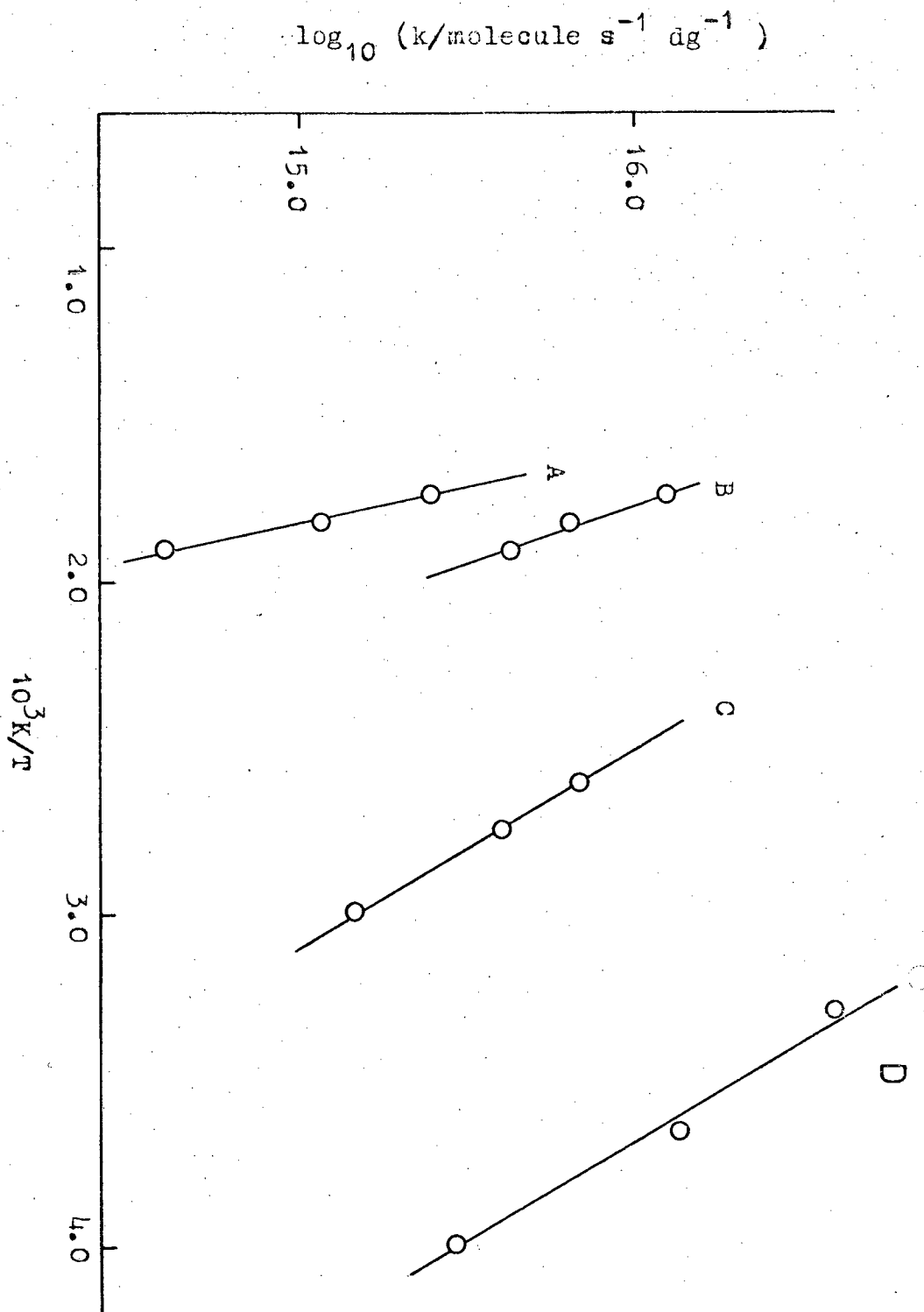


Fig.7.3- Reactions of dimethylbutenes. A = I over NaX, B = I+D<sub>2</sub>O over NaX, C = II over NaX, and D = II over CuX(10).

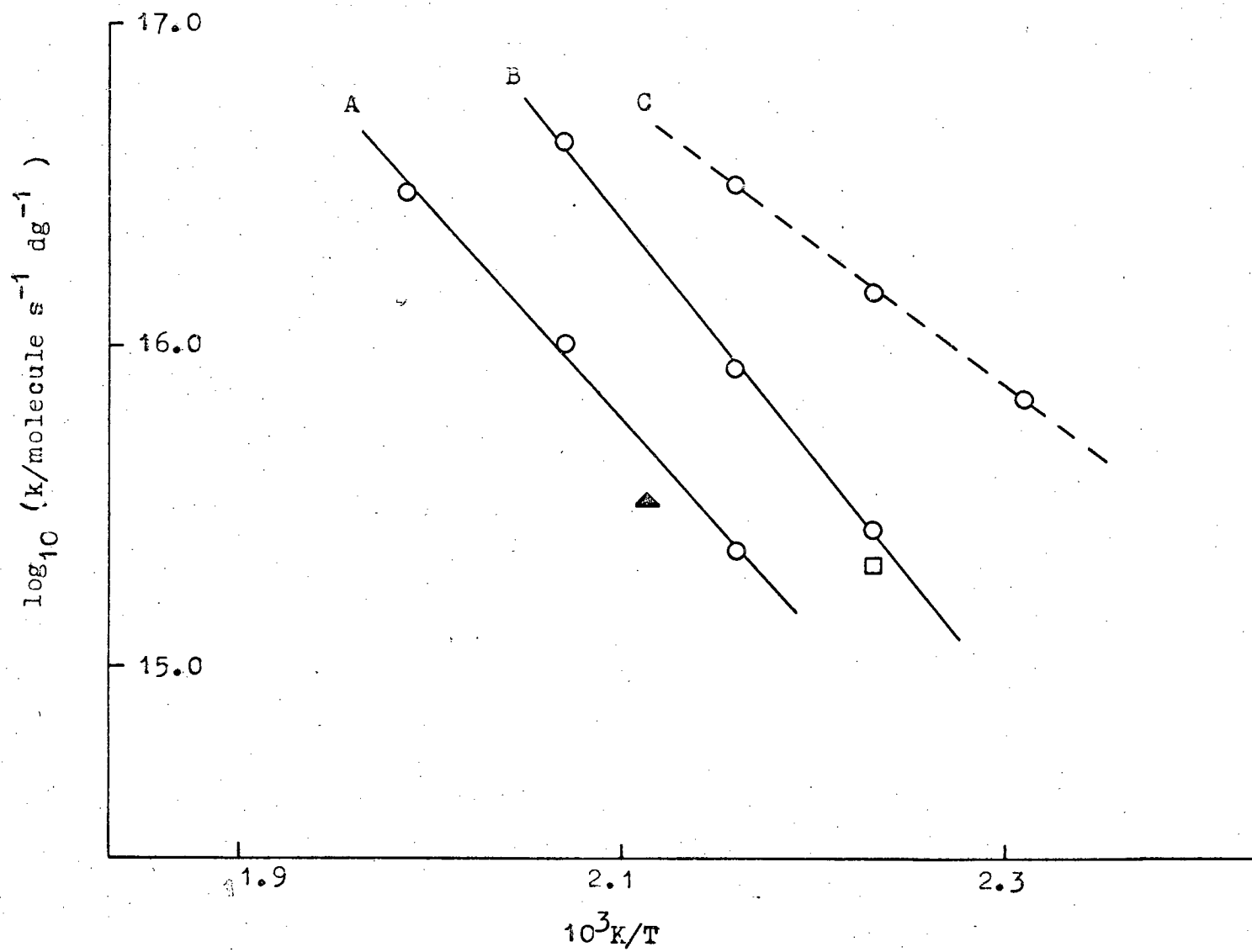


Fig. 7.4- Exchange reactions of dimethylbutenes over CuX(10). A = I+D<sub>2</sub>, B = I+D<sub>2</sub>O, C = isomerisation of I ( from fig. 7.2 ),  $\square$  = I+H<sub>2</sub>O, and  $\blacktriangle$  = exchange of II+D<sub>2</sub>.

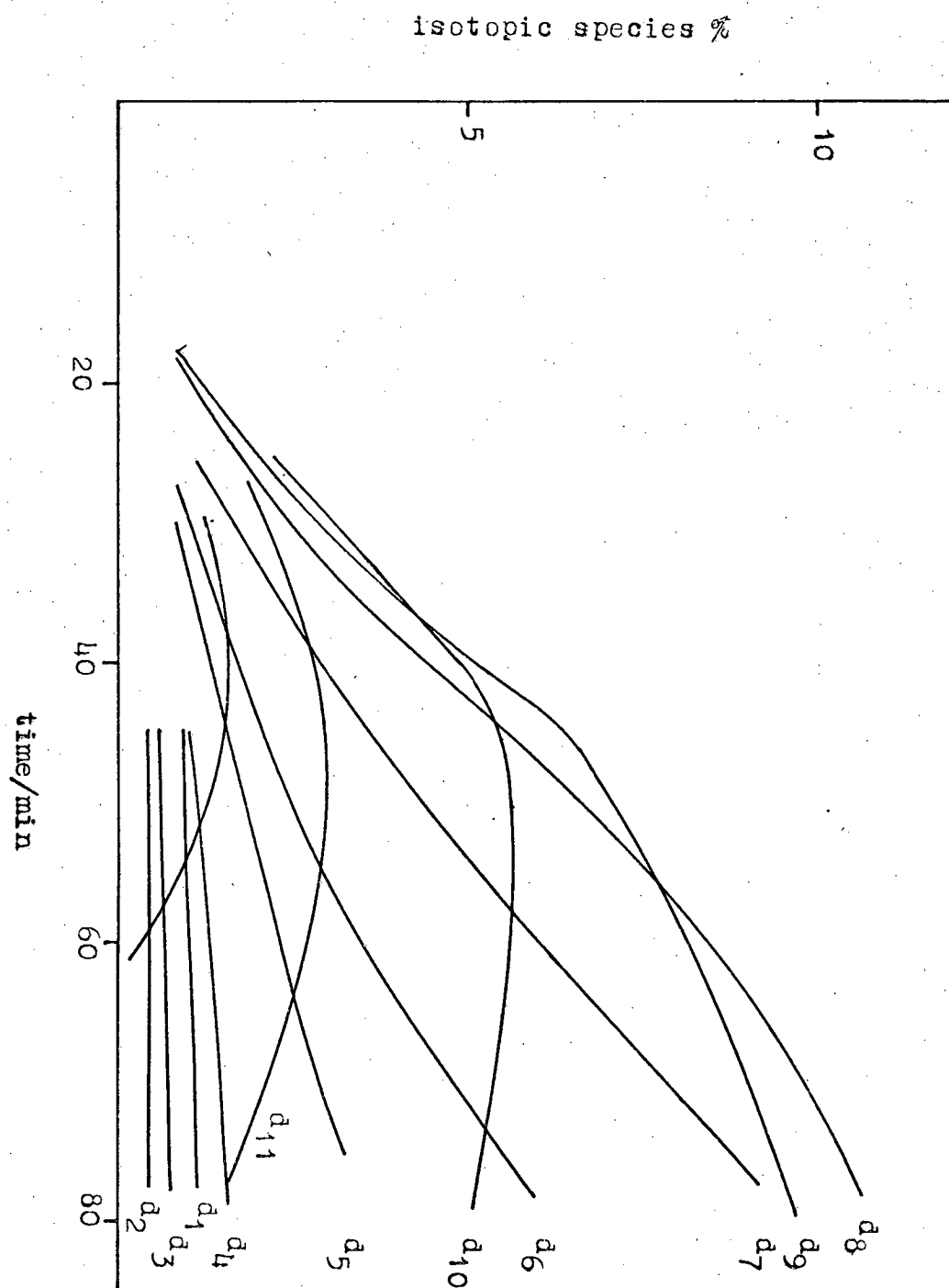


Fig.7.5- Exchange of I with  $D_2O$  over  $CuX(10)$  at 483K. Distribution of isotopic species as a function of time.

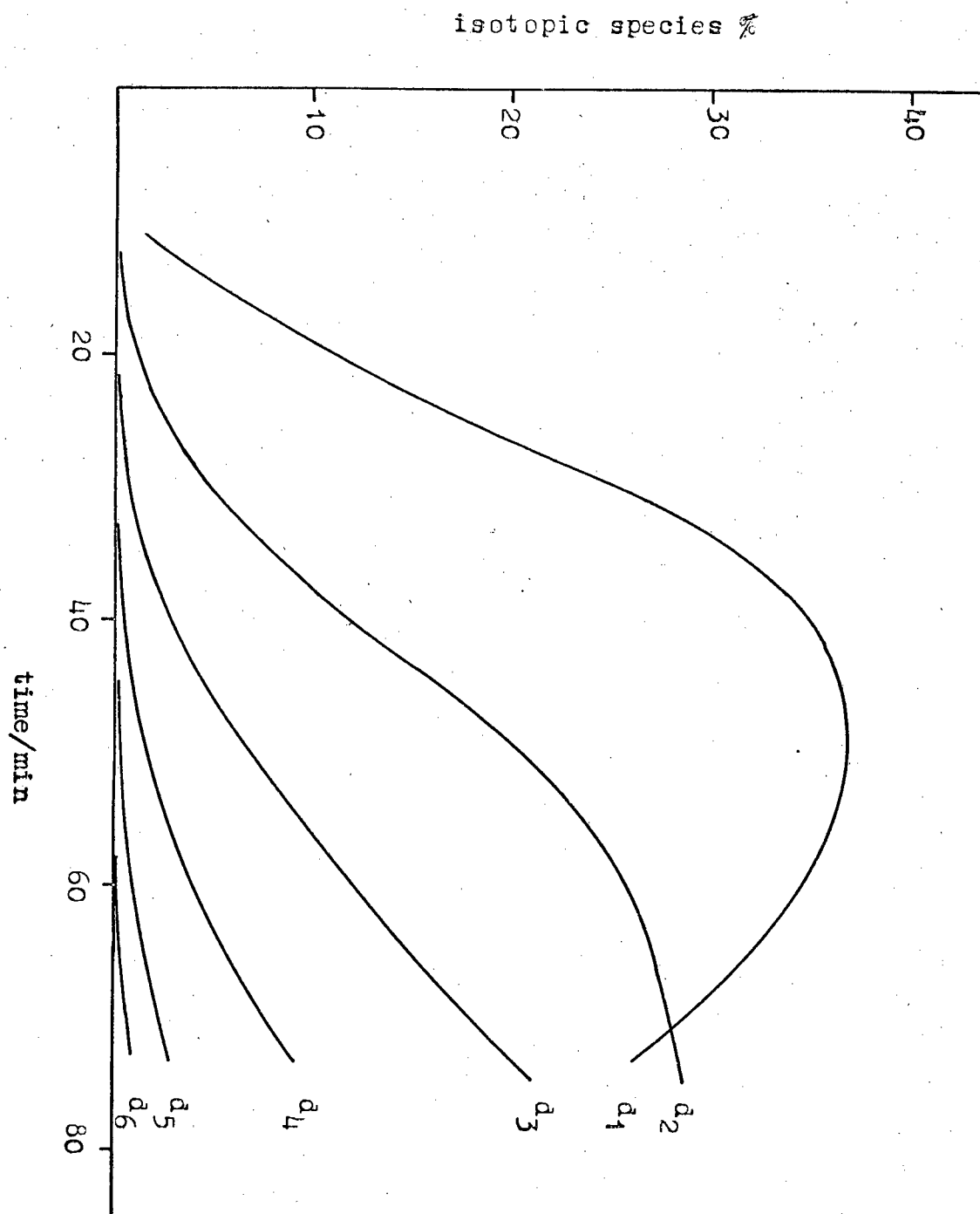


Fig.7.6- Exchange of I with  $D_2$  over  $CuX(10)$  at 503K. Distribution of isotopic species with time.



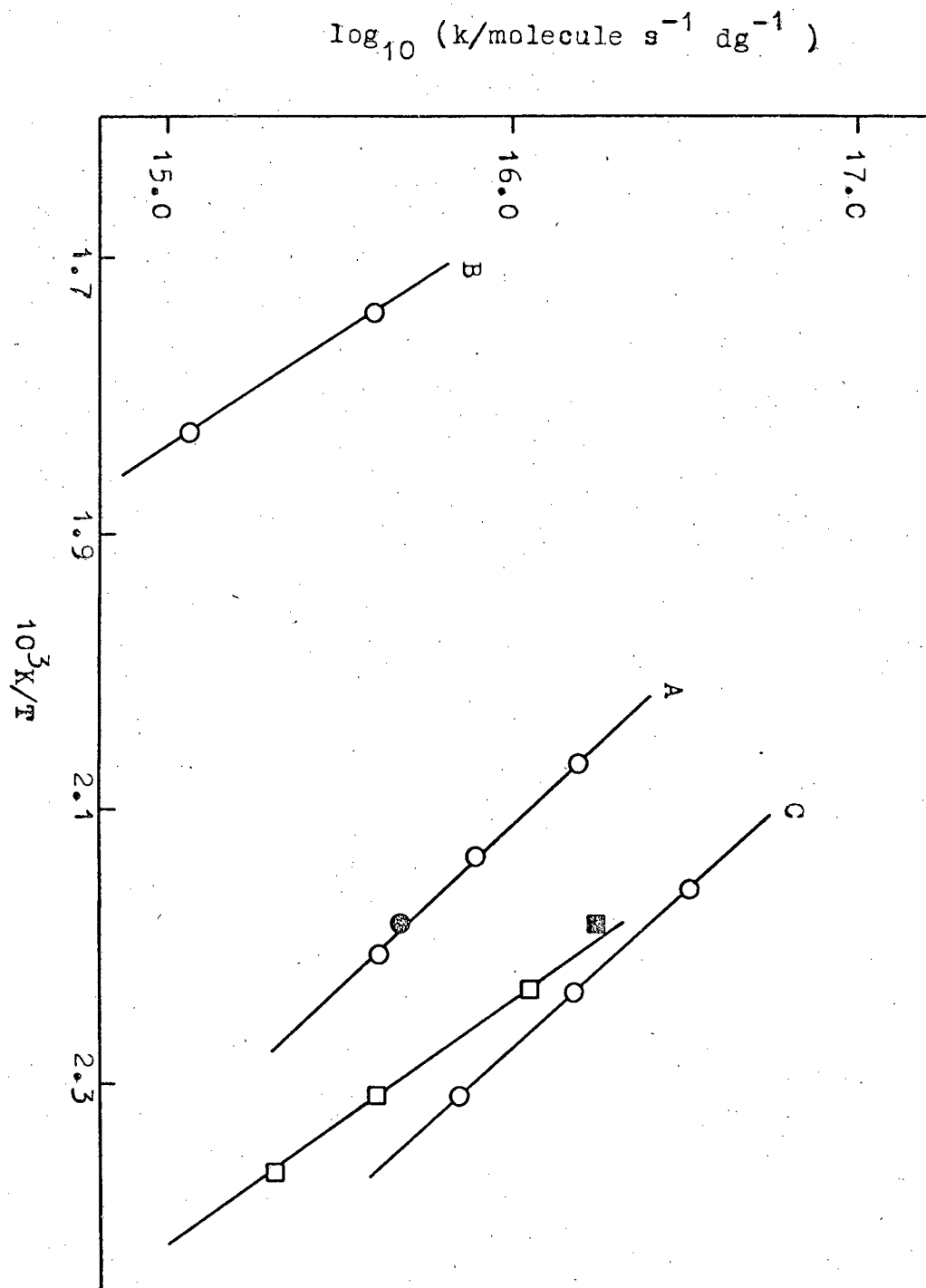


Fig.7.7- Reactions of I over CuHX(2).

A = isomerisation of I,  $\bullet$  = I+H<sub>2</sub>,  
 $\blacksquare$  = I+H<sub>2</sub>O,  $\square$  = exchange of I with D<sub>2</sub>O,  
 B and C = isomerisation of I over NaX  
 and CuX(10) resp.

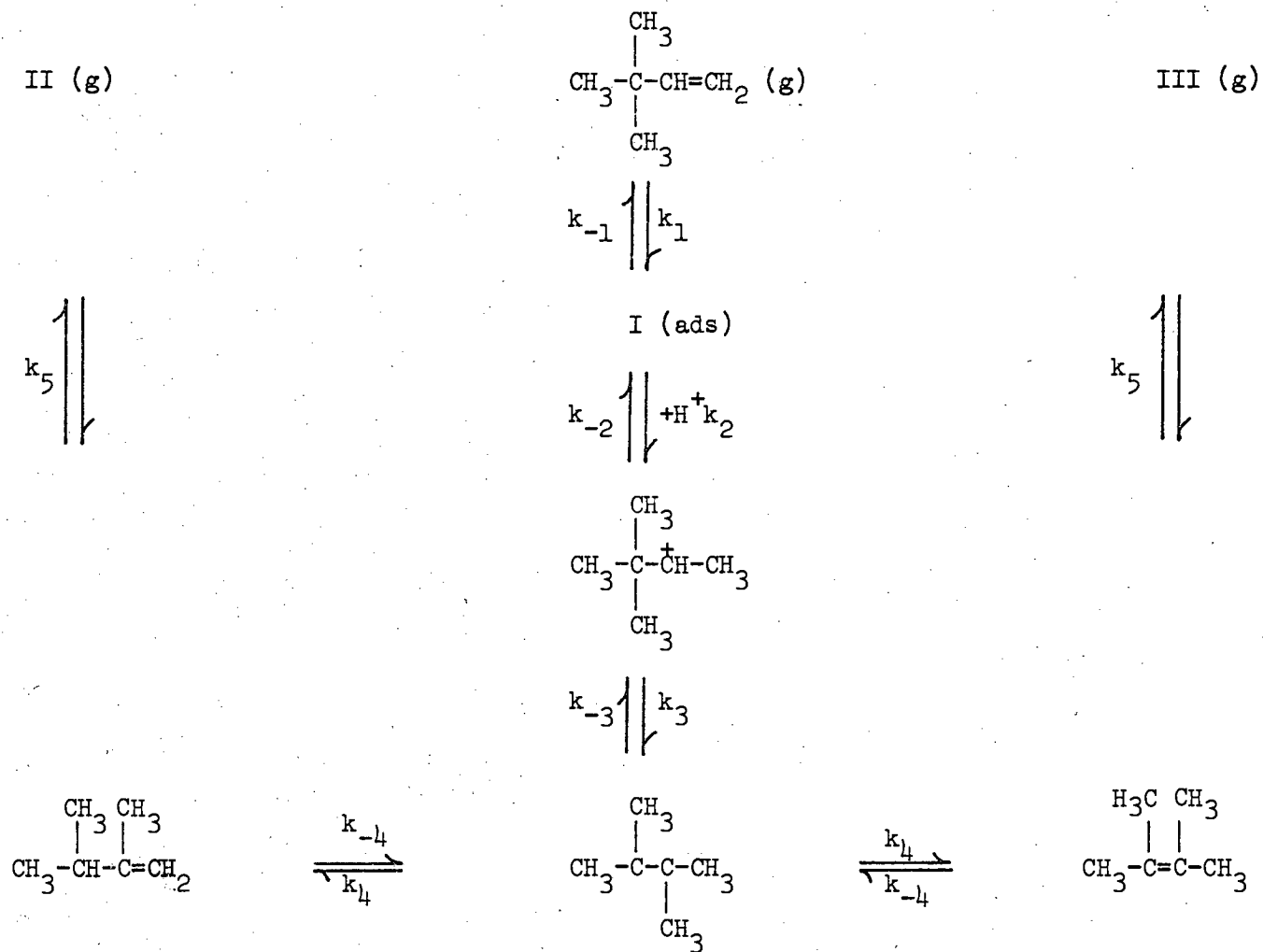


Fig. 7.8 - Reaction scheme for dimethylbutene isomerisation

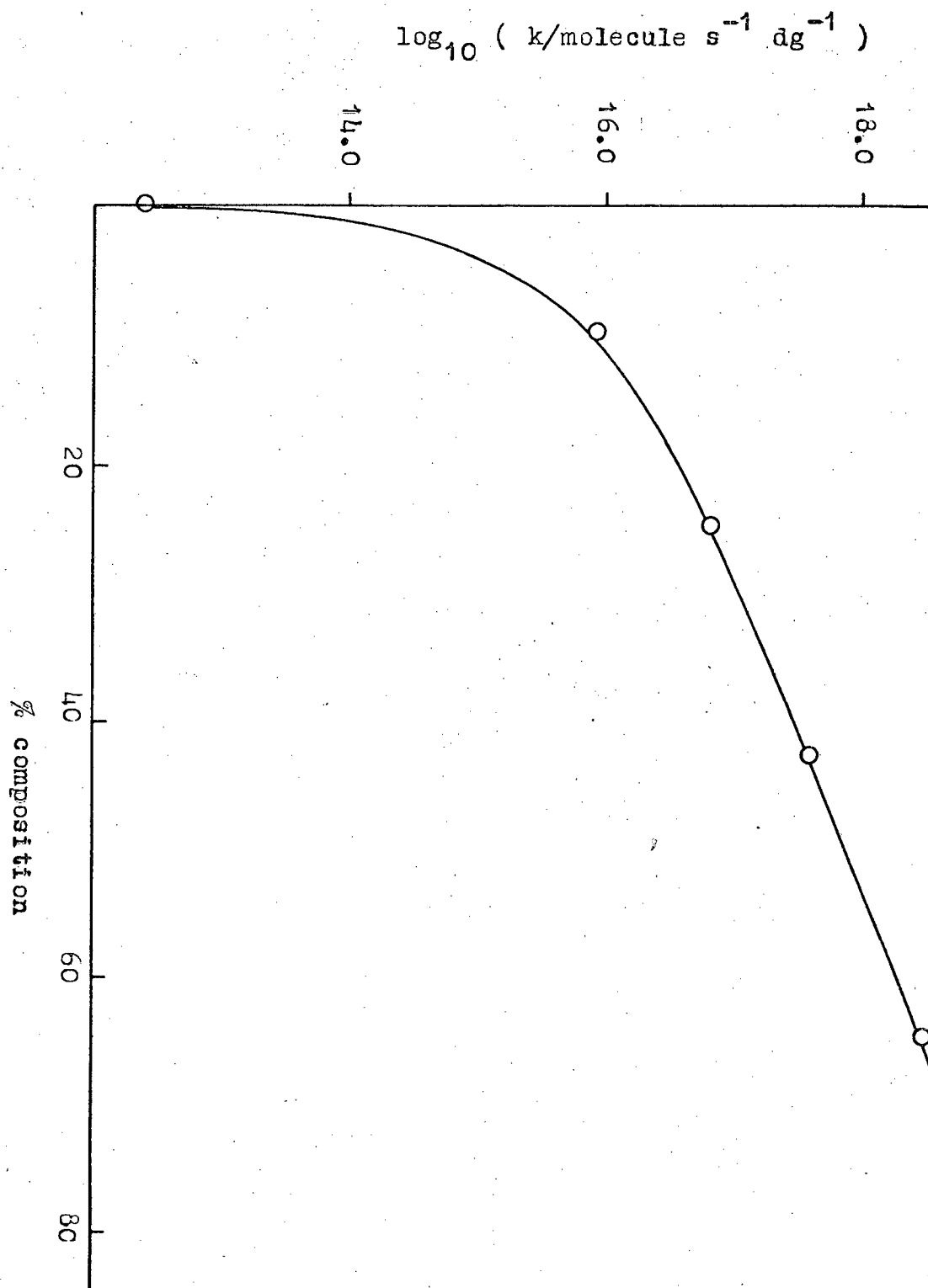


Fig.7.9- The activity for isomerisation of I as a function of extent of copper exchange. Values of  $\log_{10} k$  extrapolated to 435K.

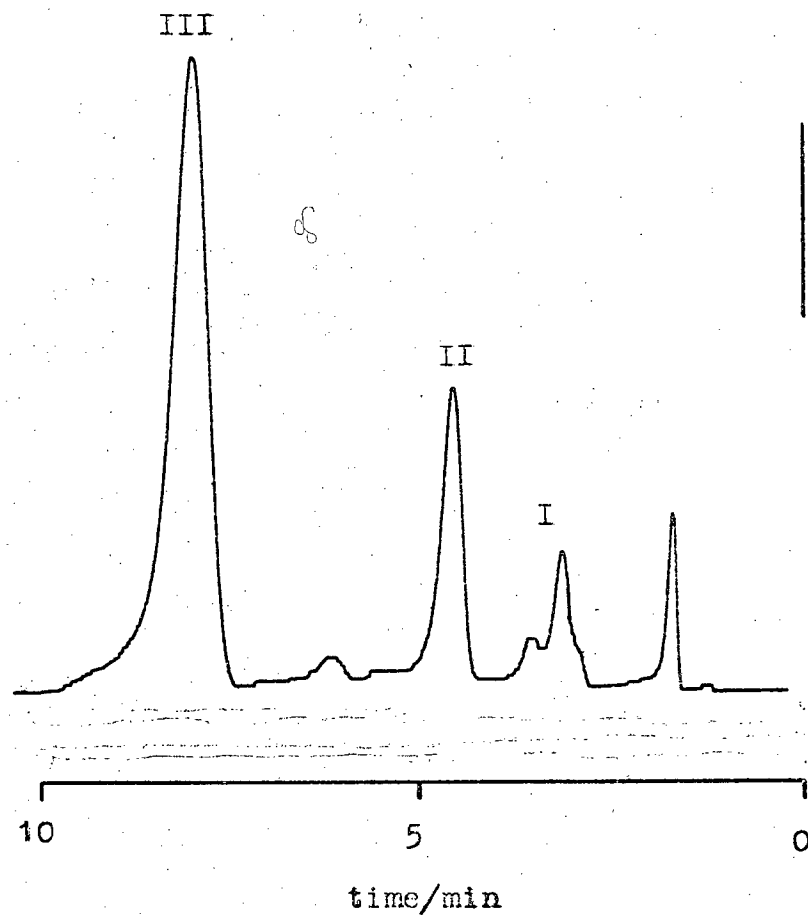
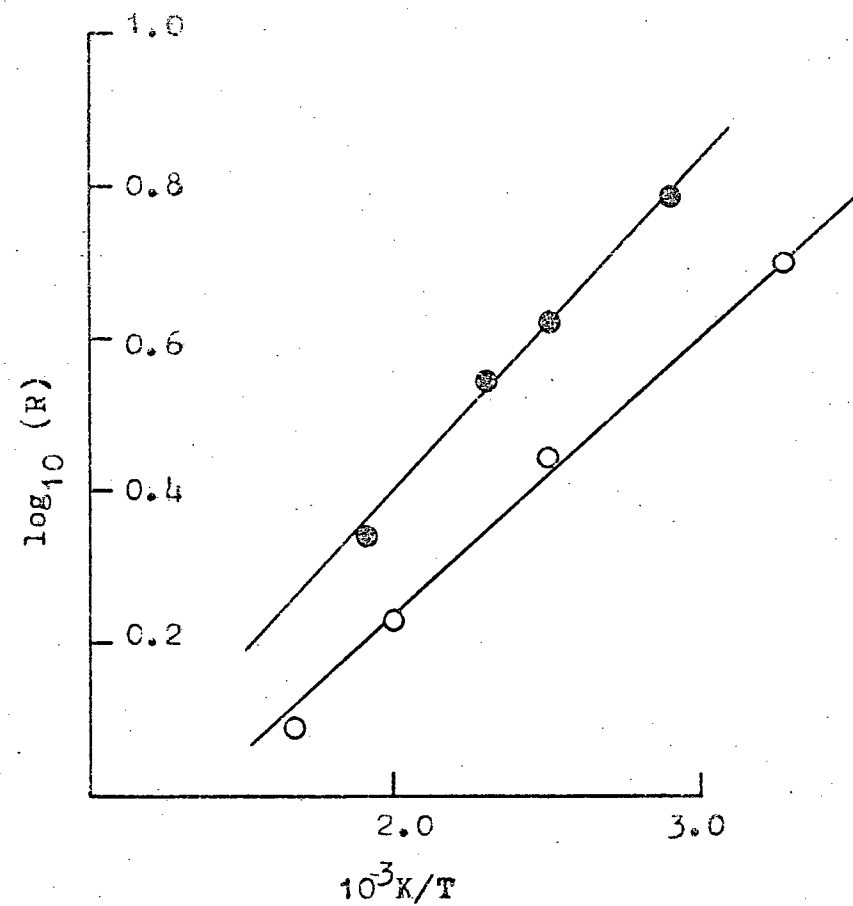


Fig.7.10(a)- Isomerisation of I ; product distribution obtained after an extended period of time.



(b)- Variation of product ratio R ( III/II ) with temperature.  
 ● = expt. and O = theoretical points resp.

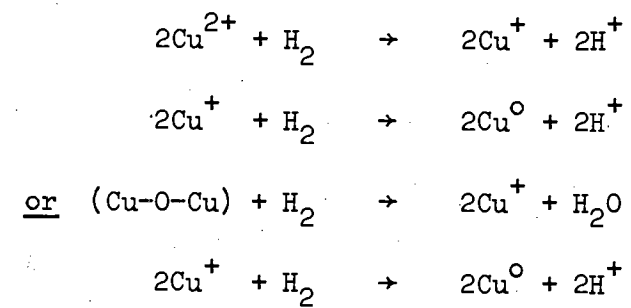
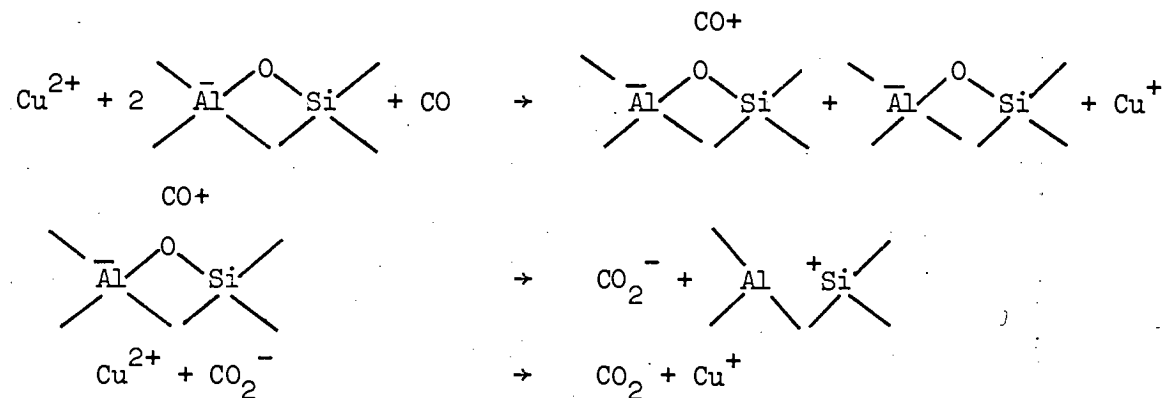


Fig. 7.11 - Reaction scheme for reduction of CuX by hydrogen.



giving overall

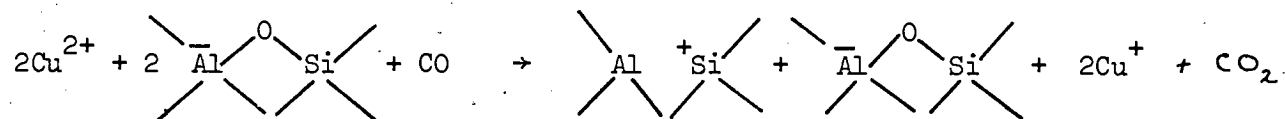


Fig. 7.12 - Reaction scheme for reduction of CuX by carbon monoxide

## Chapter VIII

### Reactions over ZnX Zeolites

#### 8.1 Olefin Isomerisation

The isomerisation of I was studied over ZnX(21) and ZnX(70), and the results are given in Table 8.1 with the corresponding Arrhenius plots in fig. 8.1(a). It can be seen that both catalysts are much more active than the parent NaX and that the catalytic activity increases with the degree of cation exchange. The character of the reaction was the same as that described for the CuX catalysts. When several experiments were carried out on the same sample of catalyst (evacuating at 673 K for 1 h between runs) it was found that the activity dropped on successive runs, this effect being much more pronounced with ZnX(70).

The effect of hydrogen and water on the rate of isomerisation of I at 428 K was examined over ZnX(21) and the results are incorporated into fig. 8.2. The presence of hydrogen was found to produce no change in rate but however, added water enhanced the rate of isomerisation by a factor of 3.

The isomerisation of II to III took place rapidly ( $3.7 \times 10^{16}$  molecule  $s^{-1} dg^{-1}$ ) at 273 K and was unaffected by hydrogen ( $k = 3.5 \times 10^{16}$  molecule  $s^{-1} dg^{-1}$ ). Water inhibited the reaction severely at low temperatures and only at 393 K was the rate of isomerisation ( $7.1 \times 10^{16}$  molecule  $s^{-1} dg^{-1}$ ) comparable to that at 273 K in the absence of water.

#### 8.2 Exchange Reactions

##### Exchange with D<sub>2</sub>O

The exchange of I with D<sub>2</sub>O was studied over ZnX(21) at 413 K. Multiple exchange was observed forming initial products with an average of 6 to 7 deuterium atoms per molecule, and the rate of reaction (expressed in terms of  $k_0$ ) agreed with the enhanced rate of isomerisation expected in the presence of water as shown in fig. 8.2.

The exchange of II with  $D_2O$  was examined over ZnX(21) at 387 K and initial products containing an average of 2.2 deuterium atoms per molecule were formed. The rate of exchange ( $k_o = 9.4 \times 10^{15} \text{ molecule s}^{-1} \text{ dg}^{-1}$ ) was comparable to the rate of isomerisation of II in the presence of water.

The reaction of I with  $D_2O$  over ZnX(70) was studied at 363 K. The rate of exchange was  $2.7 \times 10^{15} \text{ molecule s}^{-1} \text{ dg}^{-1}$  and an M value of 5 was found.

#### $H_2/D_2$ Exchange

The  $H_2/D_2$  exchange reaction was studied over ZnX(21) between 273-323 K and the following Arrhenius parameters were derived:

$$E_A = 13 \pm 3 \text{ kJ mole}^{-1} \text{ and}$$

$$\log_{10} A = 19.0 \pm 1.0 \text{ (A/molecule s}^{-1} \text{ dg}^{-1}\text{)}.$$

Pretreatment of the catalyst with hydrogen at 673 K for 1 h followed by evacuation at this temperature produced no change in the activity of the catalyst.

The reaction was also studied over ZnX(70) but the reaction became poisoned; an initial rate of  $1.8 \times 10^{16} \text{ atom s}^{-1} \text{ dg}^{-1}$  was obtained at 273 K.

The  $H_2/D_2$  exchange reaction was inhibited over ZnX(21) by preadsorbing a charge of I equivalent to 1.5 molecules per supercage and no appreciable exchange was found below 413 K.

#### Exchange with $D_2$

Stepwise exchange with deuterium occurred at similar rates starting with either I or II; the results are presented as an Arrhenius plot shown in fig. 8.2. The derived Arrhenius parameters were:

$$E_A = 52 \pm 8 \text{ kJ mole}^{-1} \text{ and}$$

$$\log_{10} A = 21.4 \pm 1.0 \text{ (A/molecule s}^{-1} \text{ dg}^{-1}\text{)}.$$

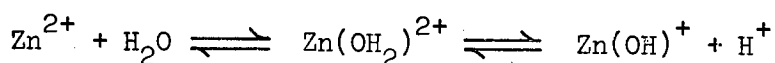


These exchange reactions were very much slower than the rates of isomerisation of the olefins (e.g. see fig. 8.2) and it was clear that a near-equilibrium mixture of olefins must have been formed before any appreciable exchange took place.

### 8.3 Discussion

The results obtained for ZnX zeolites are similar in nature to those observed for CuX zeolites and demonstrate quite clearly that these catalysts possess acidic properties. Infra-red investigations by Ward<sup>105,108,169</sup> have shown the presence of acidic structural silanol groups in X and Y zeolites containing  $\text{Zn}^{2+}$  ions and that Bronsted but not Lewis acidity is displayed at dehydration temperatures below 753 K.

In contrast to the behaviour observed with CuX, the addition of water was found to enhance the rate of isomerisation of I over ZnX(21). Ward<sup>108</sup> has observed that rehydration of ZnY resulted in the dissociation of the water and structural hydroxyl groups were formed. In the present case the observed increase in catalytic activity (despite the large amount of water used) may be due to the ready hydrolysis of the divalent cation in the following manner,



forming additional Bronsted acid sites. Cross<sup>102</sup> in a study of but-1-ene isomerisation over the ZnX zeolites used here obtained further evidence for the acidic nature of these catalysts. The initial product distribution was indicative of a carbonium ion mechanism and the presence of  $\text{D}_2\text{O}$  was found to enhance the rate of isomerisation. Fig. 8.1(b) illustrates the pronounced enhancement in catalytic activity for the isomerisation of I upon replacing  $\text{Na}^+$  ions by  $\text{Zn}^{2+}$  ions in the zeolite lattice, and emphasises that if cation-adsorbate interactions determine the activity then even at low levels of exchange some divalent cations must be present in surface

sites. Several studies have been made on the positions occupied by  $\text{Zn}^{2+}$  ions in X and Y zeolites. Barry and Lay<sup>60,61</sup>, utilising esr spectroscopy, observed that  $\text{Zn}^{2+}$  ions tend to favour type II, I' or II' sites where they acquire tetrahedral coordination rather than the octahedral site I positions especially if residual water fragments make the coordination tetrahedral. The origin of this preference is related to the covalent character of bonds to  $\text{Zn}^{2+}$  and the fact that  $\text{Zn}^{2+}$  is smaller and less electropositive than most of the group IA and IIA metal ions. Egerton and Stone<sup>65</sup> using the technique of CO adsorption found that the majority of  $\text{Zn}^{2+}$  ions are in internal sites but that considerably more divalent ions in ZnY occupy surface sites than in CuY. Upon raising the outgassing temperature from 643 to 843 K, a significant increase in the amount of CO adsorption occurred and this was thought to be due to  $\text{Zn}^{2+}$  ions in the sodalite unit (sites I' and II') becoming less stable due to removal of water, and moving to sites II or II<sup>0</sup>. The results from these studies indicate that for the ZnX(21) catalyst used here, under the experimental conditions employed, most of the  $\text{Zn}^{2+}$  ions are in hidden sites but relatively more  $\text{Zn}^{2+}$  ions are accessible to reagent molecules than  $\text{Cu}^{2+}$  ions in CuX.

Zinc does not exhibit multiple valence to any important degree, forms no compounds in which the 3d shell is other than full, and is normally considered as a non-transition element<sup>184</sup>. There are no known olefin complexes with zinc and so it is doubtful whether adsorbate-cation interactions are as important as in the case of CuX zeolites in determining the activity of the catalyst. A purely electrostatic interaction between the  $\text{Zn}^{2+}$  ion and olefin may be envisaged causing polarisation of the olefin molecule. The Bronsted acid sites (structural hydroxyl groups) present in the dehydrated zeolite are probably the primary active centres.

The exchange reaction of I with  $D_2O$  over ZnX catalysts was similar in nature to that observed over CuX(10) in that the olefin had to undergo isomerisation before exchange occurred. The exchange of II with  $D_2O$  was a more facile process and again the interconversion  $II \rightleftharpoons III$  occurred simultaneously with exchange.

For the exchange reactions of I and II with  $D_2$  nearly equilibrated mixtures of olefins would be present at the temperatures required for exchange and so the reactions can be considered to be equivalent.  $H_2/D_2$  exchange occurred readily over the ZnX catalysts and the higher temperatures required for olefin/ $D_2$  exchange may reflect the poisoning effect of the olefin on the sites which activate  $D_2$  or it may be that deuterium has to be supplied in the form of  $D^+$  species. However, as for CuX, it is likely that both effects are important.

Although NaX is relatively inactive for the  $H_2/D_2$  exchange reaction and replacement of  $Na^+$  ions by  $Zn^{2+}$  ions enhances the activity<sup>190</sup>, comparison of the results obtained by McCosh<sup>190</sup> and those in the present study does not reveal a correlation between activity and degree of ion-exchange as was found for the isomerisation of I. However, little is known about the nature of the sites active for  $H_2/D_2$  exchange and how these sites are affected by varying the degree of ion-exchange.

TABLE 8.1      ARRHENIUS PARAMETERS FOR THE ISOMERISATION OF I OVER ZnX ZEOLITES

catalyst	temp. range/K	E/kJ mole <sup>-1</sup>	log <sub>10</sub> (A/molecule s <sup>-1</sup> dg <sup>-1</sup> )	initial product ratio <sup>*</sup>
ZnX(21)	398-428	87	26.6	4.7
ZnX(70)	298-333	40	22.8	8.0

\* values refer to the lowest temperature quoted for each catalyst.

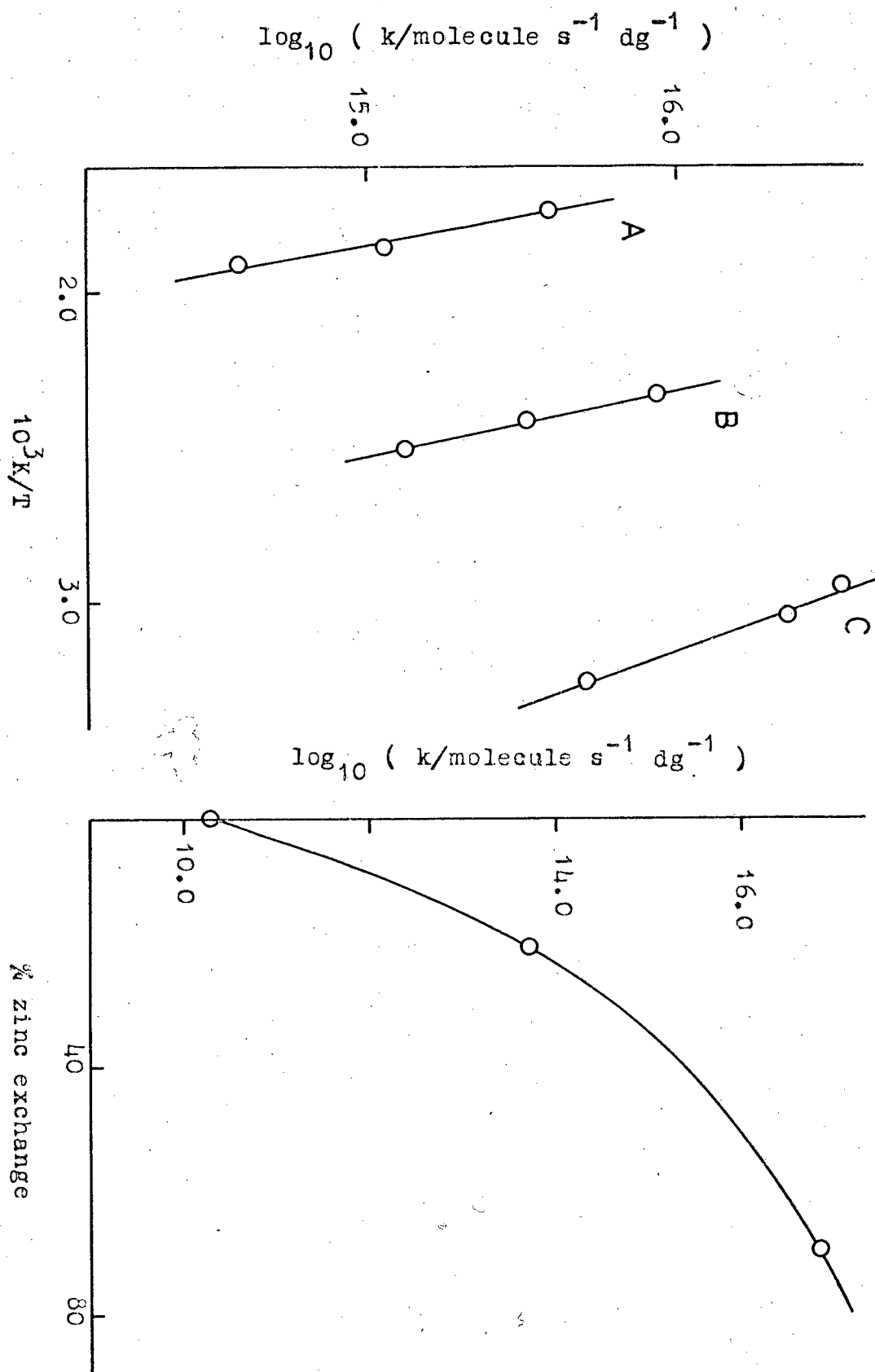
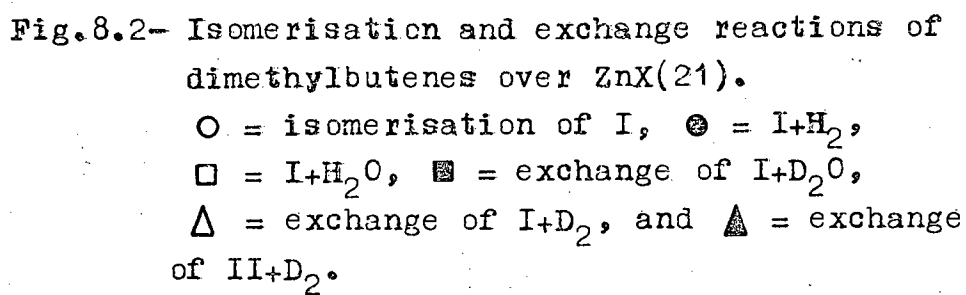


Fig.8.1- (a) Isomerisation of I over NaX and ZnX.  
A = I over NaX, B = I over ZnX(21),  
and C = I over ZnX(70).

(b) The activity for isomerisation as a  
function of extent of zinc content.  
Values of  $\log_{10} k$  extrapolated to 357K.



## Chapter IX

### Reactions over NiX Zeolites

#### 9.1 Olefin Isomerisation

The isomerisation of I was studied on a series of NiX catalysts which had been exchanged to differing extents. The character of the reaction on all catalysts was similar to that discussed for CuX catalysts. The results are presented as Arrhenius plots in fig. 9.1 and the derived parameters are summarised in Table 9.1. All of the catalysts studied were more active than the parent NaX which as reported in section 7.1, required temperatures above 523 K to promote the reaction. More detailed studies were made on the NiX(21) catalyst and to a lesser extent on NiX(9) and these will be discussed in the following sections.

#### 9.2 Reactions over NiX(21)

##### Olefin Isomerisation

When the isomerisation of I was carried out in the presence of water at 443 K, the rate was enhanced by a factor of 5. This is shown in fig. 9.2. The isomerisation of II to III occurred at an initial rate of  $1.8 \times 10^{17}$  molecule  $s^{-1}$  dg $^{-1}$  at 273 K, the character of the reaction being the same as for CuX and ZnX zeolites.

##### Hydrogen-Deuterium Exchange

The exchange of  $H_2-D_2$  was studied in the temperature range 273-328 K and the results are given in Table 9.2.

##### Hydrogenation Reactions

The most striking differences between NiX(21) and CuX or ZnX catalysts were observed when reactions of the olefins were studied with hydrogen or deuterium.

NiX(21) hydrogenated I exclusively to 2,2-dimethylbutane at temperatures well below those required to isomerise the olefin; a typical reaction is given in fig. 9.3 which shows that there was

a short induction period followed by a zero order reaction. These induction periods, which were difficult to measure, varied from 5 to 35 minutes and showed no definite trend with temperature; the subsequent rates of hydrogenation gave an Arrhenius plot but with some scatter of points (fig. 9.4). The Arrhenius parameters were,

$$E_A = 90 \pm 11 \text{ kJ mole}^{-1} \text{ and}$$
$$\log_{10} A = 28.9 \pm 1.6 \text{ (A/molecule s}^{-1} \text{ dg}^{-1}\text{)}.$$

When II was reacted with hydrogen over NiX(21) the usual rapid low temperature isomerisation to III occurred ( $k = 1.5 \times 10^{17}$  molecule  $\text{s}^{-1} \text{ dg}^{-1}$ ) at 273 K and then at 363 K both olefins were hydrogenated to 2,3-dimethylbutane as shown in fig. 9.5. The rates of hydrogenation of all 3 olefins were comparable at this temperature as shown in fig. 9.4. Once again an induction period was observed before the zero order hydrogenation reaction took place (fig. 9.5).

#### Exchange/Deuteration of I

Some exchange together with deuteration occurred with I and deuterium over NiX(21) and both reactions could be followed by means of the mass spectrometer. The neohehexane gave negligible contributions to the peaks in the  $C_6$  region which after corrections for naturally occurring isotopes and fragmentation were used to estimate the exchange of the olefin. The sum ( $\Sigma$ ) of the corrected peak heights of the parent peaks from mass 84 upwards was used as a measure of the olefin not yet converted to alkane. The main types of ion contributing to the  $C_5$  region of the mass spectrum were the  $C_5X_{11}^+$  ions (X representing H or D) from mass 71 upwards from the neohehexane and  $C_5X_9^+$  ions from mass 69 upwards from the olefin. It was possible to allow for the contributions to masses 71 and 72 from the exchanged olefins and then the corrected peak heights



from mass 71 upwards were used to estimate the isotopic composition of the neohexanes as  $C_5X_{11}^+$  species. The sum (X) of the amounts of these ions gave a measure of the total neohexane formed. The percentage deuteration Z was obtained from the relationship,

$$Z = 100 X / (X + a_1 Y_1) \quad 9.1$$

where  $a_1$  is a factor allowing for the relative sensitivities of the two kinds of ions.

A second method of calculating the percentage deuteration was based upon the sum ( $Y_2$ ) of the corrected amounts of  $C_5X_9^+$  ions as a measure of the unreacted olefin in an equation equivalent to 9.1, with an appropriate sensitivity factor  $a_2$ . The values for  $a_1$  and  $a_2$  were 2.81 and 0.74 respectively.

The reaction of I with  $D_2$  over NiX(21) was studied at 373 K. After an induction period of 10 to 15 minutes stepwise exchange of the olefin occurred at a rate of  $8.0 \times 10^{15}$  molecule  $s^{-1}$   $dg^{-1}$  producing up to the  $d_3$  compound. This reaction was accompanied by a zero order formation of 2,2-dimethylbutanes. There was good agreement between the rates of deuteration measured in the two ways as demonstrated in fig. 9.4. The isotopic composition of the products estimated as  $C_5X_{11}^+$  ions at two stages of the reaction are given in Table 9.3.

### 9.3 Reactions over treated NiX(21)

The hydrogenation and isomerisation of I were examined over NiX(21) catalysts subjected to different pretreatments in order to gain more information about the nature of the sites responsible for the two reactions. Most of the results are shown as additional points on figs. 9.2 and 9.4.

#### Oxygen Pretreatment

The catalyst was heated in oxygen ( $13 \text{ kNm}^{-2}$ ) at 673 K for 12 h and then evacuated for 1 h at the same temperature. This

had virtually no effect upon the rate of isomerisation of I at 423 K, but reduced the rate of hydrogenation at 398 K by a factor of about  $3 \times 10^4$  with the consequence that isomerisation of the olefin, which now took place, was faster than hydrogenation on the oxygen-treated catalyst.

#### Hydrogen Pretreatment

The catalyst was heated in hydrogen ( $5 \text{ kNm}^{-2}$ ) at 673 K for 1 h and then evacuated for 10 minutes at the same temperature. This pretreatment enhanced the rate of isomerisation of I at 423 K by a factor of 10 but the rate of hydrogenation increased by a factor of  $10^4$  to  $10^5$  at 293 K and no induction periods were now observed. The hydrogen-deuterium exchange reaction was too fast to follow at 293 K after this pretreatment.

#### Carbon Monoxide Pretreatment

A charge of  $8.0 \times 10^{19}$  molecules of CO, which is equivalent to one molecule per nickel ion, was contacted with the catalyst at 293 K for 30 minutes and then evacuated for 5 minutes at this temperature. The uptake of carbon monoxide measured by use of a McLeod gauge, appeared to be very small and less than one molecule per 100 nickel ions. This pretreatment had no influence upon the rate of isomerisation of I but the rate of hydrogenation was reduced by a factor of  $10^3$  to  $10^4$  at 428 K. The same effect was observed if the excess CO was not pumped off but allowed to remain in the reaction vessel. The rate of exchange of hydrogen with deuterium was reduced by a factor of 7 at 293 K by the preadsorption of CO.

A few experiments were carried out on hydrogen-treated catalysts subsequently exposed to CO. The uptake of CO was no greater than observed for the untreated catalysts but the high activity of the hydrogen-treated catalysts was destroyed, i.e.

catalysts subjected to hydrogen pretreatment and then exposed to CO behaved in a similar manner to untreated catalysts for the reaction of I with hydrogen.

#### 9.4 Reactions over NiX(9)

##### Olefin Isomerisation

The results are presented on the Arrhenius plot shown in fig. 9.6. The effect of water was to reduce the rate of isomerisation of I at 453 K by a factor of about 10. The isomerisation of II to III occurred readily at 273 K with a rate of  $5.5 \times 10^{16}$  molecule  $s^{-1}$  dg $^{-1}$ . Water completely inhibited the reaction at this temperature and isomerisation was only observed at 373 K ( $k = 2.2 \times 10^{15}$  molecule  $s^{-1}$  dg $^{-1}$ ).

##### H<sub>2</sub>/D<sub>2</sub> Exchange

This reaction was studied in the temperature range 273-323 K. The results are summarised in Table 9.2. Oxygen pretreatment of this catalyst (using the method described above) resulted in no appreciable exchange taking place below 363 K.

##### Hydrogenation

The hydrogenation of I to 2,2-dimethylbutane was studied at 333 K and as observed with NiX(21), when II was reacted with hydrogen only rapid isomerisation to III took place ( $1.8 \times 10^{17}$  molecule  $s^{-1}$  dg $^{-1}$ ) at 273 K but on raising the temperature to 338 K, both olefins were hydrogenated to 2,3-dimethylbutane. Small induction periods were observed as for NiX(21).

##### Exchange/Deuteration of I

The reaction of I with deuterium was studied over NiX(9) at 293, 316 and 373 K and stepwise exchange was observed forming up to the d<sub>3</sub> compound. From the results the following Arrhenius parameters were derived,

$$E_A = 31 \pm 4 \text{ kJ mole}^{-1} \text{ and}$$
$$\log_{10} A = 20.5 \pm 0.6 \text{ (A/molecule s}^{-1} \text{ dg}^{-1}\text{)}.$$

Deuteration of I, studied at 293 and 316 K, occurred simultaneously with exchange and the results were similar in nature to those obtained for NiX(21). The rates of deuteration calculated using the two forms of equation 9.1 were in excellent agreement. The rates of hydrogenation of the C<sub>6</sub> olefins (previous section) agreed well with the data for the deuteration of I and when the results were combined the following values were obtained,

$$E_A = 19 \pm 2 \text{ kJ mole}^{-1} \text{ and}$$
$$\log_{10} A = 18.8 \pm 0.5 \text{ (A/molecule s}^{-1} \text{ dg}^{-1}\text{)}.$$

#### Exchange with D<sub>2</sub>O

The reaction of I with D<sub>2</sub>O was studied at 453 K and multiple exchange was observed, with initial products containing an average of 9 deuterium atoms per molecule. The rate of disappearance of the light hydrocarbon correlated well with the rate of isomerisation of I in the presence of water (fig. 9.6) indicating that isomerisation and exchange were occurring simultaneously.

### 9.5 Discussion

#### Olefin Isomerisation

The results clearly demonstrate that NiX zeolites have catalytic properties of a dual function type. Firstly, they show behaviour typical of acidic catalysts in being active for the isomerisation of I. The infra-red studies of Ward<sup>105,108,169</sup> have shown that NiY zeolites possess acidic structural hydroxyl groups and that Bronsted but not Lewis acidity is exhibited by samples calcined at low temperatures (<753 K).

The increase in activity when the isomerisation of I was carried out in the presence of water over NiX(21) is typical of a proton donor enhancing the rate of a carbonium ion type reaction. A similar effect was observed with NiX(25) and NiX(41) and may be ascribed either to hydrolysis of the divalent cation or to the strong electrostatic field of the cation causing dissociation of adsorbed water molecules. In support of this Ward<sup>169</sup> has observed that water adsorbed on to NiY zeolites was transformed into structural hydroxyl groups.

All of the NiX catalysts examined in this work displayed high activity for the isomerisation of I and this illustrates once again that replacing  $\text{Na}^+$  ions by divalent cations ( $\text{Ni}^{2+}$ ) has a profound effect upon the catalytic activity. Any discussion about the catalytic activity of NiX zeolites requires information on the positions occupied by nickel ions in the zeolite framework, and from adsorption<sup>65</sup>, ir<sup>58</sup>, uv<sup>185</sup> and X-ray diffraction studies<sup>186</sup> it appears that nickel ions have a preference for site I positions. In recent detailed studies of NiY zeolites<sup>187,188</sup> Gallezot et al. found that nickel ions migrate into the hexagonal prisms upon progressive removal of water and on total dehydration the nickel ions strongly preferred site I where they have octahedral coordination but their number was limited to 12 per unit cell. The  $\text{Ni}^{2+}$  ions occupying site I positions were not displaced by large reagent molecules such as pyridine. This situation is in marked contrast to that encountered for  $\text{Cu}^{2+}$  ions<sup>175,176</sup> which were located preferentially in site I' positions and found to migrate under the influence of various adsorbates. The consequences for the catalytic activity of NiX zeolites are that for low-exchanged samples increasing the dehydration temperature would decrease the activity and since the cations in the hexagonal prisms are not catalytically active

because they have achieved a stable coordination they can neither move easily towards the supercages to react with adsorbed molecules nor can they be reached by these molecules. However, as the results of this work demonstrate, if nickel ions do influence the catalytic activity then even in low exchanged samples some  $\text{Ni}^{2+}$  ions must be available outside the hexagonal prisms.

#### Comparison of Transition Metal Zeolites

The isomerisation of I has proved to be a useful test reaction for measuring the ability of a catalyst to form carbonium ions from the olefin and it is interesting to compare the activities of the TM zeolites used in the present work for this reaction. The data, presented in Table 9.4, refers to 21% exchanged samples the results for which have been extrapolated to a common temperature of 435 K. The activity of a CuX(21) sample was determined from fig. 7.9. The data shows that the different TM zeolites display comparable activity for this acid catalysed reaction.

The isomerisation of II to III can also be described in terms of a carbonium mechanism (fig. 7.8) and the results obtained from the various studies of this reaction have been extrapolated to 273 K and are presented in Table 9.5. The ion-exchanged zeolites display much greater activity than the parent NaX but there is very little difference in activity among the TM zeolites. However, the interconversion  $\text{II} \rightleftharpoons \text{III}$  need not necessarily involve carbonium ion intermediates and others may be invoked e.g. allylic carbanion or radical, and it is not possible to say whether the same mechanism applies to all the zeolite catalysts or if the zeolites display an individual preference.

Other test reactions for carbonium ion activity have been studied over zeolites containing Cu, Ni and Zn. For o-xylene isomerisation Ward<sup>105</sup> found that NiY displayed much greater activity

than CuY and ZnY which were of comparable activity and these three catalysts were more active than conventional silica-alumina catalysts. Merrill and Arey<sup>189</sup> observed that the differences in activity between zeolites containing Ni, Cu and Zn were slight for the cracking of methylcyclopentane and toluene disproportionation.

#### Radical Type Behaviour

The most striking behaviour shown by NiX zeolites, in marked contrast to CuX and ZnX zeolites, was their ability to catalyse the hydrogenation of the C<sub>6</sub> olefins and to bring about the low temperature exchange of I with deuterium. The nature of these reactions is more typical of metallic catalysts where radical intermediates are postulated than of oxide catalysts where charged or polarised intermediates are invoked. Similar observations have been made by other workers; NiX zeolites have been shown to possess high activity for H<sub>2</sub>/D<sub>2</sub> exchange<sup>190</sup>, to promote simultaneous exchange and deuteration in reactions of ethylene and propylene with deuterium<sup>191</sup>, to exhibit metallic character for alkylbenzene exchange with deuterium<sup>192</sup> and to give results indicative of a radical type mechanism from isomerisation and hydrogenation studies of n-butenes<sup>103</sup>.

In order to account for this radical type behaviour it is proposed that reduction of certain Ni<sup>2+</sup> ions in the zeolite lattice (either to Ni<sup>+</sup> and/or Ni<sup>0</sup>) produces the active catalyst and the reduced nickel species function as active centres. There are several observations which support this view. Induction periods were a feature of the hydrogenation studies (and of others mentioned above) and are compatible with such a reduction process. Oxygen pretreatment of the catalyst resulted in a severe loss of hydrogenation activity due to, presumably, the oxidation of any reduced nickel species present back to Ni<sup>2+</sup>. If this is so, it would appear that in a

normally outgassed catalyst a limited but variable amount of reduction has occurred and this would account not only for the variation in hydrogenation activity (as shown by the scatter of points in fig. 9.4) but also in the lengths of the induction periods.

Further evidence for the presence of reduced nickel species in NiX zeolites comes from esr studies. Cross<sup>103</sup> observed a broad signal from outgassed NiX and this is in agreement with the results obtained from a preliminary investigation of the NiX(9) catalyst used in the present study<sup>193</sup>. In this, a broad signal was present in the spectrum of the dehydrated catalyst and after heating in but-1-ene at 473 K the intensity of the broad signal developed and superimposed on this was a sharp signal. A tentative explanation is that the broad signal may be attributed to the formation of  $\text{Ni}^0$  and the sharp signal to  $\text{Ni}^+$ . Since  $\text{C}_6$  olefins are known to be more efficient than but-1-ene for reducing  $\text{Cu}^{2+}$  ions in CuX zeolites<sup>175</sup> they should be capable of producing the above changes with NiX zeolites at lower temperatures. The results indicate the importance of interaction between the olefin and nickel ions, and the reduction resulting from such interactions may be responsible for the induction periods.

Hydrogen pretreatment produced a catalyst which displayed enhanced hydrogenation activity and resulted in the elimination of the induction periods. Several studies<sup>183,194,195</sup> have shown that nickel ions in the zeolite lattice may be reduced to the metal by such a pretreatment. The formation of crystalline metallic nickel on the external surface of the zeolite is believed to arise from the aggregation of either metal atoms or very small crystallites showing that the metal atoms formed are only loosely held to the lattice at the temperature of reduction. In the present study due



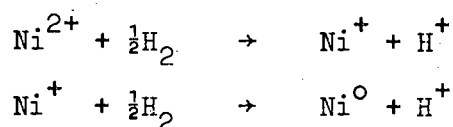
to the technique employed it was not possible to determine the extent of reduction but from previous work<sup>183,194-196</sup> where factors such as temperature, pressure of hydrogen and time of exposure were studied it seems probable that the reduction process was irreversible. In agreement with this Pope and Kemball<sup>192</sup> found that whereas pretreating NiX with hydrogen at 521-573 K produced reversible changes treatment at 623 K gave rise to irreversible change as evidenced by esr spectroscopy. This enhanced catalytic activity subsequent to hydrogen pretreatment has been noted in the studies of n-butenes<sup>103</sup> and alkylcyclopropanes<sup>155</sup> over some of the NiX catalysts used in the present study. This, together with the elimination of the induction periods may be rationalised in terms of the pretreatment leading to the reduction of  $\text{Ni}^{2+}$  ions at certain active sites in the lattice.

Carbon monoxide was chosen as a suitable 'poison' because it is thought to be too large a molecule to penetrate the sodalite unit at the relatively low temperatures used in the present work and so should be capable of interacting only with exposed or surface nickel ions. One of the most striking features of this work was the extremely small uptake of CO by the catalyst and although the amount of adsorption is small it does indicate that some nickel species are present in surface sites. Assuming that one CO molecule interacts with one nickel ion then less than 1% of the nickel ions occupy surface sites. Even after hydrogen pretreatment there was no significant increase in CO adsorption. This was unexpected and may be due to the reduced nickel species being present in hidden sites with little migration having occurred or that only  $\text{Ni}^{2+}$  ions in certain sites have been reduced since it is known that nickel ions in different environments are reduced at different rates<sup>196</sup>.

The effect of CO adsorption is dramatic causing marked inhibition of hydrogenation activity. If the active centres are reduced nickel species then the results indicate that the number of

such catalytically active centres is extremely small. CO has been shown to coordinate more strongly with surface  $\text{Ni}^+$  than  $\text{Ni}^{2+}$  <sup>59</sup>, a temperature of 298 K being sufficient to remove the CO from  $\text{Ni}^{\text{II}}\text{Y}$  but much higher temperatures required to desorb CO from  $\text{Ni}^{\text{I}}\text{Y}$ . In the present work the poisoning effect of CO remained unaltered despite evacuation at 293 K indicating the interaction of CO with reduced nickel and although higher temperatures were not employed Wall et al. <sup>197</sup> noted that CO adsorption inhibited but-1-ene isomerisation over the  $\text{NiX}(41)$  catalyst used in the present study but that the original activity could be restored by evacuation at 393 K. Therefore, if the active centre is  $\text{Ni}^+$ , and this has been shown to possess a remarkable chemical activity <sup>59</sup>, coordination of the CO molecule with the reduced nickel species would prevent the interaction of the olefin and hydrogen molecules with the latter.

The results demonstrate that the various catalyst pretreatments greatly affected the hydrogenation activity but had virtually no effect upon the activity of  $\text{NiX}$  for the isomerisation of I. This must reflect a difference in the nature of the two reactions and suggests the participation of at least two different active sites. For the isomerisation reactions no induction periods were observed and only the hydrogen pretreatment produced an appreciable change in activity. This reaction is envisaged as taking place primarily on Bronsted acid sites (structural hydroxyl groups) in the zeolite framework with hydrogen pretreatment leading to an increase in the population of such sites as depicted below.



The nickel ions are thought to play an important role in the hydrogenation reaction with reduction of  $\text{Ni}^{2+}$  ions producing the active centres and it appears that there is direct interaction between the reduced nickel species and the reactants.

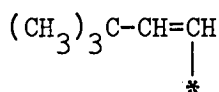
#### Exchange of I with Deuterium

The reaction of I with  $\text{D}_2$  over NiX catalysts was markedly different in character to that observed over CuX and ZnX catalysts. Over NiX exchange and isomerisation of I were independent processes, exchange taking place at temperatures well below those required for isomerisation. Over CuX and ZnX however, temperatures much higher than those required for isomerisation were necessary before exchange occurred and under such conditions a near equilibrium mixture of olefins would be present.

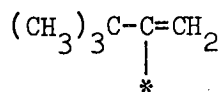
The exchange of I with  $\text{D}_2$  has been studied on several catalyst systems; over alumina<sup>198</sup> at 291 K only the three vinyl hydrogens exchanged with the two terminal hydrogens reacting faster than the non-terminal one, and over  $\text{MgO}$ <sup>148</sup> at 393 K the vinyl hydrogens exchanged at the same rate. In a further study over  $\text{MgO}$ <sup>199</sup> the vinyl hydrogen atoms were found to react much more quickly than the hydrogen atoms of the methyl groups attached to the quaternary carbon atom. In the present work it is concluded that the three vinyl hydrogen atoms of I exchanged with  $\text{D}_2$  over NiX and further support for this comes from the fact that no exchange was observed when the saturated neohexane molecule was reacted with  $\text{D}_2$  over NiX(9). However, if the interaction between the  $\pi$ -electron system of the olefin and the nickel ions leads to the formation of the active catalyst then the apparent inactivity of the neohexane molecule would be expected.

The character of the exchange reactions of I over NiX catalysts is greatly influenced by the nature of the source of deuterium i.e.  $\text{D}_2$  or  $\text{D}_2\text{O}$ . The exchange reaction with  $\text{D}_2\text{O}$  is similar in nature to that

observed over CuX and ZnX; a carbonium ion mechanism is envisaged with exchange and isomerisation of the olefin occurring simultaneously. The multiple exchange character of the reaction is presumably due to the ability of the catalyst to provide a plentiful supply of  $D^+$  from the  $D_2O$ . However with  $D_2$  exchange and deuteration occur simultaneously and this is evidence for a radical type mechanism being involved. A carbonium ion mechanism must be ruled out because this would lead to isomerisation of the olefin molecule and a carbanion mechanism is unlikely since only three hydrogen atoms were exchanged and those in the methyl groups attached to the quaternary carbon atom would be expected to exchange albeit slowly if such a mechanism was involved. The saturated products arising from the deuteration of I contain substantial amounts of compounds containing 0 and 1 deuterium atoms respectively and this indicates that dissociative adsorption of the olefin is taking place on the catalyst surface. The exchange/deuteration of I may proceed through the formation of radical type intermediates such as those shown below.

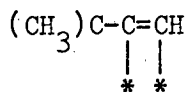


(1)

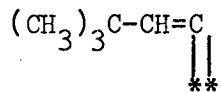


(2)

Species such as (3) and (4) are not believed to be involved otherwise some multiple exchange would be expected



(3)



(4)

TABLE 9.1 ARRHENIUS PARAMETERS FOR THE ISOMERISATION OF I' OVER NiX ZEOLITES

catalyst	temp. range/K	E/kJ mole <sup>-1</sup>	log <sub>10</sub> (A/molecule s <sup>-1</sup> dg <sup>-1</sup> )	initial product ratio <sup>*</sup>
NiX(9)	398-428	134	32.5	4.5
NiX(21) <sup>†</sup>	408-443	76	25.0	3.8
NiX(25)	423-473	86	25.2	3.1
NiX(44)	368-413	51	22.2	5.7
NiX(56)	368-398	54	23.0	6.3

\* values refer to the lowest temperature quoted for each catalyst.

† prepared by Cross<sup>37</sup>, all others prepared by Coutts<sup>22</sup>.

TABLE 9.2      ARRHENIUS PARAMETERS FOR  $H_2/D_2$  EXCHANGE OVER NiX ZEOLITES

catalyst	temp. range/K	E/kJ mole <sup>-1</sup>	log <sub>10</sub> (A/atom s <sup>-1</sup> dg <sup>-1</sup> )
NiX(9)	273-323	19	20.6
NiX(21)	273-323	19	20.6

TABLE 9.3 - ISOTOPIC COMPOSITION OF THE SATURATED HYDROCARBON FORMED FROM  
THE REACTION OF I WITH D<sub>2</sub> ON NiX(21) AT 373 K

% deuteration	d <sub>0</sub>	d <sub>1</sub>	d <sub>2</sub>	d <sub>3</sub>	d <sub>4</sub>	d <sub>5</sub>
2.5	10.7	22.2	63.3	3.8	-	-
52	13.3	29.2	41.8	10.9	3.8	1.1

TABLE 9.4      COMPARISON OF THE ACTIVITY OF 21% EXCHANGED TRANSITION METAL  
ZEOLITES FOR THE ISOMERISATION OF I AT 435 K

catalyst	$\log_{10} (\text{k/molecule s}^{-1} \text{ dg}^{-1})$	relative activity
NiX	16.05	1
ZnX	16.13	1.2
CuX	16.60	3.5



TABLE 9.5      COMPARISON OF THE ACTIVITY OF ZEOLITE CATALYSTS FOR THE  
ISOMERISATION OF II

catalyst	$\log_{10}(\text{k/molecule s}^{-1} \text{ dg}^{-1})$	relative activity
NaX	13.82	$5 \times 10^{-3}$
CuX(10)	16.12	1
NiX(9)	16.74	4.1
NiX(21)	17.25	13.4
ZnX(21)	16.57	2.8

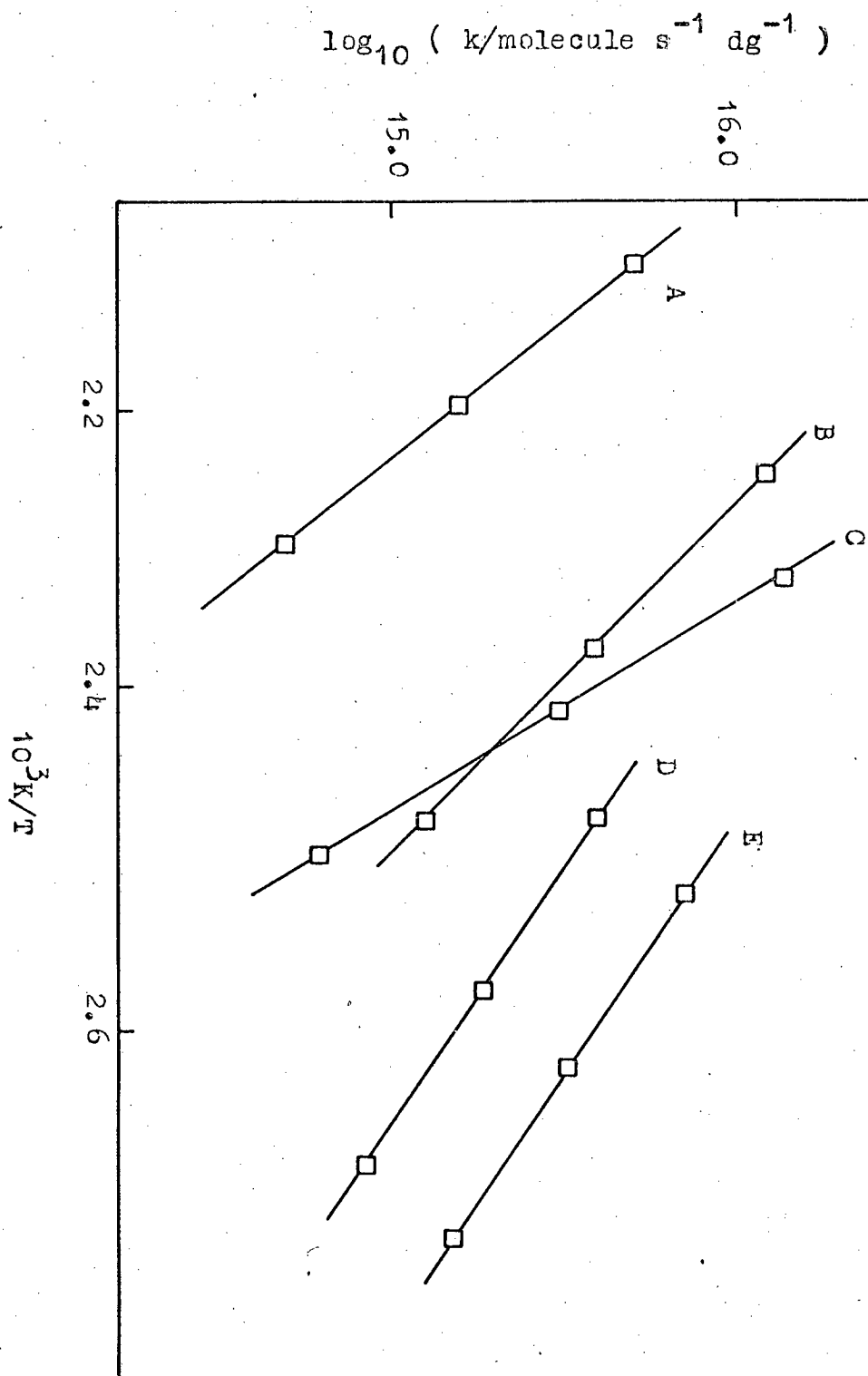


Fig.9.1- Isomerisation of I over NiX zeolites.

A = I over NiX(25), B = I over NiX(21),  
 C = I over NiX(9), D = I over NiX(44),  
 and E = I over NiX(56).

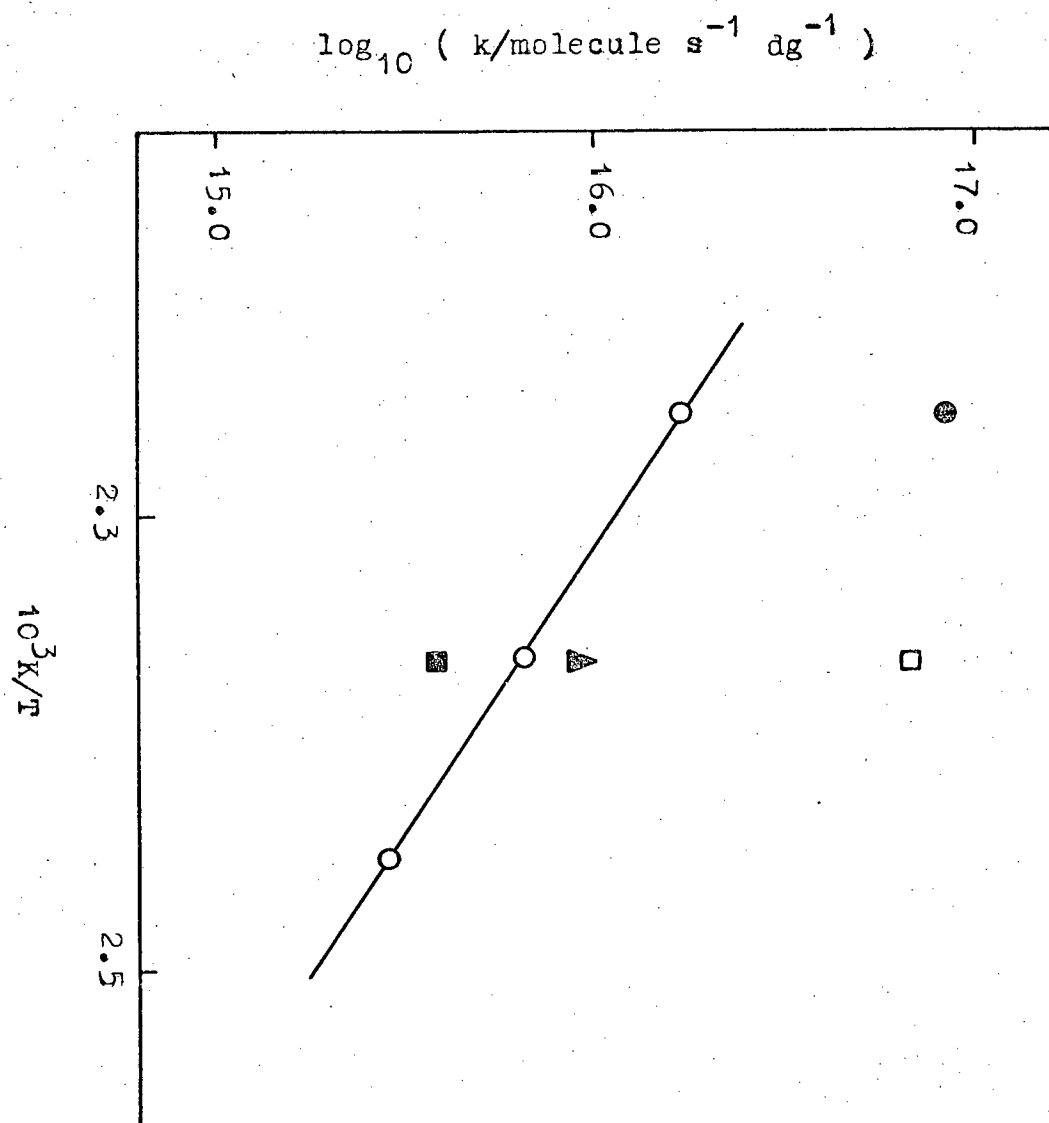


Fig.9.2- Isomerisation of I over NiX(21).

O = isomerisation of I, ● = I+H<sub>2</sub>O,  
 ■ = after CO pretreatment, ▲ = after  
 oxygen pretreatment, and □ = after  
 hydrogen pretreatment.

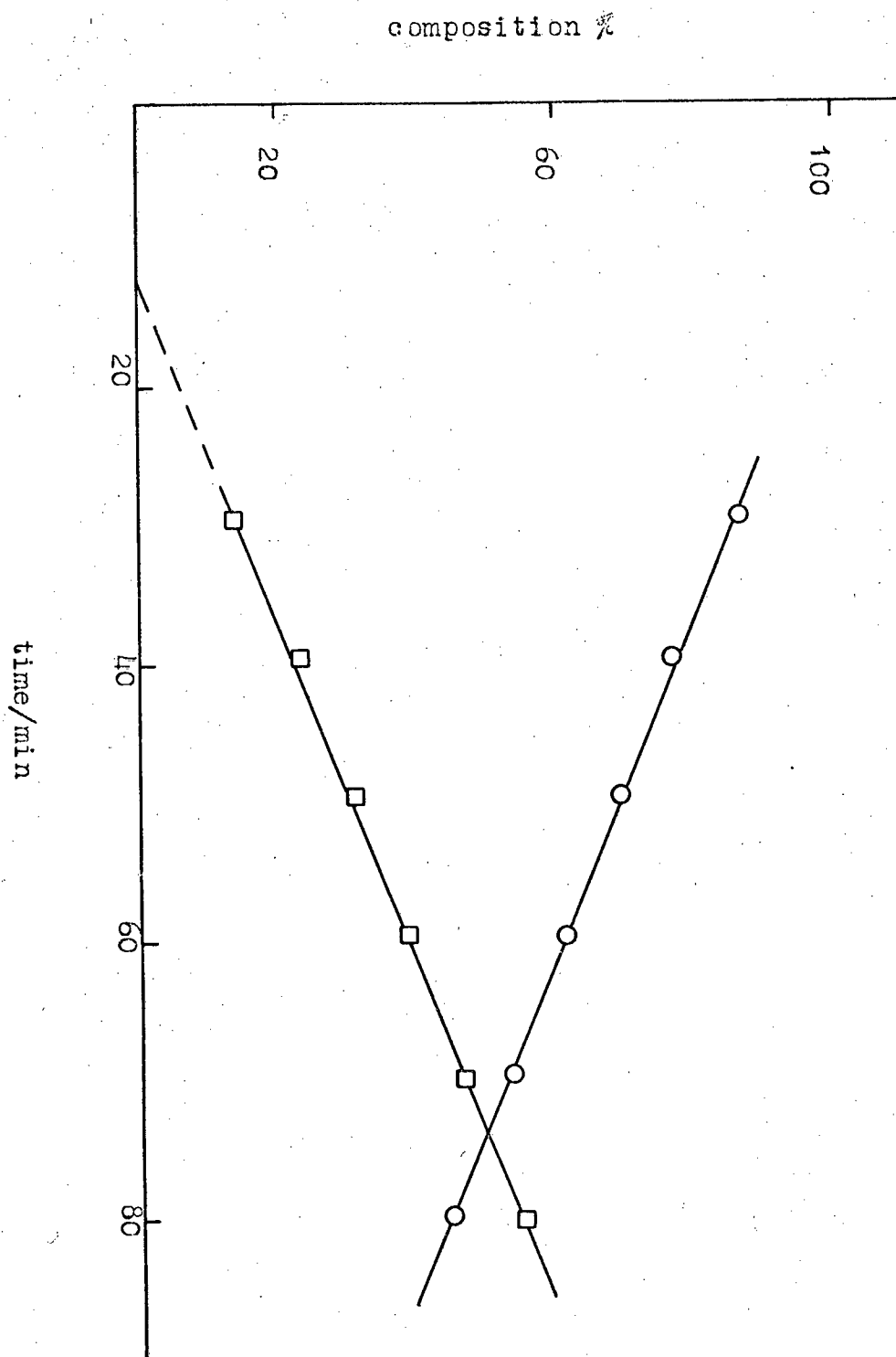


Fig.9.3- Hydrogenation of I over NiX(21) at 363K.  
O = I and  $\square$  = neoheptane.

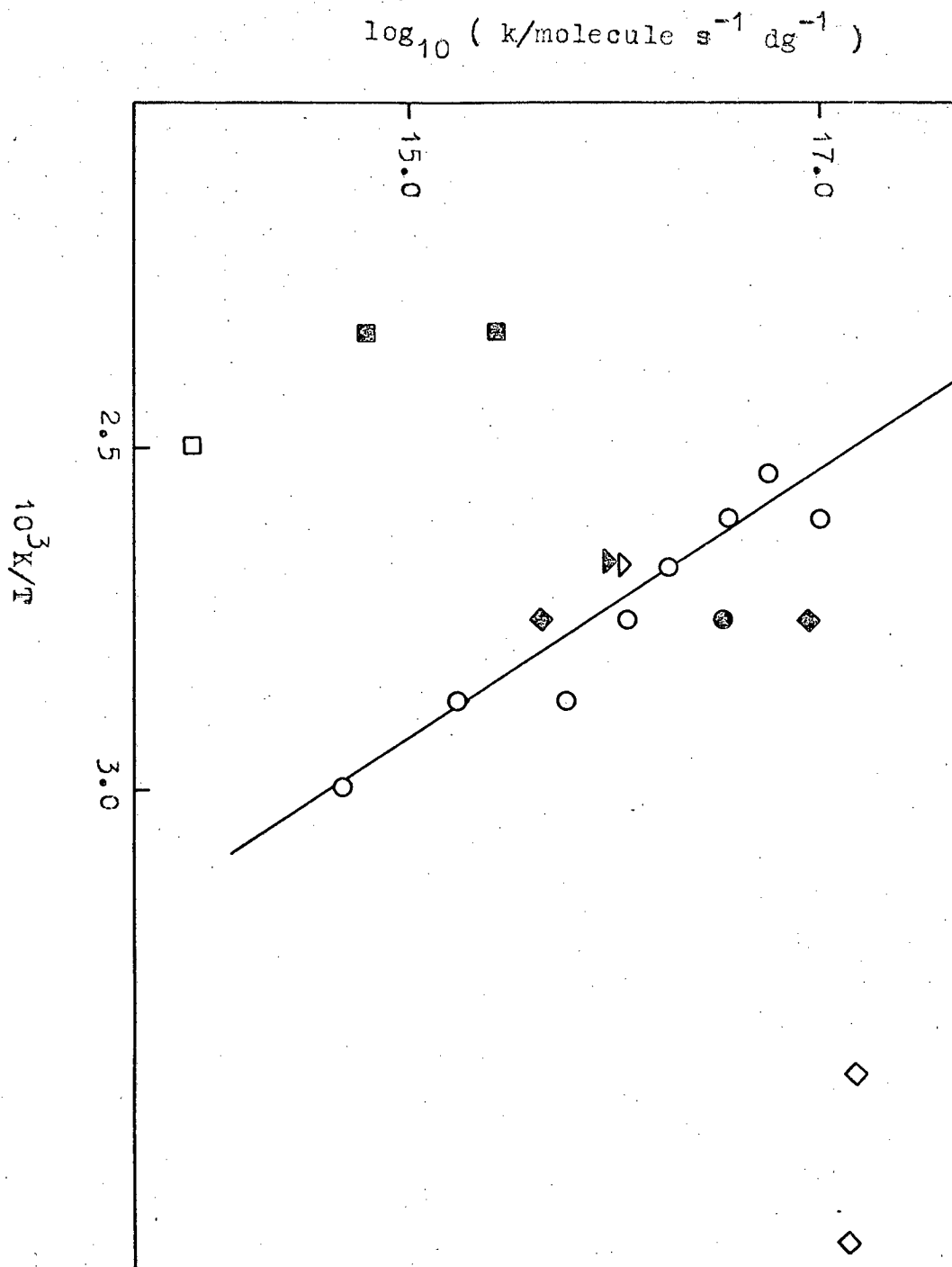


Fig.9.4- Hydrogenation of I over NiX(21).

○ = I+H<sub>2</sub>, □ = I+H<sub>2</sub> after oxygen pre-treatment, ■ = I+H<sub>2</sub> after CO pretreatment, ◇ = I+H<sub>2</sub> after hydrogen pretreatment, ◆ = I+H<sub>2</sub> after CO adsorption on reduced NiX, ⊙ = II/III+H<sub>2</sub>, Δ and ▲ = I+D<sub>2</sub> (calculated from mass spec. data using C<sub>6</sub><sup>+</sup> and C<sub>5</sub><sup>+</sup> ions resp.).

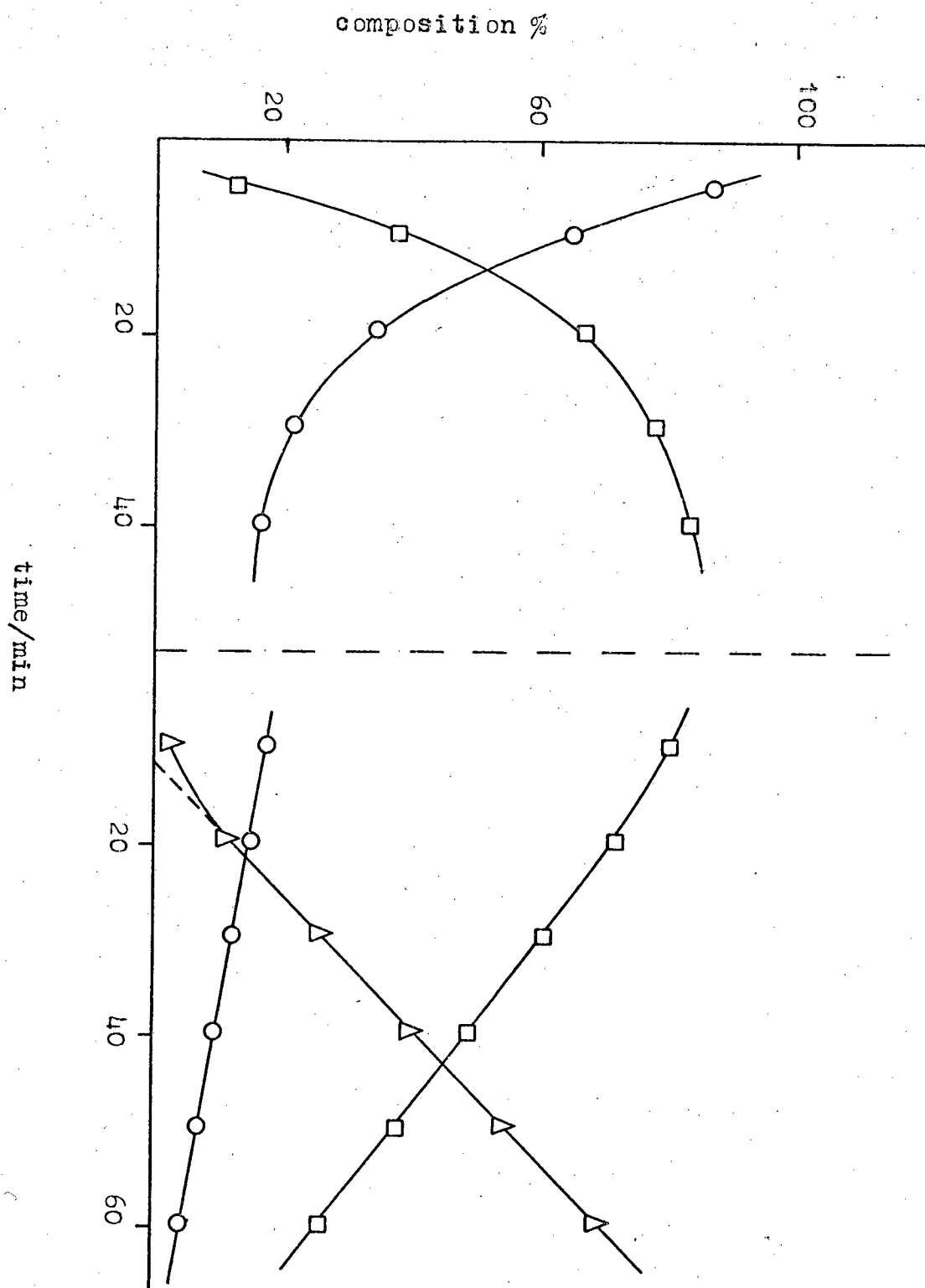


Fig.9.5- Reaction of  $\text{II} + \text{H}_2$  over  $\text{NiX}(21)$ .

(a) at 273K,  $\circ$  = II, and  $\square$  = III.

(b) at 363K,  $\Delta$  = 2,3-dimethylbutane.

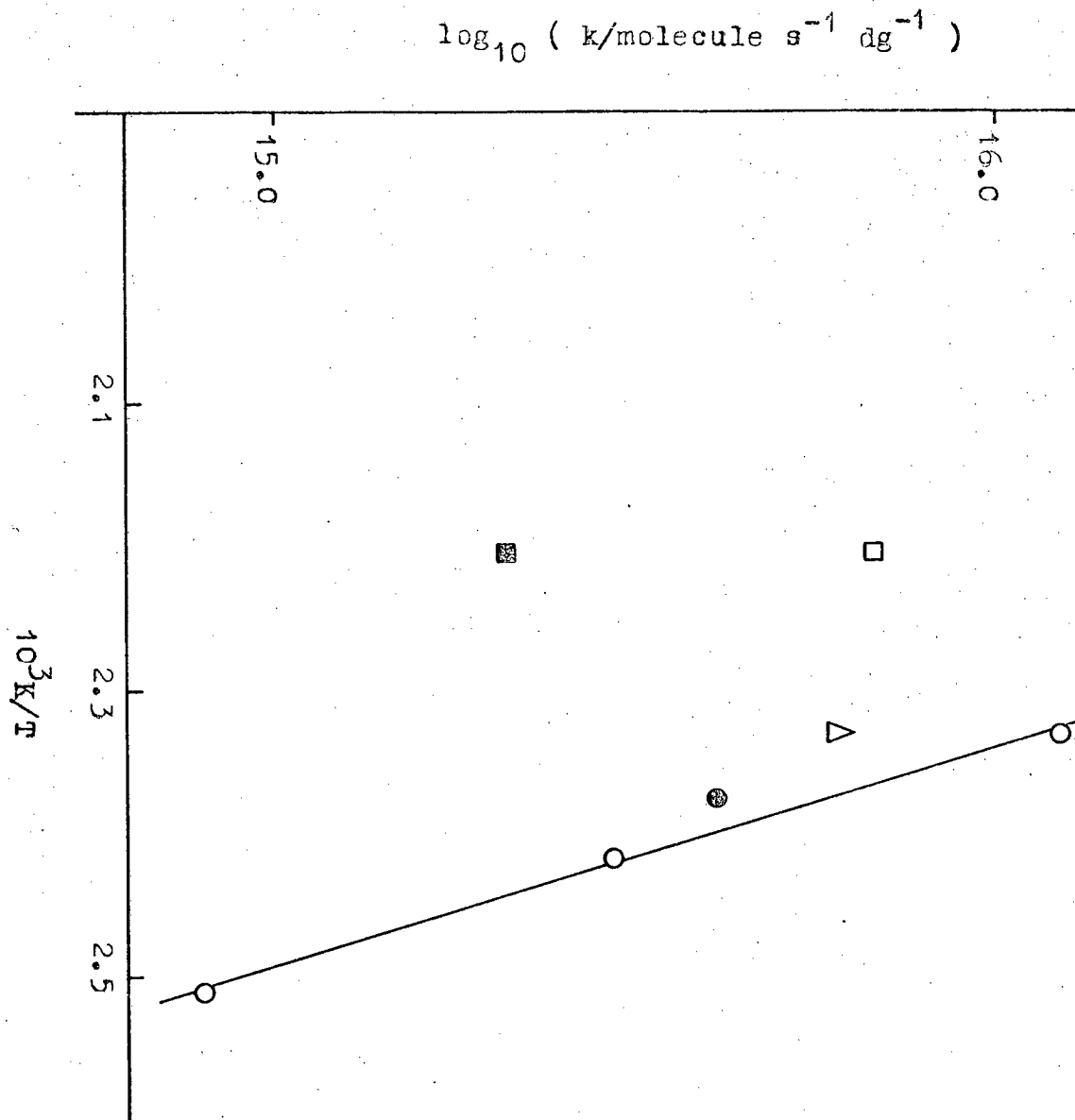


Fig.9.6- Isomerisation of I over NiX(9).

○ = isomerisation of I, □ = I+H<sub>2</sub>O,  
 △ = after oxygen pretreatment, ● = after  
 hydrogen pretreatment, and ⊠ = exchange of  
 I+D<sub>2</sub>O.

## Part IV

### The Exchange Reactions of m-Xylene over Ion-Exchanged X Type Zeolites



## Chapter X

### Exchange Reactions of Alkylbenzenes

#### 10.1 Introduction

The exchange reactions of alkylbenzenes provide a useful method of investigating the properties of catalysts because information about the probable mechanisms can be gained from a study of the relative rates of exchange of the different types of hydrogen atoms present in the aromatic molecule. The exchange of m-xylene with  $D_2$  has been studied on a number of catalyst systems and striking variations have been shown in the abilities of the catalysts to bring about the exchange of side-group and ring hydrogen atoms. In general, where adsorbed radicals are thought to be involved, e.g. on metals<sup>200</sup>, exchange of the side-group hydrogen atoms tends to be as fast, if not faster than, ring atoms (and there is usually some evidence of multiple exchange) whereas for systems where carbonium ion intermediates are important, e.g. alumina and silica-alumina<sup>201</sup>, exchange of the ring atoms takes place more rapidly than side-group exchange.

The exchange of m-xylene has been studied on a number of cation-exchanged zeolites. When m-xylene was exchanged with  $D_2$  over NiX Pope<sup>192</sup> found that side-group exchange was faster than ring exchange, the four ring positions reacting at the same rate. This result is in keeping with previous findings<sup>103,190,191</sup> which indicate the metallic character of NiX. On the other hand when m-xylene was exchanged with  $D_2O$  over CoX<sup>202</sup> ring exchange was found to be faster than side-group exchange, behaviour which is typical of acidic catalysts and supports the view that CoX zeolites are important only for reactions which involve carbonium ion intermediates<sup>102,190</sup>.

## 10.2 Object of the Present Study

The aim of the present study was to extend the previous work carried out on the exchange reactions of m-xylene over ion-exchanged zeolites. Since m-xylene can react in different ways particular emphasis was placed upon investigating the role played by  $D_2$  and  $D_2O$  in influencing the type of mechanism. As Kemball and McCosh have discussed<sup>191</sup> carbonium ions are probably favoured by  $D_2O$  relative to  $D_2$  and radicals by  $D_2$  relative to  $D_2O$ , and so it was important to determine whether the character of the reaction could be attributed to the source of deuterium or to the nature of the catalyst. Therefore the exchange reactions of m-xylene over NiX and CoX zeolites were studied using both  $D_2$  and  $D_2O$  as the source of labelling isotope. A few experiments were also carried out over CaX zeolite since it was thought that this catalyst would show properties typical of a divalent cation-exchanged zeolite and, unlike transition metal cations,  $Ca^{2+}$  ions would be unlikely to undergo changes in oxidation state under the reaction conditions employed.

In the study of exchange reactions of alkylbenzenes by conventional methods, i.e. those carried out under isothermal reaction conditions, it is frequently necessary to do several reactions at different temperatures to obtain a full comparison of the rates of exchange of the different hydrogen atoms in the molecules. However McCosh<sup>202</sup> has shown that equivalent information can be obtained from a single experiment using a temperature-programming technique in which a linear rate of increase in temperature during the course of the reaction was employed. The second aim of the present work was to develop and apply a temperature-programming technique to the study of the exchange reactions of m-xylene in order to show that the use of such a technique provides a valid and reliable means of investigating such reactions.

### 10.3 Experimental

The apparatus was the same as that used for the earlier work (Gas Line A) and has been described in detail (chapter 5). The reactions were studied in a static system and the reaction vessel was connected to the mass spectrometer via a fine capillary leak thus allowing continuous analysis of the isotopic composition of the reaction mixture. An ionising beam of 18 eV was employed in all studies.

For hydrocarbon/D<sub>2</sub>O mixtures known pressures of reactants (equivalent to 2.0 molecules of m-xylene and 10.0 molecules of D<sub>2</sub>O respectively per supercage) were frozen into the reaction vessel whereas for hydrocarbon/D<sub>2</sub> mixtures the hydrocarbon was frozen into the reaction vessel and the desired amount of D<sub>2</sub> (varying from 5 to 14 times the amount of m-xylene) was expanded from the mixing volume into the reaction vessel.

A close fitting furnace of high thermal capacity was placed around the reaction vessel and by carefully adjusting the temperature controls a linear increase in temperature with time was achieved. The exact temperature was measured by means of a chromel-alumel thermocouple connected to an XL DVM. The thermocouple was inserted into an inlet in the reaction vessel so that it was situated just above the surface of the catalyst. Temperature readings were taken at regular time intervals during a run. The procedure for recording mass spectra was the same as described previously.

### 10.4 Treatment of Results

The raw data were first given a preliminary treatment which involved plotting peak heights against time so that by drawing smooth curves a suitable number of points at regular time intervals could be selected. These points were then further corrected for background, the presence of naturally

occurring isotopes and fragmentation in the usual manner and hence the distributions of isotopic species at particular times were obtained.

By examining the distribution of products during the course of the exchange reaction it was possible to divide the hydrogen atoms into groups according to their ease of replacement by deuterium. A typical run, for m-xylene/D<sub>2</sub> over NiX(41), is shown in fig. 10.1 and indicates clearly that six hydrogen atoms were replaced more rapidly than the remaining four.

The methods used to analyse the kinetic data were similar to those used for conventional experiments<sup>203</sup> and gave approximate values of the initial rates of exchange of the different groups of hydrogen atoms at a series of temperatures. The method will be illustrated with reference to the above example in which there are two Groups D and E containing six and four hydrogen atoms respectively.

As discussed in chapter III, when all the hydrogen atoms in a molecule react at the same rate, the course of the exchange reaction is given by the equation

$$-\log_{10}(\phi_{\infty} - \phi) = k_{\phi} t / 2.303 \phi_{\infty} - \log_{10}(\phi_{\infty}) \quad (10.1)$$

and the initial rate of disappearance of the d<sub>0</sub> hydrocarbon in percentage in unit time, k<sub>0</sub>, may be obtained from the equation

$$-\log_{10}(d_0 - (d_0)_{\infty}) = k_0 t / 230.3 - \log_{10}(100 - (d_0)_{\infty}) \quad (10.2)$$

When the molecule contains hydrogen atoms which react at different rates, the quantities k<sub>φ</sub> and k<sub>0</sub> will be composite terms of the type

$$k_{\phi} = k_D + k_E \quad (10.3)$$

and

$$k_0 = k_{0D} + k_{0E} \quad (10.4)$$

and plots according to Eq.(10.1) will not be linear. Approximate methods may be used to determine the rates of exchange of the

groups of hydrogen atoms and work satisfactorily provided  $k_D > k_E$ .

In order to determine  $k_{\phi_E}$  it was assumed that the  $d_6$  compound had exchanged the Group D hydrogen atoms and that the formation of the  $d_7$  to  $d_{10}$  compounds was due to the exchange of the four atoms in Group E.

Thus  $\phi_E$  was defined by the relationship

$$\phi_E = 100 \frac{\sum_{i=7}^{10} (i-6) d_i}{\sum_{i=6}^{10} d_i} \quad (10.5)$$

In order to determine  $k_{\phi_D}$ ,  $\phi_D$  was defined as follows

$$\phi_D = \sum_{i=1}^5 i d_i + 6 \sum_{i=6}^{10} d_i \quad (10.6)$$

The method used to calculate  $(\phi_E)_{\infty}$  was as follows: an equilibrium distribution corresponding to  $\phi_{\infty} = 773$  (i.e. D/H ratio of 3.4) for the exchange of 10 hydrogen atoms in the molecule was calculated assuming a random distribution of the 7.73 deuterium atoms among the various isotopic species. Values of  $(d_6)_{\infty}$ ,  $(d_7)_{\infty}$ ,  $(d_8)_{\infty}$ ,  $(d_9)_{\infty}$  and  $(d_{10})_{\infty}$  of 11.9, 23.2, 29.6, 22.4 and 7.6% respectively were obtained in this manner and hence by Eq. (10.5)  $(\phi_E)_{\infty} = 190$  was obtained.  $(\phi_D)_{\infty}$  was calculated in a statistical manner using the relation

$$(\phi_D)_{\infty} = 100.H.D / (H+D)$$

where H and D represent the number of hydrogen and deuterium atoms respectively.

After evaluating  $\phi_D$  and  $\phi_E$  from the relevant sets of data plots were drawn of  $\log(\phi_{\infty} - \phi)$  against time and these showed curvature concave to the time axis as should be expected of an accelerating reaction. From these plots, two  $\phi$  values were taken at a reasonably close time interval along the reaction coordinate and a rate was calculated using these two  $\phi$  values assuming that the temperature

remained constant over the time interval under consideration. The value of the temperature chosen was that at the mid-point of the time interval and this is equivalent to drawing tangents to the appropriate  $\phi$  plots and is sufficiently accurate provided that small enough time intervals are chosen. No allowance was made for the fact that the initial rate is the sum of the rates for all the processes since these had widely differing rates and thus the corrections would have been negligible. In this way it was possible to obtain a series of rates at differing temperatures for the two processes and thus Arrhenius plots could be drawn as shown in fig. 10.2 (broken lines).

In the method of analysis discussed above the results were calculated assuming that the molecule possessed two groups of hydrogen atoms of differing reactivity and the results obtained were taken as justification for this approach. However, when the results were calculated on the basis that all ten hydrogen atoms are equally reactive then the Arrhenius plot which was obtained (fig. 10.2) clearly demonstrates that this was not the case and so lends further support for the methods adopted here.

## 10.5 Results

### Exchange reactions of m-xylene over NiX zeolites

The exchange of m-xylene with  $D_2O$  was examined over NiX(9) and NiX(41). The character of the reaction was the same over both catalysts and is illustrated in fig. 10.3 for the reaction over NiX(41). It can be clearly seen that three hydrogen atoms exchanged faster than a fourth which, in turn, reacted faster than the remaining six atoms. Although from mass spectrometric data alone the positions of the various hydrogen atoms in the molecule cannot be determined, it seems likely that the first two groups of atoms to exchange are those in the aromatic ring with the last group consisting of the six hydrogen atoms in the two methyl side groups. The results are presented in Table 10.1 and the

Arrhenius plots for the reaction over NiX(41) are shown in fig. 10.4. Stepwise exchange was observed over both catalysts and the results indicate that NiX(41) was more active than NiX(9) for exchange of the ring hydrogen atoms but of comparable activity for side group exchange.

The exchange of m-xylene with  $D_2$  was studied over NiX(41) and in this case it was observed that six hydrogen atoms were replaced faster than the remaining four. The hydrogen atoms in the first group are believed to be those in the methyl side groups and the ring atoms are thought to comprise the second group. The course of the reaction is illustrated in fig. 10.1 where it can be seen that for the first group of atoms there is multiple exchange with a tendency to complete the exchange of a methyl group during one sojourn of the molecule at the catalyst surface, whereas the ring atoms are replaced in a stepwise manner. The results for this reaction are presented as Arrhenius plots in fig. 10.4 (where they may be compared with the  $D_2O$  exchange results) and the derived parameters are summarised in Table 10.2. Table 10.3 shows the comparison between an experimental product distribution obtained in the later stages of the reaction and the corresponding binomial distribution. At this point the exchange of the side group hydrogen atoms will have reached a near equilibrium situation and the build up of the  $d_5$  and  $d_6$  compounds demonstrates the much slower exchange of the ring hydrogen atoms.

When a further experiment was carried out on a fresh sample of NiX(41) considerable variation in the activity of the two samples of catalyst for side group exchange was observed whereas comparable activity for ring exchange was observed. These effects are shown in fig. 10.5 where the results are presented in the form of Arrhenius plots, the derived parameters are given in Table 10.2. When the results are extrapolated to 556 K, for the first reaction side group exchange is faster than ring exchange by a factor of

of approximately 2000 whereas the difference in rate observed in the second run is only a factor of 6. However, this last point serves to illustrate the sensitivity of the technique for detecting small differences in rate.

#### 10.6 Exchange reactions of m-xylene over CoX(52)

Examination of the distribution of products with time during the exchange of m-xylene with  $D_2O$  showed that the hydrogen atoms could be divided according to their rate of exchange into three groups A, B and C consisting of 3, 1 and 6 atoms respectively. The character of the reaction was the same as that observed over NiX catalysts, exchange taking place in a stepwise manner, and again it is believed that ring exchange is faster than side group exchange. The results are given in Table 10.1 and the corresponding Arrhenius plots shown in fig. 10.6. When the results of the present work are compared with those of McCosh<sup>202</sup> (broken lines) for m-xylene/ $D_2O$  exchange over this same CoX(52) catalyst the very close agreement demonstrates the reproducibility of the technique.

#### Mesitylene

In order to determine which of the ring hydrogen atoms was exchanging more slowly than the other three, the exchange of 1,3,5-trimethylbenzene (mesitylene) with  $D_2O$  was examined over CoX(52). Mesitylene was chosen because the ring hydrogen atoms in the molecule are equivalent and should be equally reactive. Also the ring atom in m-xylene which is ortho to both methyl groups is analogous to the ring atoms in mesitylene and hence would be expected to show similar reactivity. The reaction was studied at 493 K and the result has been incorporated into fig. 10.6. The good agreement between the rate of exchange of the ring hydrogen atoms in mesitylene and the rate of exchange of the Group B hydrogen atom in m-xylene indicates that this latter atom lies between the methyl groups.

The exchange of m-xylene with  $D_2$  over CoX(52) gave a product



distribution (fig. 10.7) which indicated that all ten hydrogen atoms in the molecule were reacting at the same rate. When the results were calculated on this basis the Arrhenius plots shown in fig. 10.6 were obtained for the two experiments studied. The results are summarised in Table 10.2. As can be seen from fig. 10.6 the agreement between the two runs is moderate. Comparison of the experimental product distribution with the corresponding binomial distributions showed that in the early stages of reaction the exchange took place in a stepwise manner but as Table 10.4 illustrates there was evidence for multiple exchange occurring later.

#### 10.7 Exchange reactions of m-xylene over CaX(59)

The exchange of m-xylene with  $D_2O$  was similar in nature to the reactions observed over NiX and CoX zeolites. There was stepwise replacement of the hydrogen atoms and the ease of exchange was  $3>1>6$ , indicating that ring exchange was faster than side group exchange. The results are presented in Table 10.2.

Two experiments were carried out to examine the exchange of m-xylene with  $D_2$  over this catalyst. The first reaction was studied in a Pyrex reaction vessel and temperatures above 628 K were necessary before exchange took place and there was some indication of multiple exchange character. When the reaction was carried out in a silica reaction vessel no exchange was observed below 723 K and the reaction was stepwise in nature.

In both cases it was observed that all ten hydrogen atoms in the molecule were equally susceptible to exchange.

#### 10.8 Discussion

The most striking feature of the results is that the choice of  $D_2$  or  $D_2O$  as the source of labelling isotope has a critical influence upon the nature of the reaction. For the exchange of m-xylene with  $D_2O$  over all the zeolites studied ring exchange was faster than side-group

exchange, behaviour which is taken to be typical of acidic catalysts<sup>201</sup>. It has previously been discussed<sup>191</sup> that reactions which involve the formation of carbonium ion intermediates are likely to proceed more readily in the presence of  $D_2O$  than  $D_2$ . Zeolite catalysts should be capable of splitting the  $D_2O$  molecule heterolytically to provide a ready supply of  $D^+$ .

The zeolite catalysts (with the exception of NiX(9)) show comparable activity for the exchange of the ring atoms in m-xylene with  $D_2O$  but the NiX catalysts are less active for side-group exchange with  $D_2O$ . The behaviour of NiX(41) illustrates that found for the series of zeolites; when the results were extrapolated to 500 K it was found that Group A exchanged faster than Groups B and C by factors of 260 and 1300 respectively.

It is interesting to note that if the electron donating effects of the substituent groups were important then it would be expected that the ease of replacement of the various ring hydrogen atoms would parallel the ease of electrophilic attack at these positions and on this basis the position meta to both methyl groups in m-xylene should be the least reactive. However, it was observed that the position ortho to both side groups was the least reactive indicating that steric and not electronic effects are dominant.

The results reported here for exchange with  $D_2O$  are similar to those obtained in the homogeneous acid catalysed exchange reactions of alkylbenzenes<sup>204-206</sup>. The common feature is that the ring hydrogen atoms react in preference to those in the side group. However, there are a number of differences between the two systems. On the zeolites studied there are no directing effects caused by substituent groups, and it was found that side group exchange does occur whereas in homogeneous systems this is found only in exceptional cases e.g. with aromatic molecules

containing the t-butyl side group<sup>207</sup>. In basic media the results are diametrically opposed to those in acidic media and the exchange of alkylbenzenes has been observed to proceed most readily when primary carbanions are formed<sup>208,209</sup>.

The presence of different reaction rates among the various ring hydrogen atoms demonstrates that at the temperatures employed the isomerisation of m-xylene was unimportant compared with exchange. If isomerisation had been rapid compared with exchange it would not have been possible to detect differences in the rates of reaction for the various ring positions.

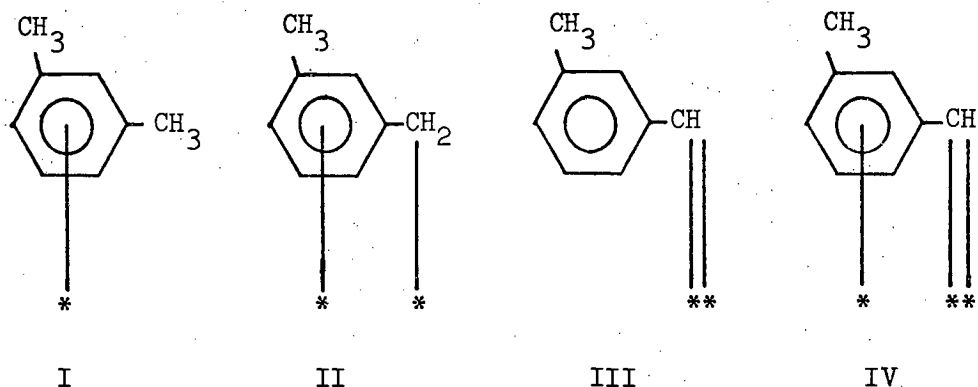
The fact that the character of the reaction was the same on all zeolites and that with the exception of NiX(9) the catalysts displayed comparable activity suggests that a common mechanism is involved. The exchange of the ring hydrogen atoms is most likely to proceed via carbonium ion intermediates and the simplest explanation is that of electrophilic substitution by attack at a single carbon atom with  $D^+$  as the electrophile, as in ordinary aromatic substitution<sup>210</sup>, with addition of  $D^+$  followed by elimination of  $H^+$ . Another possibility is that exchange may only take place readily with deuterium which is present in the form of OD groups at special sites in the zeolite framework and this affords an explanation for the stepwise nature of the exchange and the absence of directing effects due to side groups. Alternatively the reaction may proceed by a mechanism in which the aromatic ring is bound to the surface by donation of  $\pi$  electrons to Lewis acid sites prior to exchange. Surface divalent cations may function as such electron acceptor sites and adsorption would render the ring positions more equivalent since the electron densities at the various ring positions will be different from those found in isolated gas phase molecules. The exchange of this adsorbed

molecule may then proceed by an addition-elimination reaction with subsequent desorption. This would appear the most likely mechanism since the orientation of the molecule will be important and hence it is to be expected that attack at the ring position ortho to both methyl groups will be sterically hindered.

For exchange of the side group hydrogen atoms the slow step must involve activation of the hydrocarbon. A dissociative mechanism involving heterolytic cleavage of a C-H bond is most likely. However, it is not possible to say whether a carbonium ion or a carbanion mechanism is involved and in order to distinguish between these possibilities it would be necessary to examine other alkylbenzenes such as ethylbenzene and cumene.

When  $D_2$  is used as the source of labelling isotope instead of  $D_2O$  there is a complete change in the character of the reaction. This effect is most pronounced for NiX where side group exchange now becomes a more facile process than ring exchange. The exchange reactions of m-xylene demonstrate quite clearly the dual function nature of NiX catalysts. They show properties typical of acidic catalysts when  $D_2O$  is present but display radical type behaviour when  $D_2$  is used. As fig. 10.4 illustrates, NiX exhibits high activity for ring exchange with  $D_2O$  and side-group exchange with  $D_2$  but ring exchange with  $D_2$  occurs more readily than side group exchange with  $D_2O$ . CoX and CaX however only show acidic type behaviour and are extremely inactive for exchange with  $D_2$ .

For the exchange of the side group hydrogen atoms with  $D_2$  over NiX it is possible that radical type intermediates such as I→III depicted below are involved, as was postulated for the reaction over metals<sup>200, 203</sup>,



and that interconversion between I and II or the formation of III and IV could lead to the complete exchange of a methyl group during one sojourn of the molecule at the catalyst surface. The observed variation in activity of NiX catalysts for side group exchange with  $D_2$  may be compared with the same effect found in the hydrogenation of I and is probably due to variable reduction of the catalyst during outgassing. The activity of NiX zeolites for reactions involving radical type intermediates appears to depend greatly upon the state of reduction of the catalyst. The exchange of the ring hydrogen atoms with  $D_2$  occurs over NiX at temperatures lower than those observed over CoX and CaX and it is possible that radical or polarised intermediates are involved in this process. The exchange of the hydrocarbon may only take place readily with deuterium atoms which are present in the form of OD groups at special sites on the catalyst surface with the hydrocarbon being desorbed before more deuterium can be supplied to the system by exchange of these OH groups with deuterium from the gas phase; or, as previously discussed adsorption of the hydrocarbon may involve the donation of  $\pi$  electrons to Lewis acid centres on the surface

and this adsorbed molecule may react with molecular or dissociated deuterium. This may explain the stepwise nature of the reaction, the equality between the rates of exchange of the ring atoms and the absence of directing effects due to side groups.

With CoX and CaX the change in the character of the reaction when  $D_2$  is used instead of  $D_2O$  may reflect the inability of these catalysts to suitably activate  $D_2$ . Hydrogen-deuterium exchange has been noted over CoX(52) in the temperature range 373-423 K<sup>190</sup> and the higher temperatures necessary for the exchange of m-xylene might reflect a change in the character of the reaction. Although the hydrogen-deuterium exchange reaction may be envisaged as proceeding via homolytic fission it might well be necessary in the present study to supply deuterium in the form of  $D^+$  (a less facile process). An alternative explanation could be that the preferential adsorption of the aromatic molecule leads to the blocking of the sites active for hydrogen-deuterium exchange. It is probable however, that both effects are important.

CaX appears to be active only for reactions involving carbonium ion intermediates and this ability to display acidic but not metallic properties is even more marked than for CoX. Calcium is a non-transition metal and since the  $Ca^{2+}$  ions present inside the zeolite lattice contain no 3d electrons a purely electrostatic bond between cation and adsorbate would be expected. The exchange of m-xylene with  $D_2$  took place only with great difficulty over CaX, the reaction being slightly more facile when a Pyrex rather than a silica reaction vessel was employed. A similar pattern of behaviour was observed by McCosh<sup>190</sup> who found that CaX was extremely inactive for  $H_2/D_2$  exchange and that in blank runs, using both Pyrex and silica reaction vessels, the reaction took place more readily in the Pyrex vessel. This

suggests that the inability of CaX to activate  $D_2$  is the important factor and that the reaction is probably taking place on the walls of the reaction vessel.

TABLE 10.1 - ARRHENIUS PARAMETERS FOR THE EXCHANGE OF m-XYLENE WITH D<sub>2</sub>O.

catalyst	group*	temp. range/K	E/kJ mole <sup>-1</sup>	log <sub>10</sub> (A/molecule s <sup>-1</sup> dg <sup>-1</sup> )
NiX(9)	A	462-514	110	27.8
	B	546-625	69	21.6
	C	625-713	91	22.9
NiX(41)	A	434-464	57	23.3
	B	488-542	40	19.4
	C	554-590	55	20.1
CoX(52)	A	417-463	152	35.0
	B	483-513	85	24.6
	C	532-563	111	26.2
CaX(59)	A	436-468	56	23.2
	B	478-526	84	24.4
	C	532-562	40	19.6

\* groups A, B and C refer to the exchange of the first three, fourth and last six hydrogen atoms respectively.



TABLE 10.2 - ARRHENIUS PARAMETERS FOR THE EXCHANGE OF m-XYLENE WITH D<sub>2</sub>

catalyst	group	temp. range/K	E/kJ mole <sup>-1</sup>	log <sub>10</sub> (A/molecule s <sup>-1</sup> dg <sup>-1</sup> )
NiX(41)	side-group	463-503	123	31.4
	ring	503-543	42	20.5
NiX(41)	side-group	433-463	152	32.5
	ring	493-563	48	21.4
CoX(52)	all 10	423-673	119	27.1
CoX(52)	all 10	423-673	79	23.2
CaX(59)	all 10	628-752	42	19.3

TABLE 10.3 - PRODUCT DISTRIBUTION DURING EXCHANGE OF m-XYLENE WITH D<sub>2</sub> ON NiX(41)

	d <sub>0</sub>	d <sub>1</sub>	d <sub>2</sub>	d <sub>3</sub>	d <sub>4</sub>	d <sub>5</sub>	d <sub>6</sub>	d <sub>7</sub>	d <sub>8</sub>	d <sub>9</sub>	d <sub>10</sub>	M <sub>D</sub>
expt.	5.3	2.0	2.2	4.2	11.3	27.2	32.6	12.3	2.6	0.4	0.0	5.06
binomial <sup>a</sup>	0.1	0.9	4.1	11.2	20.0	24.6	21.0	12.3	4.7	1.1	0.1	5.06

<sup>a</sup> Binomial distribution calculated assuming all ten hydrogen atoms react at same rate

TABLE 10.4 - PRODUCT DISTRIBUTION DURING EXCHANGE OF m-XYLENE WITH D<sub>2</sub> ON CoX(52)

	d <sub>0</sub>	d <sub>1</sub>	d <sub>2</sub>	d <sub>3</sub>	d <sub>4</sub>	d <sub>5</sub>	d <sub>6</sub>	d <sub>7</sub>	d <sub>8</sub>	d <sub>9</sub>	d <sub>10</sub>	M <sub>D</sub>
expt.	29.1	14.3	12.4	13.4	11.2	7.0	5.5	3.7	2.2	1.1	0.2	2.47
binomial <sup>a</sup>	5.9	19.2	28.4	24.8	14.3	5.6	1.5	0.3	-	-	-	2.47

<sup>a</sup> Binomial distribution calculated assuming all ten hydrogen atoms in the molecule are equally exchangeable.

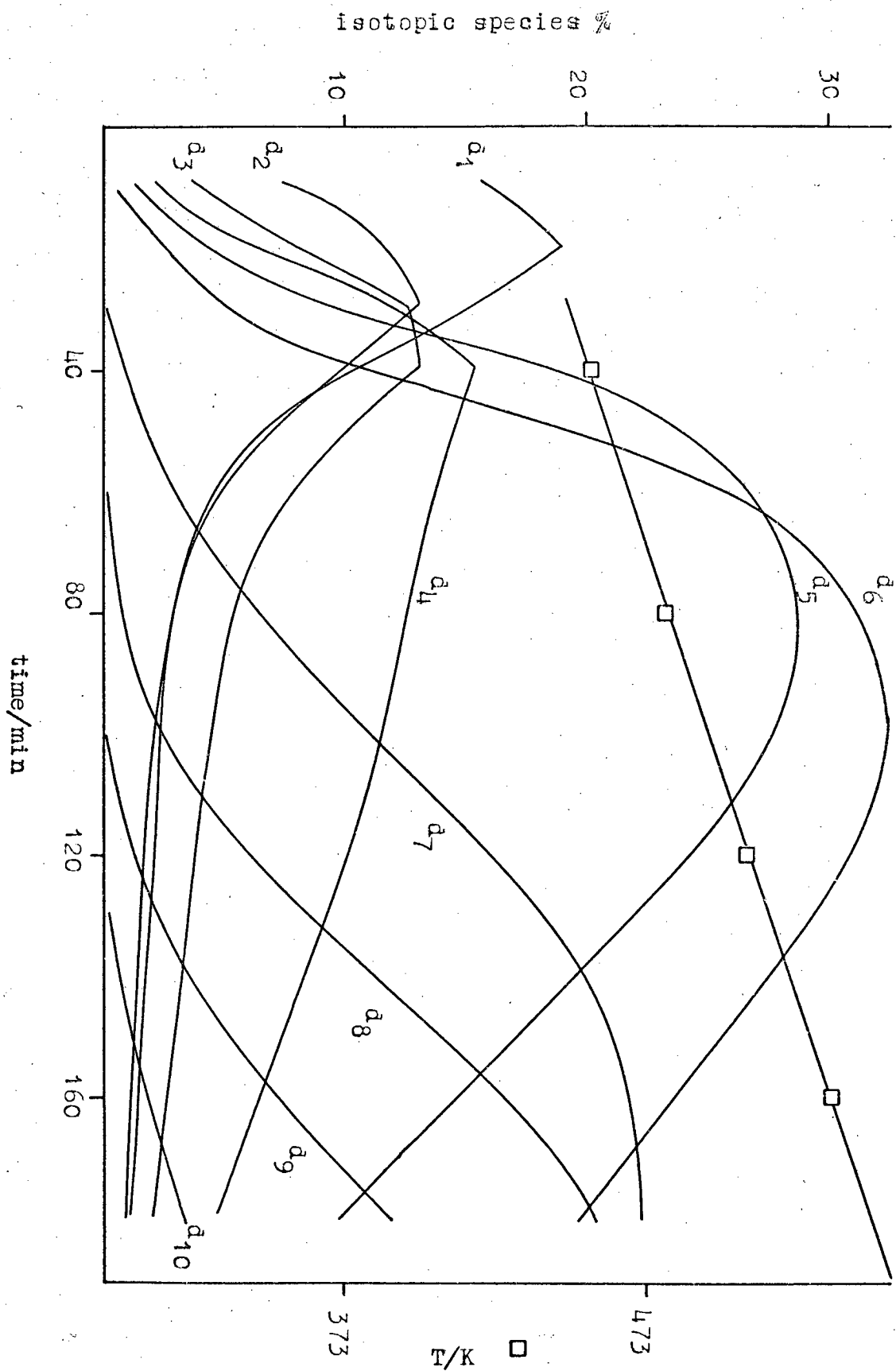


Fig.10.1- Exchange of m-xylene with  $D_2$  over NiX(41).  
Distribution of isotopic species with time.

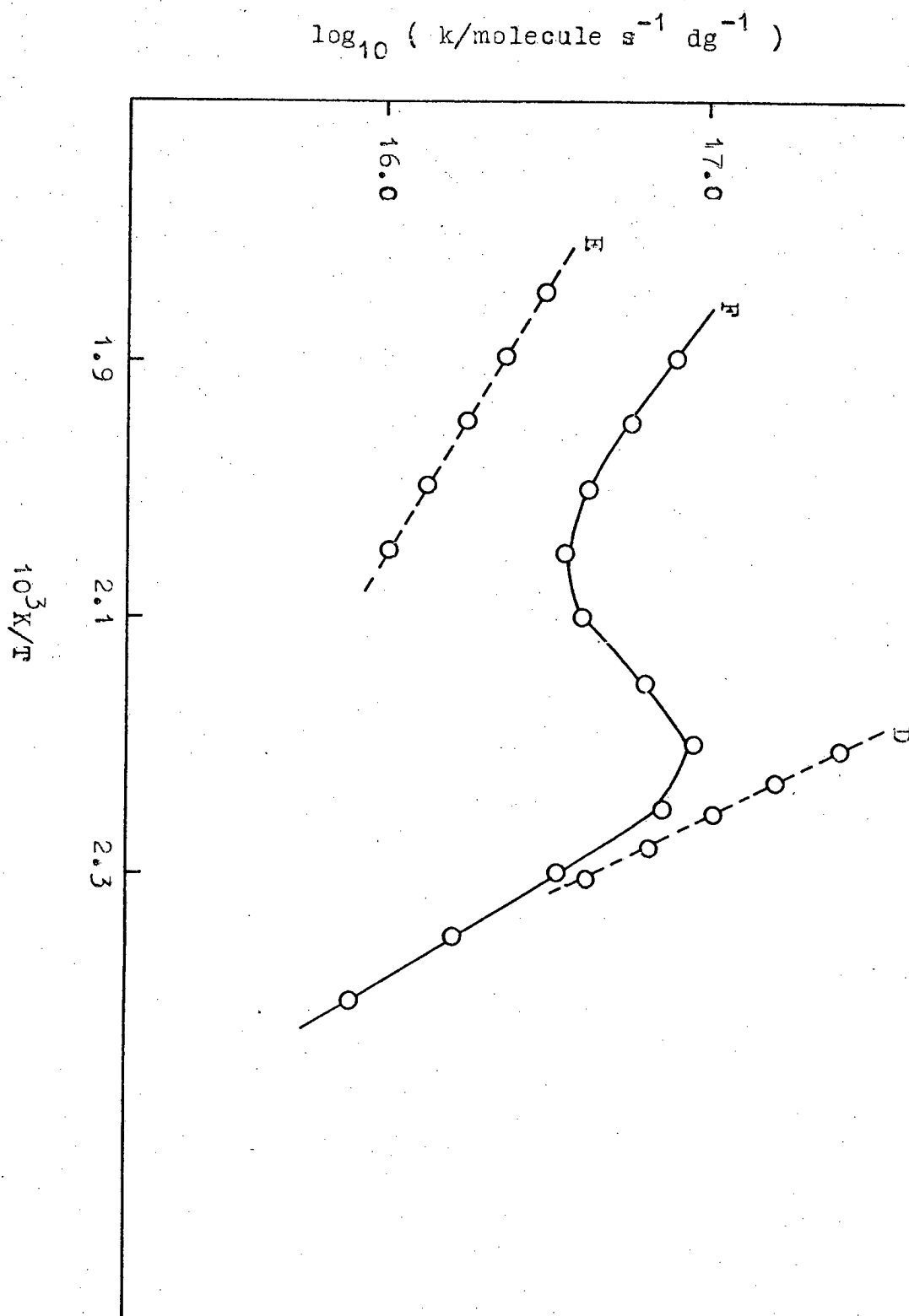


Fig.10.2- Arrhenius plots for m-xylene/D<sub>2</sub> exchange over NiX(41). D = side-group exchange, E = ring exchange, and F = plot obtained assuming all ten hydrogen atoms equally reactive.

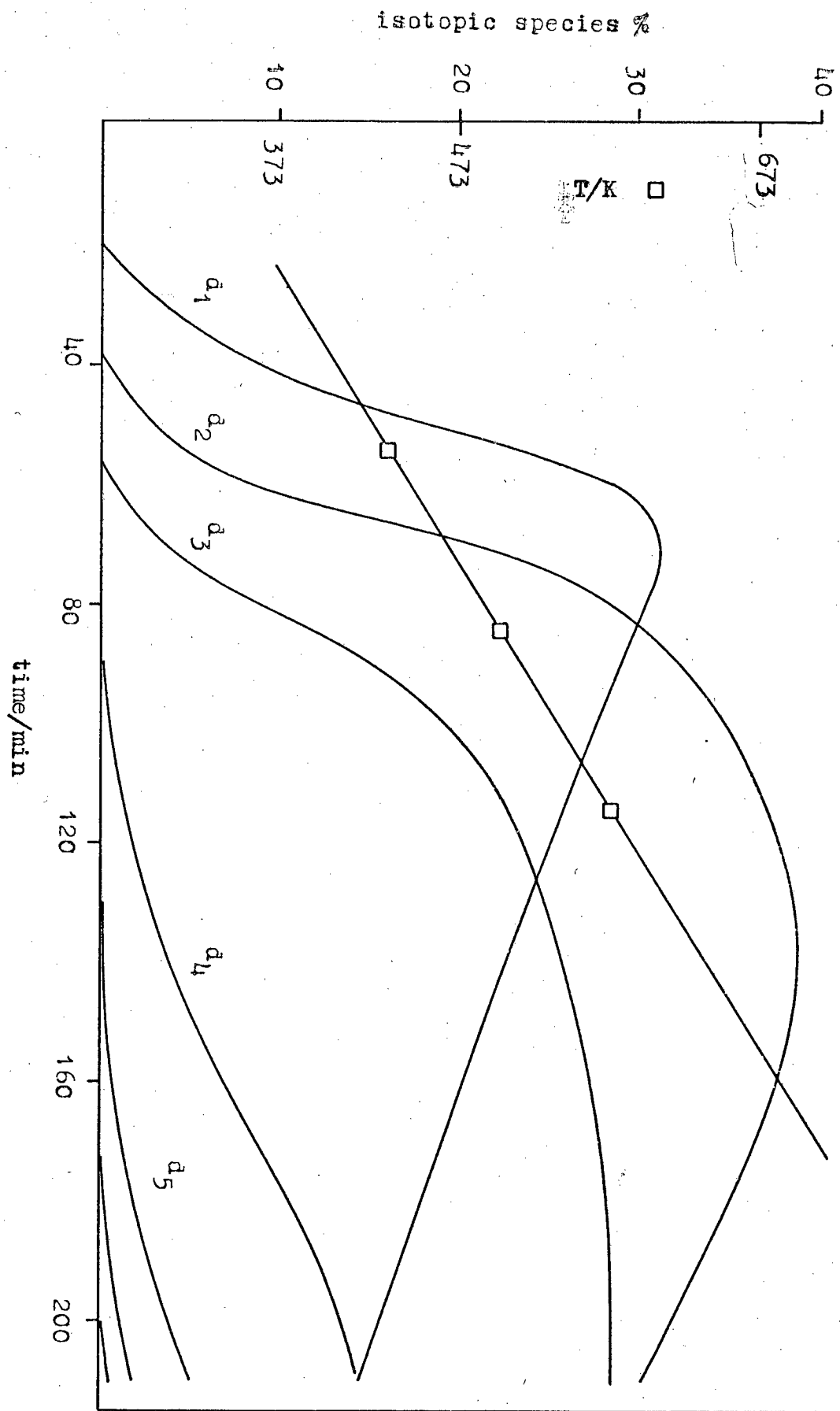


Fig.10.3- Exchange of m-xylene with D<sub>2</sub> over NiX(41).

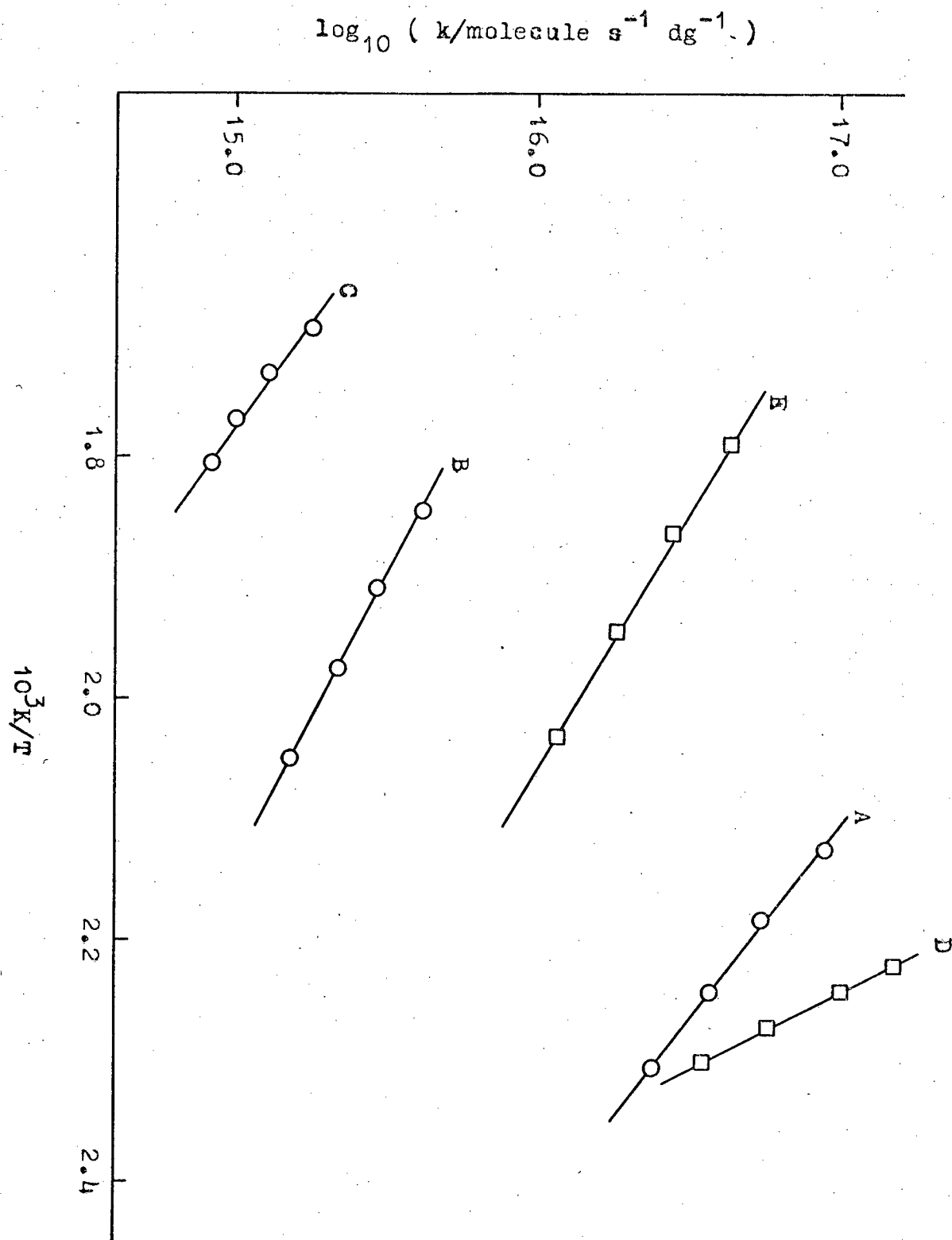


Fig.10.4- Arrhenius plots for m-xylene exchange with D<sub>2</sub> and D<sub>2</sub>O over NiX(41). A,B and C = exchange of 3,1 and 6 atoms resp. with D<sub>2</sub>O; D and E = side-group and ring exchange with D<sub>2</sub>.

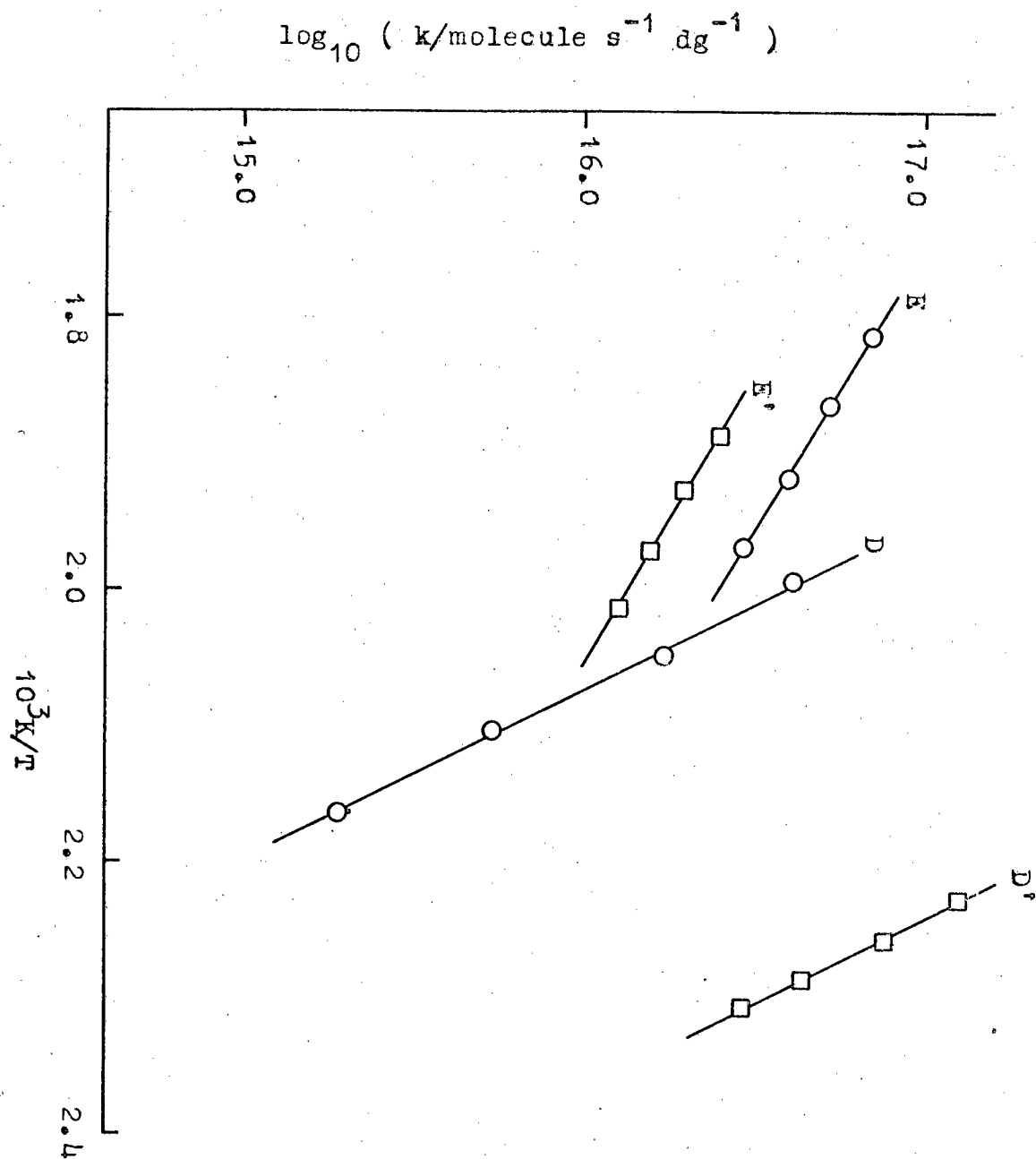


Fig.10.5- Variation in activity of NiX(41) for side-group exchange with D<sub>2</sub>.  
D and D' = side-group exchange, and  
E and E' = ring exchange.



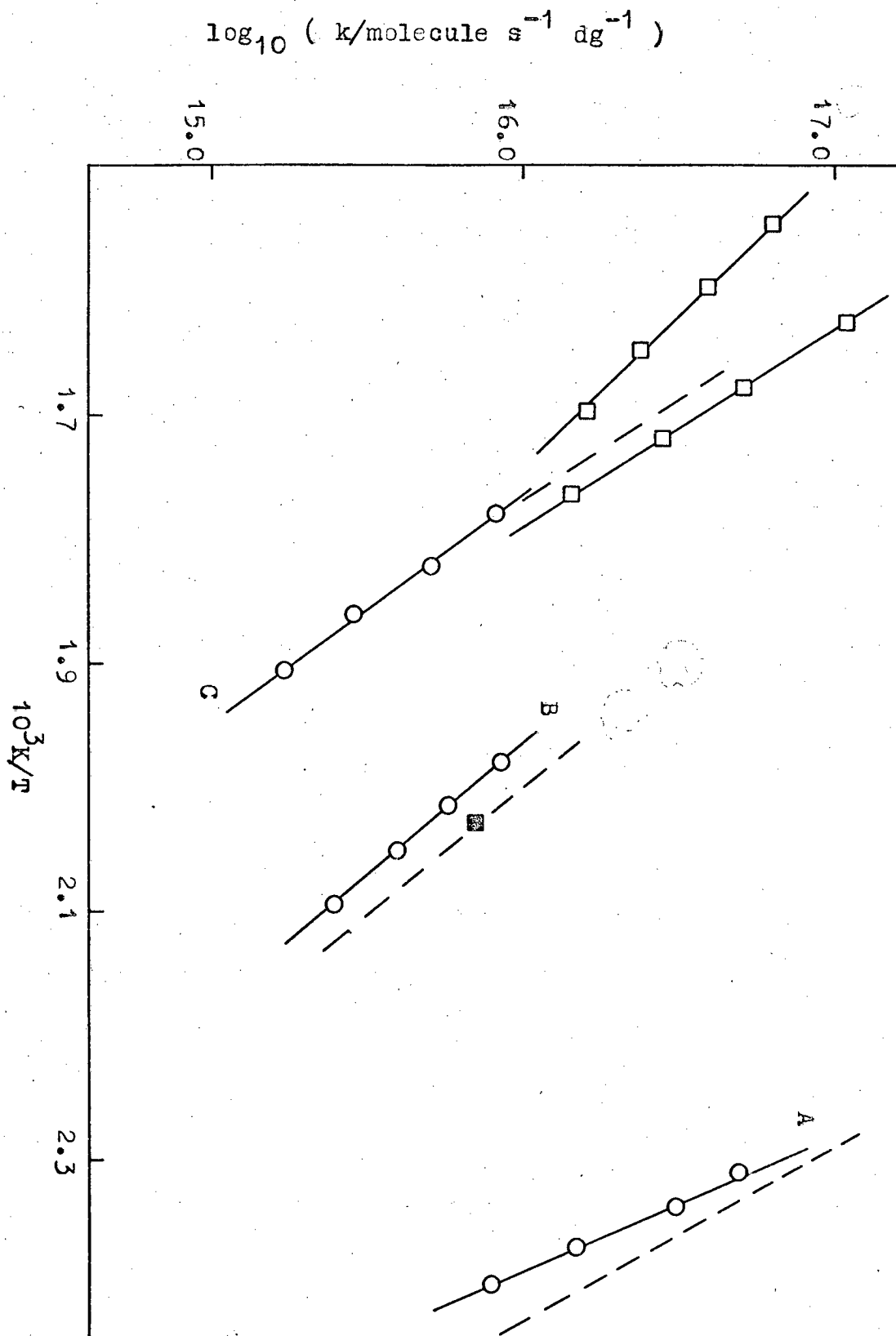


Fig.10.6- Exchange of m-xylene with  $D_2$  and  $D_2O$  over CoX(52). A,B and C = exchange of 3,1 and 6 atoms resp. with  $D_2O$  ( broken lines are the corresponding results of M<sup>c</sup>Cosh ),  
 ■ = exchange of ring atoms of mesitylene with  $D_2O$ , and □ = exchange of all ten atoms of m-xylene with  $D_2$ .

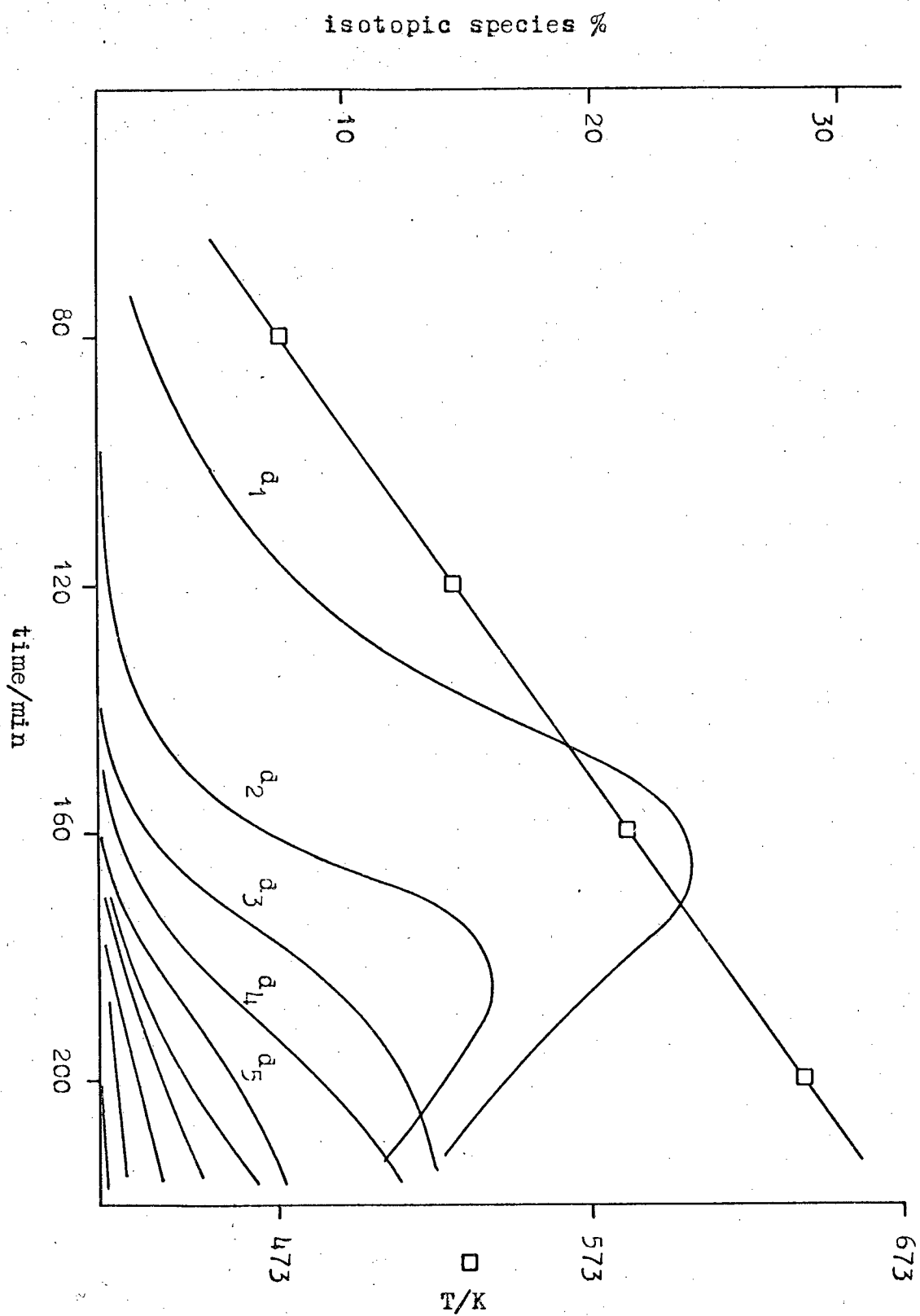


Fig.10.7- Exchange of m-xylene with D<sub>2</sub> over CoX(52).

References

1. Berzelius, J., Jahresber. Chem., 15, 237 (1836).
2. Ostwald, W., Physik., 3, 313 (1902).
3. Faraday, M., Phil. Trans., 114, 55 (1834).
4. Sabatier, P., La Catalyse en Chemie Organique (Paris and Liege, 1913).
5. Langmuir, I., Phys. Rev., 6, 79 (1915).
6. Brunauer, S., "The Physical Adsorption of Gases and Vapours", (O.U.P., Lond., Princeton U.P., Princeton, 1943).
7. Hayward, D.O., and Trapnell, B.M.W., "Chemisorption", (Butterworth, Lond., 1964).
8. Brunauer, S., Emmett, P.H. and Teller, E., J. Am. Chem. Soc., 56, 35 (1934).
9. Gregg, S.J. and Sing, K.S., "Adsorption, Surface Area and Porosity", (Academic Press, Lond. and New York, 1967).
10. Langmuir, I., J. Am. Chem. Soc., 40, 1361 (1918).
11. Wheeler, A., Adv. Catalysis, 3, 249 (1951).
12. Hinshelwood, C.N., "The Kinetics of Chemical Change", (Clarendon Press, Oxford, 1940).
13. Laidler, K.J., Catalysis, ed. Emmett, P.H., (Reinhold, New York, 1954).
14. Rideal, E.K., Sabatier Lecture: J. Soc. Chem. Ind., 62, 335 (1943).
15. Eley, D.D., Quart. Rev., 3, 209 (1949).
16. Beeck, O., Smith, A.E. and Wheeler, A., Proc. Roy. Soc. A177, 62 (1940).
17. Beeck, O., Disc. Faraday Soc., 8, 118 (1950).
18. Balandin, A.A., Z. phys. Chem., 132, 289 (1929).
19. Allpress, J.G. and Sanders, J.V., Phil. Mag., 9, 645 (1964).
20. Boudart, M., J. Am. Chem. Soc., 72, 1040 (1950).
21. Schwab, G.M., Disc. Faraday Soc., 8, 166 (1950).
22. Kemball, C., Proc. Roy. Soc., A124, 413 (1952).

41. Milton, R.M., U.S. Patent 2,882,243 and 2,882,244, April 14, 1959.
42. Walker, G.P.L., Miner Mag., 32, 503 (1960).
43. Coombs, D.S., Trans. Roy. Soc. N.Z., 82, 65 (1954).
44. Breck, D.W., Flanigen, E.M. and Milton, R.M., Abstract of Papers,  
137th Meeting of the ACS, April 1960.
45. Selbin, J. and Mason, R.B., J. Inorg. Nucl. Chem., 20, 222 (1961).
46. Barrer, R.M. et al., J. Chem. Soc., 195 (1959).
47. Flanigen, E.M. and Grose, R.W., Adv. Chem. Ser., 101, 76 (1971).
48. Reed, T.B. and Breck, D.W., J. Am. Chem. Soc., 78, 5972 (1956).
49. Meier, R.M., Z. Krist., 115, 439 (1961).
50. Cundy, H.M. and Rollett, A.P., "Mathematical Models", 2nd ed.,  
Oxford, London, 1961, pp.104,106.
51. Smith, J.V., Adv. Chem. Ser., 101, 171 (1971).
52. Breck, D.W., J. Chem. Ed., 41, 678 (1964).
53. Olson, D.H., J. Phys. Chem., 72, 1400 (1968).
54. Dempsey, E., J. Phys. Chem., 73, 3600 (1969).
55. Sherry, H.S., J. Phys. Chem., 70, 1158 (1966).
56. Ibid., 72, 4086 (1968).
57. Olson, D.H., J. Phys. Chem., 74, 2758 (1970).
58. Angell, C.L. and Schaffer, P.C., J. Phys. Chem., 70, 1413 (1966).
59. Rabo, J.A., Angell, C.L., Kasai, P.H. and Schomaker, V., Disc.  
Faraday Soc., 41, 328 (1966).
60. Barry, T.I. and Lay, L.A., J. Phys. Chem. Solids, 27, 1823 (1966).
61. Ibid., 29, 1395 (1968).
62. ✓ Richardson, J.T., J. Catalysis, 9, 178 (1967).
63. Mikheikin, I.P., Shvets, V.A. and Kazanskii, V.B., Kinet. Katal.,  
11, 747 (1970).
64. Egerton, T.A. and Stone, F.S., Trans. Faraday Soc., 66, 2364 (1970).
65. Ibid., 69 (1), 22 (1973).
66. Delgass, W.N., Garten, R.L. and Boudart, M., J. Phys. Chem., 73,  
2970 (1969).

41. Milton, R.M., U.S. Patent 2,882,243 and 2,882,244, April 14, 1959.
42. Walker, G.P.L., Miner Mag., 32, 503 (1960).
43. Coombs, D.S., Trans. Roy. Soc. N.Z., 82, 65 (1954).
44. Breck, D.W., Flanigen, E.M. and Milton, R.M., Abstract of Papers,  
137th Meeting of the ACS, April 1960.
45. Selbin, J. and Mason, R.B., J. Inorg. Nucl. Chem., 20, 222 (1961).
46. Barrer, R.M. et al., J. Chem. Soc., 195 (1959).
47. Flanigen, E.M. and Grose, R.W., Adv. Chem. Ser., 101, 76 (1971).
48. Reed, T.B. and Breck, D.W., J. Am. Chem. Soc., 78, 5972 (1956).
49. Meier, R.M., Z. Krist., 115, 439 (1961).
50. Cundy, H.M. and Rollett, A.P., "Mathematical Models", 2nd ed.,  
Oxford, London, 1961, pp.104,106.
51. Smith, J.V., Adv. Chem. Ser., 101, 171 (1971).
52. Breck, D.W., J. Chem. Ed., 41, 678 (1964).
53. Olson, D.H., J. Phys. Chem., 72, 1400 (1968).
54. Dempsey, E., J. Phys. Chem., 73, 3600 (1969).
55. Sherry, H.S., J. Phys. Chem., 70, 1158 (1966).
56. Ibid., 72, 4086 (1968).
57. Olson, D.H., J. Phys. Chem., 74, 2758 (1970).
58. Angell, C.L. and Schaffer, P.C., J. Phys. Chem., 70, 1413 (1966).
59. Rabo, J.A., Angell, C.L., Kasai, P.H. and Schomaker, V., Disc.  
Faraday Soc., 41, 328 (1966).
60. Barry, T.I. and Lay, L.A., J. Phys. Chem. Solids, 27, 1823 (1966).
61. Ibid., 29, 1395 (1968).
62. ✓ Richardson, J.T., J. Catalysis, 9, 178 (1967).
63. Mikheikin, I.P., Shvets, V.A. and Kazanskii, V.B., Kinet. Katal.,  
11, 747 (1970).
64. Egerton, T.A. and Stone, F.S., Trans. Faraday Soc., 66, 2364 (1970).
65. Ibid., 69 (1), 22 (1973).
66. Delgass, W.N., Garten, R.L. and Boudart, M., J. Phys. Chem., 73,  
2970 (1969).

67. Breck, D.W. et al., J. Am. Chem. Soc., 78, 5963 (1956).
68. Sherry, H.S., Adv. Chem. Series, 101, 350 (1971).
69. Rees, L.V.C., Ann. Reports (A), 67, 191 (1970).
70. Barrer, R.M., Proc. Chem. Soc., 99 (1958).
71. Barrer, R.M. et al., Helv. Chim. Acta, 39, 518 (1956).
72. Breck, D.W. and Flanigen, E.M., Proc. Intern. Symp. Mol. Sieves,  
1st, London, 10, 1968.
73. Barrer, R.M. and Gibbons, R.M., Trans. Faraday Soc., 59, 2569 (1963).
74. Barrer, R.M., Endeavour, 23, 122 (1964).
75. Barrer, R.M. and Baynham, J.W., J. Chem. Soc., 2892 (1956).
76. Barrer, R.M. and Peterson, D.L., J. Phys. Chem., 68, 3427 (1964).
77. Smith, J.V., Acta Cryst., 15, 835 (1962).
78. Barrer, R.M., Trans. Brit. Ceram. Soc., 56, 155 (1957).
79. Venuto, P.B. and Landis, P.S., Adv. Catalysis, 18, 259 (1968).
80. Rabo, J.A., Angell, C.L. and Schomaker, V., Intern. Congr. Catalysis,  
4th, Moscow, 1968, Preprint 54.
81. Barrer, R.M. and Bratt, G.C., J. Phys. Chem. Solids, 12, 130 (1960).
82. Stamires, D.N. and Turkevich, J., J. Am. Chem. Soc., 86, 749 (1964).
83. Kerr, G.T., J. Phys. Chem., 71, 4155 (1967).
84. McDaniel, C.V. and Maher, P.K., 'Molecular Sieves', p.186, Society  
of the Chemical Industry (London) 1968.
85. Ward, J.W., Adv. Chem. Series, 101, 380 (1971).
86. Dollish, F.R. and Hall, W.K., J. Phys. Chem., 71, 1005 (1967).
87. ✓ Flockhart, B.D., McLoughlin, L. and Pink, R.C., J. Catalysis, 25,  
305 (1972).
88. ✓ Hirschler, A.E., J. Catalysis, 2, 428 (1963).
89. Okamoto, Y., Imanaka, T. and Teranishi, S., Bull. Chem. Soc.  
Japan, 43, 3353 (1970).
90. Tsutsumi, K. and Takahashi, H., J. Phys. Chem., 74, 2710 (1970).

91. ✓ Bolton, A.P., J. Catalysis, 22, 9 (1971).
92. ✓ Tung, S.E., J. Catalysis, 17, 24 (1970).
93. Dyer, A., Gettins, R.B. and Townsend, R.P., J. Inorg. Nuclear Chem., 32, 2395 (1970).
94. Gallezot, P., Ben Taarit, Y. and Imelik, B., Compt. rend., C, 272, 261 (1971).
95. Mikheiken, I., Shvets, V.A. and Kazanskii, V.B., Kinetika i Kataliz, 11, 747 (1970).
96. Lygin, V.I., Adv. Chem. Series, 102, 86 (1971).
97. ✓ Stevenson, R.L., J. Catalysis, 21, 113 (1971).
98. ✓ Venuto, P.B., Hamilton, L.A. and Landis, P.S., J. Catalysis, 5, 484 (1966).
99. Eberley, P.E. Jr., J. Phys. Chem., 71, 1717 (1967).
100. Bartley, B.H., Habgood, H.W. and George, Z.M., J. Phys. Chem., 72, 1689 (1968).
101. ✓ Dimitrov, C. and Leach, H.F., J. Catalysis, 14, 336 (1969).
102. Cross, N.E., Kemball, C. and Leach, H.F., Adv. Chem. Ser., 102, 389 (1971).
103. Cross, N.E., Kemball, C. and Leach, H.F., J. Chem. Soc. (A), 3315 (1971).
104. Mays, R.L. and Pickert, P.E. in 'Molecular Sieves', Society of Chemical Industry, London, 1968, p.112.
105. ✓ Ward, J.W., J. Catalysis, 22, 237 (1971).
106. ✓ Ibid., 10, 34 (1968).
107. ✓ Ibid., 11, 259 (1968).
108. ✓ Ibid., 14, 365 (1969).
109. Bolton, A.P., Lanewala, M.A. and Pickert, P.E., J. Org. Chem., 35, 1513 (1968).
110. Lanewala, M.A. and Bolton, A.P., Natl. Meeting, North American Catalysis Society, 1st, Atlantic City, 1969.

111. ✓ Csicsery, S.M. and Hickson, D.A., J. Catalysis, 19, 386 (1970).
112. Galick, P.N. et al., Neftekhim., Akad. Nauk. Turkm. SSR, 63,  
(1963); Chem. Abstr., 61, 14434 (1964).
113. Galick, P.N. et al., Neftekhim., Akad. Nauk. Ukr. SSR, Inst.  
Khim. Vysokomolekul. Saedin, 13, (1964); Chem. Abstr., 62,  
8905 (1965).
114. Borunova, N.V. et al., Izv. Akad. Nauk. SSR, Ser. Khim., 4,  
773 (1968).
115. Mochida, I., Hayata, S., Kato, A. and Seiyama, T., J. Catalysis,  
13, 314 (1969).
116. Weisz, P.B. and Frilette, V.J., J. Phys. Chem., 64, 382 (1960).
117. Rabo, J.A. and Poutsma, M.L., Adv. Chem. Ser., 102, 284 (1971).
118. Pickert, P.E., Rabo, J.A., Dempsey, E. and Schomaker, V., Proc.  
Intern. Congr. Catalysis, 3rd, Amsterdam, 714 (1964).
119. Norton, C.J., Proc. Intern. Congr. Catalysis, 2nd, Paris,  
2073 (1960).
120. Turkevich, J., Nozaki, F. and Stamires, D.N., Proc. Intern.  
Congr. Catalysis, 3rd, Amsterdam, 1964, 1, 586 (1965).
121. Kolesnikov, I.M., Panchenkov, G.M. and Tret'yakova, V.A., Russ.  
J. Phys. Chem., 41, 586 (1967).
122. ✓ Matsumoto, H., Yasui, K. and Morita, Y., J. Catalysis, 12, 84  
(1968).
123. Planck, C.J., Proc. Intern. Congr. Catalysis, 3rd, Amsterdam,  
727 (1964).
124. ✓ Ward, J.W., J. Catalysis, 13, 321 (1969).
125. ✓ Hildebrandt, R.A. and Skala, H., J. Catalysis, 12, 61 (1968).
126. ✓ Hopkins, P.D., J. Catalysis, 12, 325 (1968).
127. ✓ Ward, J.W. and Hansford, R.C., J. Catalysis, 13, 364 (1969).
128. ✓ Richardson, J.T., J. Catalysis, 9, 182 (1967).
129. Taylor, T.I., "Catalysis", (P.H. Emmett, ed.) Vol. V, p.257,  
Reinhold, New York, 1957.



130. Kemball, C., Proc. Roy. Soc., A207, 539 (1951).
131. Ibid., A223, 377 (1954).
132. Anderson, J.R. and Kemball, C., Proc. Roy. Soc., A223, 361 (1954).
133. Kemball, C., Adv. Catalysis, 11, 223 (1959).
134. Kemball, C., Proc. Roy. Soc., A214, 413 (1952).
135. Matsen, F.A. and Franklin, J.L., J. Am. Chem. Soc., 72, 3337 (1950).
136. Kemball, C., Catalysis Rev., 5, 33 (1971).
137. Burwell, R.L., Acc. Chem. Res., 2, 289 (1969).
138. Burwell, R.L., Haller, G.L., Taylor, K.C. and Read, J.F., Adv. Catalysis, 20, 1 (1969).
139. Voge, H.H., "Catalysis", (P.H. Emmett, ed.), Reinhold, New York, 435 (1958).
140. Kemball, C., Ann. New York Acad. Sci., 213, 90 (1973).
141. Pines, H. and Schaap, L.A., Adv. Catalysis, 12, 117 (1960).
142. Dunning, H.N., Ind. Eng. Chem., 45, 551 (1953).
143. Haag, W.O. and Pines, H., J. Am. Chem. Soc., 82, 2488 (1960).
144. Ibid., 82, 2471 (1960).
145. Whitmore, F.C. and Meunier, P.L., J. Am. Chem. Soc., 63, 2197 (1941).
146. Whitmore, F.C., Ropp, W.S. and Cook, N.C., *ibid.*, 72, 1507 (1950).
147. Schmerling, L. and Ipatieff, V.N., Adv. Catalysis, 2, 21 (1950).
148. ✓ Kemball, C., Leach, H.F., Skundric, B. and Taylor, K.C., J. Catalysis, 27, 416 (1972).
149. Nier, A.D., Rev. Sci. Instrum., 18, 398 (1947).
150. Halsted, R.E. and Nier, A.D., Rev. Sci. Instrum., 21, 1019 (1950).
151. Barnard, G.P., "Modern Mass Spectrometry", 112. (The Institute of Physics, London).
152. Brookes, B.I., Ph.D. Thesis, University of Edinburgh (1972).
153. McCosh, R., Ph.D. Thesis, University of Edinburgh (1968).
154. Cross, N.E., Ph.D. Thesis, University of Edinburgh (1969).
155. Coutts, N.M., Ph.D. Thesis, University of Edinburgh (1973).

156. Rudham, R. and Sanders, M.K., in "Chemisorption and Catalysis"  
(London: Institute of Petroleum 1971).
157. Walker, D.R., Ph.D. Thesis, University of Edinburgh (1967).
158. Dowie, R.S., Kemball, C., Kempling, J.C. and Whan, D.A., Proc.  
Roy. Soc. A327, 491 (1972).
159. Scurrrell, M.S., Robertson, P.J., Nisbet, J.D. and Kemball, C.,  
to be published.
160. Beynon, J.H., Mass Spectrometry (Elsevier, London, 1960).
161. Gault, F.G. and Kemball, C., Trans. Faraday Soc., 57, 1781 (1961).
162. Stevenson, D.P. and Wagner, C.D., J. Chem. Phys., 19, 11 (1951).
163. Amenomiya, Y. and Pottie, R.F., Canad. J. Chem., 46, 1741 (1968).
164. Evans, M.W., Bauer, N. and Beach, J.Y., J. Phys. Chem., 14, 701 (1946).
165. Field, F.H. and Franklin, J.L., Electron Impact Phenomena (Academic  
Press, New York, 1957), p.204.
166. Dowie, R.S., Whan, D.A. and Kemball, C., J. Chem. Soc. Faraday  
Trans. I, 68, 2150 (1972).
167. Urey, H.C. and Rittenberg, D., J. Chem. Phys., 1, 137 (1933).
168. Kilpatrick, J.E., Prosen, E.J., Pitzer, K.S. and Rossini, F.D.,  
J. Res. Nat. Bur. Stand., 36, 559 (1946).
169. Ward, J.W., Trans. Faraday Soc., 67, 1489 (1971).
170. ✓ Nacacche, C.M. and Ben Taarit, Y., J. Catalysis, 22, 171 (1971).
171. Nacacche, C.M. and Ben Taarit, Y., J. Chim. Phys., 67, 1434 (1970).
172. Christner, L.G., Liengme, B.V. and Hall, W.K., Trans. Faraday Soc.,  
64, 1679 (1968).
173. ✓ Lombardo, E.A., Sill, G.A. and Hall, W.K., J. Catalysis, 22, 54 (1971).
174. Kemball, C., Leith, I.R. and Leach, H.F., Chem. Comm., 407 (1971).
175. Leith, I.R. and Leach, H.F., Proc. Roy. Soc., A330, 247 (1972).
176. ✓ Gallezot, P., Ben Taarit, Y. and Imelik, B., J. Catalysis, 26,  
295 (1972).

177. Huang, Y. and Vansant, E.F., J. Phys. Chem., 77, 663 (1973).
178. Vansant, E.F. and Lunsford, J.H., J. Phys. Chem., 76, 2860 (1972).
179. ✓ Slot, H.B. and Verbeek, J.L., J. Catalysis, 12, 216 (1968).
180. Leith, I.R., personal communication.
181. Leith, I.R., to be published.
182. ✓ Richardson, J.T., J. Catalysis, 9, 172 (1967).
183. Rieckert, L., Bunsengesellschaft, 73, 331 (1969).
184. Cotton, F.A. and Wilkinson, G., 'Advanced Inorganic Chemistry',  
2nd ed., Interscience, London.
185. Garbowski, E., Kodratov, Y., Mathieu, M. and Imelik, B., J. Chim.  
Phys., 69, 1386 (1972).
186. Olson, D.H., J. Phys. Chem., 72, 4366 (1968).
187. ✓ Gallezot, P., Ben Taarit, Y. and Imelik, B., J. Catalysis, 26,  
481 (1972).
188. Gallezot, P. and Imelik, B., J. Phys. Chem., 77, 652 (1973).
189. Merril, H.E. and Arey, W.F., Amer. Chem. Soc. Div. Petrol. Chem.  
Prepr., 193 (1968).
190. Kemball, C. and McCosh, R., Proc. Roy. Soc., A321, 249 (1971).
191. Ibid., A321, 259 (1971).
192. Pope, C.G. and Kemball, C., Trans. Faraday Soc., 65, 619 (1969).
193. Leith, I.R., private communication.
194. Yates, D.J.C., J. Phys. Chem., 69, 1676 (1965).
195. Romanowski, W., Z. anorg. allg. Chem., 351, 180 (1967).
196. Herd, A.C. and Pope, C.G., J. Chem. Soc. Faraday Trans. I,  
69, 833 (1973).
197. Wall, J., Leach, H.F. and Kemball, C., unpublished results.
198. ✓ Hightower, J. and Hall, W.K., J. Catalysis, 13, 161 (1969).
199. Kemball, C., Leach, H.F., Moller, B.W. and Scurrrell, M.S.,  
to be published.

200. Crawford, E. and Kemball, C., Trans. Faraday Soc., 58, 2452 (1962).
201. McCosh, R. and Kemball, C., J. Chem. Soc. (A), 1967 (1968).
202. McCosh, R. and Kemball, C., Chem. Comm., 802 (1969).
203. ✓ Harper, R.J., Siegel, S. and Kemball, C., J. Catalysis, 6, 72 (1966).
204. Barrer, R.M., J. Soc. Chem. Ind., 64, 130 (1945).
205. Mackor, E.L., Smit, P.J. and Van der Waals, J.H., Trans. Faraday Soc., 53, 1309 (1957).
206. Tiers, G.V.D., J. Amer. Chem. Soc., 78, 4165 (1956).
207. Dallinga, G. and Ter Maten, G., Rec. Trav. Chem., 79, 737 (1960).
208. Dykhno, N.M. and Shatenshtein, A.I., Zur. Phys. Khim., 28, 11 (1954).
209. Shatenshtein, A.I. and Izrailevich, E.A., Zur. Phys. Khim., 32, 2711 (1958).
210. Ingold, C.K., Rasin, C.G. and Wilson, C.L., J. Chem. Soc., 915 (1936).

# ABSTRACT OF THESIS

Bernard William Moller

Name of Candidate .....

10 Brunstane Drive, Edinburgh EH15 2NF.

Address .....

Ph.D.

Degree .....

Date .....

Title of Thesis ..... Reactions of  $C_6$  Olefins and m-Xylene over Ion-Exchanged Zeolites.

In this work two test reactions have been utilised to study the nature of zeolite catalysts. Firstly, the isomerisation of 3,3-dimethylbut-1-ene(I), to give 2,3-dimethylbut-1-ene(II) and 2,3-dimethylbut-2-ene(III), was used to study the acidity of a series of copper, zinc and nickel-exchanged zeolites because the reaction is believed to proceed via the formation of carbonium ion intermediates. After a preliminary survey of each series of zeolites a more detailed examination of the isomerisation and exchange reactions of these  $C_6$  olefins over selected catalysts was undertaken. The isomerisation of both I and II was studied and the effect of the presence of  $H_2$  and  $H_2O$  upon such rates examined. The nature of the exchange reactions of the various olefins was investigated using both  $D_2$  and  $D_2O$ .

The results demonstrate that CuX and ZnX zeolites display acidic-type behaviour, being much more active than the parent NaX. Hydrogen was observed to have no effect upon the rate of isomerisation of the olefins over these catalysts but the changes in rate observed when the reactions were carried out in the presence of water could be explained in terms of interaction of water molecules with the transition metal cations. The isomerisation of II was shown to be a more facile process than that of I.

The exchange reactions of I and II with  $D_2$  and  $D_2O$  showed that substantial exchange only took place under conditions where isomerisation occurred. With  $D_2O$  the exchange of I was multiple in character whereas that of II was stepwise. These differences were rationalised in terms of the relative rates of desorption of II and III from the catalyst surface and the rate of formation of a tertiary carbonium ion from the initial olefin. The exchange reactions of the olefins with  $D_2$  all occurred via a stepwise process.

NiX zeolites were observed to display activity of a dual function type. They showed acidic behaviour in being active for the isomerisation of I and the reactions of the olefins with  $H_2O$  or  $D_2O$  could be interpreted as for CuX or ZnX. However, the most striking differences between NiX and CuX or ZnX were observed when reactions of the olefins were studied with  $H_2$  or  $D_2$ . The ability of NiX zeolites to catalyse the hydrogenation of the  $C_6$  olefins and to bring about the low temperature exchange of I with  $D_2$  was well demonstrated. Further detailed study was undertaken with selected CuX and NiX zeolites. The catalysts were subjected to various pretreatments in an attempt to gain more information about the nature of the catalytically active sites.

The second part of the thesis was concerned with studying the exchange reactions of m-xylene over nickel, cobalt and calcium-exchanged zeolites using a temperature- programming technique. The relative reactivities of the different hydrogen atoms in the aromatic molecule is thought to provide information about the operative mechanism.

The most important result to emerge was that the nature of the source of labelling isotope ( $D_2$  or  $D_2O$ ) had a profound effect upon the character of the reaction. With  $D_2O$ , ring exchange was found to be faster than side-group exchange over all catalysts, a result indicative of acidic-type behaviour. One of the ring hydrogen atoms in m-xylene was observed to react more slowly than the other three and this is believed to be the hydrogen atom ortho to both methyl groups, indicating that steric and not electronic factors are important in the exchange of the ring atoms.

When  $D_2$  was used as the source of deuterium a complete change was observed in the character of the reaction. With NiX side-group exchange was now faster than ring exchange, a result similar to that found over metals. CoX and CaX were much less active than NiX for exchange with  $D_2$ . Over these two catalysts all of the hydrogen atoms in the molecule were found to be equally reactive and the limiting factor in the exchange appeared to be the ability of the catalysts to activate  $D_2$ .